

Tectonic Evolution of the Izmir-Ankara Suture Zone in Northwest Turkey using
Zircon U-Pb Geochronology and Zircon Lu-Hf Isotopic Tracers

By

Clay Franklin Campbell
B.S., The University of Arizona, 2013

Submitted to the graduate degree program in the Department of Geology and the Graduate
Faculty of the University of Kansas in partial fulfillment of the requirements for the degree
Master of Science

Chair: Mike Taylor

Andreas Möller

Noah McLean

Mike Blum

Date Defended: 26 July, 2017

The thesis committee for Clay Franklin Campbell certifies that this is the approved version of the following thesis:

Tectonic Evolution of the Izmir-Ankara Suture Zone in Northwest Turkey using Zircon U-Pb Geochronology and Zircon Lu-Hf Isotopic Tracers

Chair: Mike Taylor

Date Approved: 26 July, 2017

Abstract

Detrital zircons from the Late Cretaceous Murdunu-Göynük forearc basin and the Paleogene Sarıcakaya foreland basin; part of the greater Central Sakarya Basin located along the Sakarya Zone of the Western Pontides were analyzed to better understand the closure history of the Tethyan oceans. In northwest Turkey, the Variscan Orogeny is characterized by abundant 350-300 Ma zircon U-Pb ages and minimally to highly evolved ϵ_{Hf} values. In ϵ_{Hf} vs. age space no distinct trends are apparent, consistent with a north dipping subduction zone that emplaced plutons into a southward growing, heterogeneous accretionary margin. From 300-250 Ma ϵ_{Hf} values trend from highly to minimally evolved, interpreted as crust thinning, a result of slab roll-back and rifting of the Intra-Pontide Ocean. The Cimmerian Orogeny is characterized by a decrease in magmatism from 250-230 Ma associated with minimally to moderately evolved ϵ_{Hf} evolution, followed by a 230-200 Ma magmatic gap consistent with crustal thickening followed by flat-slab underthrusting of the Karakaya Complex. Zircons with 200-115 Ma U-Pb ages are all but absent, interpreted as a magmatic lull. The Alpine Orogeny in northwest Turkey is characterized by an increase in magmatism from 115-85 Ma, associated with minimally intermediate to moderately evolved ϵ_{Hf} evolution of Late Cretaceous Murdunu-Göynük forearc zircons. At 100 Ma, Late Cretaceous zircons only found within Paleogene Sarıcakaya foreland basin sediments deviate from similar aged ϵ_{Hf} evolution in forearc basin sediments and plot in both the juvenile and intermediate domains. Minor zircon U-Pb age peaks and contrasting inter-basinal ϵ_{Hf} evolution are interpreted to represent onset of Andean-style subduction along the southern margin of the Sakarya Zone at ~115 Ma followed by 100 Ma initiation of intra-oceanic subduction within the İzmir-Ankara Ocean. Epsilon Hf values from zircons with 85-75 Ma U-Pb ages sampled from forearc basin sediments trend from moderately evolved to moderately

intermediate, interpreted as crustal thinning, a result of slab roll-back along the southern margin of the Sakarya Zone, responsible for final rifting of the Western Black Sea. Foreland basin zircon with U-Pb ages of 85-80 Ma deviate towards highly evolved ϵ_{Hf} values. These highly evolved and deviant ϵ_{Hf} values are interpreted to represent synchronous melting of the Tavşanlı Zone and intra-oceanic slab break-off. A single concordant ~66 Ma pre-collisional zircon grain collected from Late Cretaceous forearc basin flysch located directly beneath a regional unconformity is defined by a moderately evolved ϵ_{Hf} value prior to complete absence of young detrital grains and is interpreted to represent incipient collision between the Sakarya and Tavşanlı zones followed by total arc shut-off. Syn-collisional tuffs yield minimally evolved ϵ_{Hf} values that trend toward minimally intermediate ϵ_{Hf} values from 55-50 Ma and from minimally intermediate to highly intermediate from 50-46 Ma, interpreted to represent a second episode of slab break-off followed by crustal thickening, a result of renewed syn-collisional underthrusting.

Acknowledgements

I am deeply thankful for being given the opportunity to study with Professor Micheal Taylor at the University of Kansas. Without his encouragement, guidance, patience, and support this project would not have come to fruition. I am also indebted to my committee members; Andreas Möller, who kindly allowed me to use his analytical facilities and ensured all the data collected at the KU IGL for this project was of the highest quality, Noah McLean who continually worked with me to reduce and interpret data, and Mike Blum who reminded me to look at the rocks. I would also like to thank Alexis Licht for generously sharing his samples and knowledge of various basins in Turkey with me. Professor Doug Walker served to expand my literary geologic knowledge and taught me the basic – yet valuable statistical methods and applications for better understanding my geochemical datasets. University of Arizona Professor George Gehrels also served as an invaluable outlet for assistance with Lu-Hf data interpretation. I would like to thank Jeff Oalman who graciously took his time to help me run my DZ samples for U-Pb as well as served as a bridge of understanding between the Iolite and ET_Redux data reduction schemes. I am thankful to Ty Tenpenny for taking his time to teach me the various mineral separation procedures as well as Wayne Dickerson for helping with sample preparation. Mark Pecha, Jacob Favela and Chelsi White from Arizona Laserchron were integral pieces to this project and were patient as well as malleable.

I am incredibly grateful for financial support provided by The KU department of Geology as well as K. Christopher Beard and Michael Taylor's NSF INSPIRE grant, which supported me for 24 months. Ultimately none of this would have materialized without the echoes of enthusiasm from my family who constantly remind me there's more to life than just living.

Table of Contents

1 Introduction.....	1
2 Regional Geology.....	4
2.1 Pontides.....	5
2.2 Anatolides.....	6
2.3 Basins.....	7
3 Methods.....	9
3.1 Sampling Strategy.....	9
3.2 Sample Preparation.....	9
3.3 Zircon U-Pb Geochronology.....	10
4 Zircon U-Pb results.....	12
4.1 Southern Saricakaya Basin.....	12
4.2 Northern Saricakaya Basin.....	14
4.3 Murdunu-Göynük Basin.....	15
4.4 Orhaniye Basin.....	15
5 Lu-Hf Isotopic Tracers.....	17
6 Lu-Hf Results.....	19
7 Cumulative Plots.....	22
7.1 Cumulative Zircon PDP.....	22
7.2 Cumulative Lu-Hf Plot.....	23
8 Synthesis.....	24
8.1 350-250 Ma.....	24
8.2 250-200 Ma.....	25

8.3 200-115 Ma.....	25
8.4 115-80 Ma.....	26
8.5 80-66 Ma.....	26
8.6 <65 Ma.....	24
9 Conclusions.....	29
10 References.....	31
11 Figure Captions.....	38
12 Figures.....	40
13 Appendices.....	52
Appendix 1: Detailed Terrane and Basin Descriptions.....	52
Appendix 2: Sample Descriptions and Locations.....	61
Appendix 3: U-Pb Analytical Parameters.....	62
Appendix 4: U-Pb Standard Values.....	65
Appendix 5: LA-ICPMS Zircon Data Tables.....	66
Appendix 6: Zircon Hf Standard Plot.....	79
Appendix 7: LA-MC-ICPMS Zircon Hafnium Data Tables.....	80

List of Figures

Figure 1. Terrane Map	40
Figure 2. Tectonic Models	41
Figure 3. Sakarya River Valley Map	42
Figure 4. Southern Sakarya Basin Concordia and Probability Density Plots	43-44
Figure 5. Northern Sakarya Basin Concordia and Probability Density Plots	45
Figure 6. Murdunu-Göynük Basin Concordia and Probability Density Plots	46
Figure 7. Orhaniye Basin Concordia and Probability Density Plots	46
Figure 8. Basins Probability Density Plots	47
Figure 9. Mesozoic Lu-Hf Plots	48
Figure 10. Cenozoic Lu-Hf Plots	49
Figure 11. Zircon U-Pb and Lu-Hf Cumulative Plot	50
Figure 12. Tectonic Model	51

1. INTRODUCTION

Turkey is the eastern Mediterranean part of the Alpine-Himalayan orogen, which trends east-west from Western Europe through the Middle East and into Eastern Asia for over 8,000 km. The active Alpine-Himalayan orogen is a zone of north-south convergence, which accommodated Carboniferous-Late Cretaceous closure of the Tethyan oceans, and Cenozoic juxtaposition of terranes of Laurasian and Gondwanan affinities (Ketin 1966; Şengör and Yılmaz, 1981; Şengör et al., 1988; Okay and Tüysüz, 1999). The İzmir-Ankara-Erzincan Suture Zone (İAESZ) of central Turkey is approximately east-trending for ~1750 km, representing the closure of Paleotethys as well as the multi-branched Neotethyan oceans along a zone of collision and shortening between the Pontide (Laurasia) and Anatolide-Tauride terranes (Gondwana) (Fig. 1). The Pontides formed during Paleozoic-Mesozoic terrane accretion (e.g., Okay et al., 2002; Okay et al., 2013), similar to the development of the westernmost North American Cordillera (e.g., Coney et al., 1980; Gehrels and Pecha, 2014), which unlike North America, was followed by Early Cenozoic continental collision. This study describes the Carboniferous-Paleogene tectonic evolution of the Sakarya Zone, the southernmost terrane of the Pontides.

Large basins, such as the Central Sakarya Basin (Fig. 1) sample vast swathes of land and often serve as an ideal archive for episodes of arc magmatism over geologic time (Wu et al., 2010). Zircon is ubiquitous in crustal rocks, highly resistant to erosion, re-melting and contains high concentrations of U, Pb and Hf isotopes, making it an ideal mineral for geologic investigations (Hawkesworth and Kemp 2006).

Zircon Laser Ablation – Inductively Coupled Mass Spectrometry (LA-ICPMS) U-Pb geochronology and zircon Laser Ablation – Multicollector – Inductively Coupled Mass Spectrometry (LA-MC-ICPMS) Lu-Hf as a geochemical tracer complement paleomagnetic

reconstructions (e.g. Stampfli, 2000; Stampfli and Borel, 2002; Stampfli and Kozur 2006; van Hinsbergen et al., 2016; Maffione et al., 2017), field data based geologic studies (e.g. Şengör and Yilmaz, 1981; Altiner et al., 1991; Yilmaz et al., 1997; Tüysüz 1999; Robertson et al., 2004; Moix et al., 2008) and geophysical imaging (e.g., van Hinsbergen et al., 2010b; Salaün et al., 2012). Samples collected from the Paleogene Saricakaya foreland basin, the Late Cretaceous Murdunu-Göynük forearc basin, and the Orhaniye peripheral basin (Fig. 1) of the Western Pontides, were analyzed for detrital zircon U-Pb and zircon Lu-Hf, which serves as a tested method for testing and refining tectonic models (e.g., Ji et al., 2009; Wu et al., 2010; Pecha et al., 2016) regarding the closure history of the Tethyan oceans in northwest Turkey. Therefore, basin-scale detrital zircon U-Pb coupled with Lu-Hf can guide interpretations of geologic processes such as the isolation or connectivity of terranes and periods of crustal thinning vs. crustal thickening. Interpretations of crustal thinning or crustal thickening based on ϵ_{Hf} -age datasets that coincide with major rifting or mountain building events based upon independent datasets, such as field observations, may ultimately be related to evolving subduction zone dynamics, which control terrane accretion as well as the opening and closure of ocean basins.

This study evaluates the Late Cretaceous-Early Paleogene closure of the northern branches of the Neotethyan oceans (i.e. İzmir-Ankara and Intra-Pontide oceans), as well as northwestern Turkey's pre-, syn- and post-collisional history, which remain equivocal (e.g., Pourteau et al., 2015). Figure 2 illustrates the various tectonic models used to describe the mechanisms which facilitated the closure of the İzmir-Ankara Ocean and are as follows: (1) 'stepwise subduction models' describe how multiple north dipping, singularly active and temporally distinct subduction zones facilitated the closure of the İzmir-Ankara Ocean and collision between the Tavşanlı and Sakarya zones, where subduction zone jumps were preceded

by slab break-off events (Okay et al., 2001; Dilek and Altunkaynak, 2009); (2) ‘continuous nappe stacking models’ describe how a single north dipping subduction zone located along the southern margin of the Sakarya Zone facilitated the Maastrichtian closure of the İzmir-Ankara Ocean and collision between the Tavşanlı and Sakarya zones, where Cenozoic southward sweep of basic magmatism is attributed either slab roll-back (van Hinsbergen et al., 2010b) or lithospheric delamination (Pourteau et al., 2015); (3) ‘synchronous subduction models’ describe how multiple north dipping subduction zones, which were synchronously active facilitated the closure of the İzmir-Ankara Ocean and collision between the Tavşanlı and Sakarya zones, where the southernmost Late Cretaceous subduction zone has been placed within the Afyon Ocean (Shin et al., 2013; Speciale et al., 2014) or within the İzmir-Ankara Ocean.

The above models make predictions that can be tested based on the timing, location, and geochemical fingerprint of magmatic events as well as inception of rift basins and thrust belts, which to a first order are controlled by style of subduction (e.g., slab roll-back vs. flat-slab). In the next section we describe the regional geology of the Pontide and Anatolide-Tauride terranes. Then, we present data collected from the Sarıcakaya, Murdunu-Göynük, and Orhaniye basins within the western Sakarya Zone (Fig. 1), that bear directly on the predictions of the above models. Finally, we present a model based on detrital zircon U-Pb geochronology and Lu-Hf isotopic tracers, which resolves the timing and mechanism(s) leading to the closure of the Tethyan oceans in northwest Turkey.

2. REGIONAL GEOLOGY

In Turkey, the Strandja Zone, İstanbul Zone, and Sakarya Zone exhibit a pre-Carboniferous Laurasian affinity and are collectively known as the Pontides (Okay and Tüysüz, 1999). The Menderes Massif, Tavşanlı Zone, Afyon Zone and Central Anatolian Crystalline Complex exhibit significant yet contrasting metamorphic histories and are collectively known as the Anatolides (Okay and Tüysüz, 1999). South of the Anatolides is the Tauride Block, which is interpreted to be the unmetamorphosed equivalent of the Anatolides (Okay and Tüysüz, 1999). Collectively the Anatolides and Taurides are known as the Anatolide-Tauride Block (ATB) due to their pre-Carboniferous Gondwanan affinity (Fig. 1). A unique and enigmatic feature of the ATB is the presence of regionally distributed sub-horizontal nappe sheets containing ophiolite, mélangé, marine and transitional sediment in their hanging-wall (e.g., Okay et al., 1996). In this paper the classical definition of the ATB is adopted (e.g., Şengör & Yilmaz, 1981), where the Anatolides and Taurides are treated as a single terrane, which rifted from Gondwana during the Triassic opening of the Neotethys (e.g., Robertson et al., 2012). These composite blocks – or terranes of Laurasian and Gondwanan affinity are juxtaposed against one another along the İzmir-Ankara-Erzincan Suture Zone (İAESZ), which represents the location where a westward narrowing, Late Paleozoic oceanic embayment between Laurasia and Gondwana, known as the Tethyan Ocean closed (Şengör and Yilmaz, 1981).

Below we provide a brief geologic background of these tectonic units whose geologic histories will serve as important constraints to our conceptual model. We also provide brief descriptions of the Paleogene Sarıcakaya foreland basin, Murdunu-Göynük Late Cretaceous forearc basin, and the Paleozoic Orhaniye peripheral-forearc basin. More detailed terrane and basin descriptions are located in appendix 1.

2.1 Pontides

The Strandja Zone is located in northwestern Turkey (Fig. 1). The basement of the Strandja Zone consists of felsic gneisses and migmatites intruded by Carboniferous-Permian granitoids emplaced during the Variscan Orogeny (Okay and Tüysüz, 1999). Basement rocks are unconformably overlain by Paleozoic and Early Mesozoic continental units, volcanic rocks, and shallow marine carbonates, all of which were subjected to latest Jurassic-earliest Cretaceous greenschist metamorphism (Okay, 1986; Okay et al., 1996). Paleozoic and Mesozoic sedimentary cover rocks are intruded by Late Cretaceous calc-alkaline andesitic plutons emplaced during the closure of the Vardar Ocean, which culminated by ~115 Ma (Okay et al., 1996).

The İstanbul Zone (Fig. 1) is located along the southwestern lobe of the Black Sea, is approximately 400 km E-W by 70 km N-S (Okay and Tüysüz, 1999), and is juxtaposed against the Sakarya Zone via the Intra-Pontide Suture (e.g., Akbayram et al., 2016). The İstanbul Zone consists of a Cadomian (Pan-African) basement (P. Ustaömer et al., 2005), which is overlain by a transgressive sequence of Ordovician-Carboniferous clastic rocks, resembling similar aged sedimentary packages of the Moesian Platform (Okay et al., 1996). During the Early Devonian-Late Carboniferous (\pm Permian) Variscan Orogeny (Stampfli, 2000) these sedimentary packages were subject to varying degrees of metamorphism and deformation, which propagated from west to east (Okay and Tüysüz, 1999). Triassic transgressive sediments unconformably overlie tectonised Ordovician-Carboniferous units (Okay et al., 1996; Okay and Tüysüz, 1999) and were deformed during the Cimmerian Orogeny. Along the northern margin of the İstanbul Zone, Triassic strata is unconformably overlain by Late Cretaceous extrusive volcanic rocks and cut by their intrusive counterpart (Okay and Tüysüz, 1999) (Fig. 1; inset).

The Sakarya Zone (Fig. 1), described by Okay (1984a) combines Şengör and Yılmaz, (1981)'s Sakarya Continent and the Eastern Pontides. However, in this study, we adopt the latter definition due to the abundant and contrasting Paleozoic-Cenozoic volcanic history of the Eastern Pontides (Fig. 1; inset). The Basement of the Sakarya Zone is characterized by Early Paleozoic passive margin strata, which are metamorphosed, deformed and intruded by Carboniferous ±Devonian granitoids emplaced during the Variscan Orogeny (Okay et al., 1996). The Karakaya Complex is located structurally below the Variscan basement (Okay et al., 2002) and consists of a ca. 3 km thick package of mafic Carboniferous, Permian and Triassic sediments (Okay and Tüysüz, 1999; Ustaömer et al., 2016) that underwent varying degrees of metamorphism during the Late Triassic Cimmerian Orogeny (Okay et al., 2002). During the Early Jurassic, conglomeratic strata was deposited and is overlain by a Middle Jurassic-earliest Late Cretaceous ~2 km thick sequence of limestone (Okay and Tüysüz, 1999). Late Cretaceous-Neogene strata are in contact with this limestone sequence along an angular unconformity and coarsen upward into marine turbidites, lagoonal, deltaic and fluvial deposits with interbedded volcanic horizons.

2.2 Anatolides

The Tavşanlı Zone (Okay 1984a) strikes E-W for 250-300 km and has an average N-S width of ~50 km (Fig. 2), whose defining feature is a Late Cretaceous blueschist belt with lesser amounts of Triassic blueschist (Okay et al., 2002), the former a result of intra-oceanic subduction from 90-80 Ma and subsequent high-pressure low-temperature metamorphism (Okay et al., 1998; Sherlock et al., 1999; Sherlock and Kelly, 2002). To the east, the contact between the Tavşanlı Zone and the Central Anatolian Crystalline Complex is obscured by Upper Cretaceous-

Middle Eocene sediments of the Orhaniye, Haymana-Polatli, and Tuz Gölü basins (e.g., Nairn et al., 2013; Licht et al., 2017)

The Afyon Zone (Fig. 1) (Okay 1984a), structurally beneath the Tavşanlı Zone is characterized by Paleocene Barrovian-type metamorphism and underlain by Pan-African basement mantled by low-grade, Late Paleozoic metamorphosed sediments which fine up section from Carboniferous conglomerates to Permian neritic platform-type sediments. Overlying Mesozoic sediments consist of Triassic-Late Cretaceous turbidites, which grade into sandstone beginning in the Paleocene (Candan et al., 2005).

Cenomanian Ar/Ar apparent cooling ages (ca. ~95 Ma) of metamorphic soles of ophiolitic bodies are juxtaposed over the Tavşanlı Zone (Önen and Hall, 1993; Önen 1993), Afyon Zone (Daşçi et al., 2014), and the Taurides (Çelik et al., 2006) (van Hinsbergen et al., 2016). These ophiolitic units are related to obduction of a south-directed thrust sheet along an intra-oceanic subduction zone within the İzmir-Ankara Ocean that was active from the Aptian-Maastrichtian. During Early Paleogene syn-collisional orogenesis, these ophiolites were once more translated southward in the hanging-wall of younger south-directed thrust sheets (e.g., Pourteau et al., 2015).

2.3 Basins

The Central Sakarya Basin (Fig. 1) is the primary basin along the Sakarya Zone (e.g., Okay and Tüysüz, 1999). The northern portion of this basin is known as the Murdunu-Göynük Basin (Fig. 1), which consists primarily of Jurassic marine and Cretaceous shallow marine turbidites to transitional sediments with interbedded volcanic horizons (Altiner et al., 1991).

The Sarıcakaya Basin is located in the southern portion of the Central Sakarya Basin, due north of the İzmir-Ankara Suture. This basin consists primarily of Paleogene conglomeratic red

beds that unconformably overly basement and Early-Middle Mesozoic sediments, interpreted to be deposited within a Paleogene foreland basin, whose best outcrops can be observed in the Sakarya River Valley (Fig. 3). From north to south, 3 principal SE directed thrust can be observed in the main study area: 1) the Northern Söğüt Thrust juxtaposes the Söğüt Granite (~325 Ma; P. Ustaömer et al., 2011), metamorphosed basement units (PcB) and unconformably overlying Jurassic marine limestone (Jm), Late Cretaceous transitional sediments (Kt) and Paleogene terrigenous sediments (PET), which are folded into a broad syncline structurally above Paleogene Sarıcakaya foreland basin sediments (PET). These footwall sediments are in turn locally folded into a SE verging overturned syncline; 2) the Southern Söğüt Thrust juxtaposes the footwall of the former thrust structurally above the Permo-Triassic Karakaya Complex (Trkc); and 3) the İzmir-Ankara Suture, which juxtaposes the Permo-Triassic Karakaya Complex (Trkc) structurally above Late Cretaceous accretionary mélangé (Km) and is the contact between the Sakarya Zone and the Tavşanlı Zone (Fig. 3).

3. METHODS

3.1 Sample Strategy

To understand provenance and timing of deposition within the Murdunu-Göynük Basin, we sampled the first conglomeratic bed above Late Cretaceous turbidites (15G002) as well as an overlying volcanic horizon (15G001) near the town of Göynük (Fig. 3). To understand provenance and timing of deposition within the Saricakaya Basin, we sampled rocks in the hanging-wall of the Söğüt Thrust (i.e., Northern Saricakaya Basin) with known depositional ages of Jurassic (15YP04), Late Cretaceous (15YP13) and Eocene (15YP14). In the footwall of the Söğüt Thrust (i.e., Southern Saricakaya Basin) we sampled rocks with Carboniferous (15YP12) and Eocene (15YP09, 15YP08) depositional ages as well as two tuffaceous units (15YP11, 15YP07), which are stratigraphically below all Cenozoic samples (Fig. 3). A single sample was taken from a metamorphosed Permo-Triassic Sandstone (15KZ01) at the base of the Orhaniye Basin, located within the south pointing horn of the Sakarya Zone east of the Central Sakarya Basin in order to evaluate along strike variability in tectonic setting and provenance prior to the Alpine Orogeny (Figs. 1 & 3).

3.2 Sample Preparation

Zircon grains were separated from whole-rock samples using standard heavy-mineral separation techniques including a bottle jack, chipmunk jaw crusher, disk mill, Gemini table, heavy liquids (Methylene Iodide) and a FrantzTM isodynamic magnetic separator, which serves as a tested method to separate minerals based on their chemical and physical properties (e.g., Sircombe and Stern, 2002). Large zircon aliquots for all 11 samples were reduced to representative splits using a microsplitter up to three times, effectively reducing the samples size by one half with each split. The grains were then randomly handpicked (i.e., grains of all sizes,

crystal habits, colors and degree of weathering were indiscriminately chosen) under a binocular microscope, mounted in epoxy and polished to between one half and one third width in order to expose the internal structures of the zircon grains.

3.3 Zircon U-Pb Geochronology

Zircon U-Pb analyses were conducted at The University of Kansas Isotope Geochemistry Laboratory (KU-IGL), using a Thermo Scientific Element II Inductively Coupled Plasma Mass Spectrometer attached to a Photon Machines Analyte.G2 193 nm ArF excimer laser ablation system (LA-ICP-MS). 20 μm circular spots were ablated with the laser at 2.0 J cm^{-2} fluency and 10 Hz repetition rate to depths of ca. 15 μm , where the ablated material was carried to the ICP in He gas. Elemental fractionation, downhole fractionation and calibration drift were corrected by bracketing measurements of unknowns with the GJ1 primary reference material which has a known Thermal Ionization Mass-Spectrometry (TIMS) $^{207}\text{Pb}/^{206}\text{Pb}$ age of 608.53 ± 0.037 Ma (Jackson et al., 2004). All accepted primary standard analyses during the LA-ICP-MS analyses of this study fell within 2 standard deviations of the published age. As a means to validate the calibration of the GJ1 primary reference material, Plešovice and Fish Canyon Tuff zircons were treated as unknowns (from herein referred to as secondary reference materials) to be compared to their known Chemical Abrasion – Thermal Ionization Mass-Spectrometry (CA-TIMS) $^{207}\text{Pb}/^{206}\text{Pb}$ age of 337.13 ± 0.13 Ma and 28.642 ± 0.025 Ma respectively (Sláma et al., 2008; Wotzlaw et al., 2013). Concordant ages were then used to calculate a weighted mean and the Mean Square Weighted Deviation (MSWD). Analytical sessions in which both the Plešovice and Fish Canyon Tuff fell within 2 standard deviations of their true ages and exhibited an MSWD between 0.3 and 2.5 were deemed acceptable and allowed interpretation of true unknowns. All data was reduced using the intercept ET_Redux reduction scheme (McLean et al., 2016).

Complications in data reduction and analysis were common with the Fish Canyon Tuff secondary reference material, likely a result of unobserved inclusions or common lead contamination within fractures of individual grains. Analytical parameters used for all runs can be found in appendix 3.

4. Zircon U-Pb Results

In this section zircon U-Pb data are described from the stratigraphically lowest (oldest) to highest (youngest) sample from the southern Saricakaya Basin, northern Saricakaya Basin, Murdunu-Göynük Basin and the Orhaniye Basin (Fig. 1). Detrital zircon populations are described from youngest to oldest. Figures 4-7 contain concordia and probability density plots (PDP's) of the following results and figure 8 contains PDP's of all samples analyzed in this study organized by their location and depositional setting (i.e., detrital vs. volcanic). Analyses were inspected individually to insure satisfactory data quality. Major deviations in $^{206}\text{Pb}/^{238}\text{U}$ and $^{206}\text{Pb}/^{207}\text{Pb}$ ratios deemed not to be a consequence of random and independent data collection resulted in analysis rejection. Analytical uncertainties of standards are provided in appendix 4 and raw data specific to individual samples can be found in appendix 5.

4.1 Southern Saricakaya Basin

Sample 15YP12 was collected from a basement outcrop. 70 individual spots on a total of 70 zircons were ablated, of which 60 analyses were deemed acceptable. Sample 15YP12 yielded a single major age cluster between 312-338 Ma (n=43/60; 72%), with a minor age cluster from 345-360 Ma (n=9; 15%) and single grains analyses from 472-2512 Ma (n=8/60; 13.33%). Of the 43 ages that defined the youngest age cluster 15 were used to calculate a weighted mean of 316.7 \pm 1.2 Ma, MSWD=1.1, n=15 which is interpreted as the maximum depositional age (Figs. 3,4,8).

Sample 15YP11 was collected from a Paleogene tuffaceous unit. 150 individual spots on a total of 149 individual zircons were ablated, of which 98 were deemed acceptable. Sample 15YP11 yielded a single age cluster from 47.5-55 Ma. Of the 98 ages, 56 concordant analyses were used to calculate a weighted mean of 52.43 \pm 0.55 Ma, MSWD=0.99, n=56, which we interpret as the maximum depositional age of the unit (Figs. 3,4,8).

Sample 15YP07 was collected from a stratigraphically higher Paleogene tuffaceous unit. 60 individual spots on a total of 60 zircons were ablated, of which 36 analyses were deemed acceptable. Sample 15YP07 yielded a single age cluster from 45.5-52 Ma. Of the 36 analyses, 20 concordant ages were used to calculate a weighted mean of 48.89 ± 0.71 Ma, MSWD=1.0, n=20, which we interpret as the maximum depositional age of the unit (Figs. 3,4,8).

Sample 15YP08 was collected from a Paleogene terrigenous sandstone located just below the appearance of granitic clasts. 150 individual spots on a total of 150 individual zircons were ablated, of which 129 analyses were deemed acceptable. Sample 15YP08 yielded a complex age spectrum, with the youngest analyses yielding single Jurassic and Triassic ages (n=2/129; 1.44%). Minor age clusters appear from 275-397.5 Ma (n=21/129; 16.3%), 439-482 Ma (n=11/129; 8.5%), 592-657 Ma (n=26/129; 20.1%), and 698-904 Ma (n=18/129; 13.9%). A more significant zircon age cluster is observed from 943.5-1087 Ma (n=28/129; 21.7%), followed by single U-Pb results from 1320-2600 Ma (n= 17/129; 13.2%) (Figs. 3,4,8).

Sample 15YP09 was collected from a Paleogene terrigenous sandstone containing granitic clasts. 150 individual spots on a total of 149 individual zircons were ablated, of which 137 analyses were deemed acceptable. Sample 15YP09 yielded a complex age spectrum, with minor zircon age clusters observed at 79-89 Ma (n=14/137; 10.2%), 210-258 Ma (n=5/137; 3.6%), 294-364 Ma (n=18/137; 13.1%) and 382-418 Ma (n=22/137; 16%). A major age cluster is observed from 536-711 Ma (n=30/137; 21.9%), followed by minor age clusters from 761-865 Ma (n=7/137; 5.1%) and 917-1145 Ma (n=19/137; 13.9%), single U-Pb results are observed from 1300-3490 Ma (n=17/137; 12.4%) (Figs. 3, 4,8).

4.2 Northern Saricakaya Basin

Sample 15YP04 was collected from a Jurassic sandstone. 137 individual spots on 137 individual zircons were ablated, of which 133 analyses were deemed acceptable. Sample 15YP04 yielded a single major age cluster from 312-352 Ma (n=113/133; 85.6%), with a tail consisting of three analyses with ages from 376-382.5 Ma (n=3/133; 2.3%) and a broad minor age peak from 544-697 Ma (n=13/133; 9.8%). Single zircon analyses yielded ages of 1050-3375 Ma (n=3/133; 2.25%) (Figs. 3,5,8).

Sample 15YP13 was collected from a Late Cretaceous volcanogenic unit. 127 spots on 127 individual zircons were ablated, of which 114 analyses were deemed acceptable. A single concordant analysis is observed at 66 Ma (n=1/114; 0.88%), followed by a major age cluster from 78-92.5 Ma (n=90/114; 80%), a minor age cluster from 100-115 Ma (n=6/114; 5.3%) and sporadic single analyses with ages ranging from 167-2464 Ma (n=16/114; 14%). Of the 90 youngest analyses, 8 were used to calculate a weighted mean of 79.04 ± 0.46 Ma, MSWD=0.83, which is a conservative interpretation of the units maximum depositional age due to the presence of a single ~66 Ma concordant analysis (Figs. 3,5,8).

Sample 15YP14 was collected from a Paleogene terrigenous sandstone. 140 individual spots on a total of 139 zircons were ablated, of which 130 analyses were deemed acceptable. Sample 15YP14 yielded a complex zircon age spectrum with a major age cluster from 75.5-86.5 Ma (n=33/130; 25.4%), a minor age cluster from 99.5-106.7 Ma (n=5/130; 3.8%), and a subsequent major and minor age cluster from 308-347.5 Ma (n=28/130; 21.5%) and 365.5-418 Ma (n=16/130; 12.3%). Minor age clusters were also observed from 446-475 Ma (n=8/130; 6.1%), 540-657 Ma (n=18/130; 13.8 %), 899-1128 Ma (n=8/130; 6.1 %), and 1865.5-2029.5 Ma

(n=7/130; 5.4 %). Single zircon analyses from 2475-3304 Ma (n=3/130; 2.4%) are also observed (Figs. 3,5,8).

4.3 Murdumu-Göynük Basin

Sample 15G001 was collected from a Late Cretaceous tuffaceous unit. 96 individual spots on a total of 83 zircons were ablated, of which 91 analyses were deemed acceptable. Analyses from sample 15G001 consistently clustered between 72 and 84 Ma. Of the 91 acceptable analyses, 50 were used to calculate a weighted mean of 77.8 ± 1.2 Ma, MSWD=0.47, n=50 (Figs. 3,6,8).

Sample 15G002 was collected from a Late Cretaceous conglomeratic unit. 147 spots on 111 individual zircons were ablated, of which 130 analyses were deemed acceptable. Sample 15G002 yielded major age clusters from 67-107.5 Ma (n=55/130; 42.6%) and 298.5-342.5 Ma (n=34/130; 25.75%). Minor age clusters appear at 363-461 Ma (n=10/130; 7.57%), 565-630 Ma (n=8/130; 6%), 935-997 Ma (n=5/130; 3.8%), and 1792-1999 Ma (n=6/130; 4.5%). Of the 55 analyses that define the youngest age peak, 15 ages were used to calculate a weighted mean of 76.05 ± 0.93 Ma, MSWD= 1.0, n=15, which we interpret as the units maximum depositional age (Figs. 3,6,8).

4.4 Orhaniye Basin

Sample 15KZ01 was collected from a metamorphosed Permo-Triassic sandstone. 100 spots on 95 individual zircons were ablated of which 93 analyses were deemed acceptable. Sample 15KZ01 yields a major Permo-Triassic age cluster from 225-270 Ma (n=42/93; 45.2%) and a smaller major age cluster in the Carboniferous from 305-405 Ma (n=37/93; 39.8%). A minor age peak is observed from 635-775 Ma (n=7/93; 7.5%). Single analyses have ages between 1040-2725 Ma (n=7/93; 7.5%). Of the 42 analyses that define the youngest age peak, 36

were used to calculate a weighted mean of 250.6 ± 4.2 Ma, MSWD= 0.99, n=36, which we interpret as the units maximum depositional age (Figs. 3,7,8).

5. Lu-Hf Isotopic Tracers

All zircon U-Pb samples were analyzed for Hf isotopes at The University of Arizona's geochronology facility; Arizona LaserChron (ALC). For samples with complex zircon age distributions approximately 50 zircons, representative of the samples minor and major age clusters were analyzed (e.g., Gehrels and Pecha, 2014). Zircons with concordant ages of interest were pre-screened using Cathodoluminescence (CL) imagery in order to select U-Pb spots located exclusively on zircon rims or cores. Hf isotopic analysis was achieved using a 50 μm beam diameter placed over the original U-Pb spot in order to ensure initial $^{176}\text{Hf}/^{177}\text{Hf}$ ratios being measured were representative of the isotopic composition measured during U-Pb analysis. To accommodate the analysis of smaller grains, the beam diameter was reduced to 40 μm . Data was collected using a Nu Plasma HR ICP-MS, coupled to a Photon Machines Analyte G2 laser equipped with a LeLEX cell. The ICP-MS is outfitted with 12 fixed Faraday detectors equipped with $3 \times 10^{11} \Omega$ resistors, 10 of which measure masses ^{171}Yb through ^{180}Hf . This configuration provides an enhanced signal to noise ratio for low intensity ion beams generated by laser ablation. The instrument has a factor of ~two improvement in the signal to noise ratio compared to standard $1 \times 10^{11} \Omega$ resistors, however is limited to a maximum signal intensity of 3.4 V on each Faraday collector. Hf-Yb-Lu solutions are introduced in Ar carrier gas via a Nu DSN-100 desolvating nebulizer in order to calibrate the machine prior to the analysis of unknowns. Minerals are analyzed via laser ablation, with He carrier gas mixed with Ar make-up gas before introduction to the plasma torch (See Arizona LaserChron 'Hf analytical methods description' webpage). Appendix 6 contains all Hf reference material analyses (organized in a single plot).

Age vs. ϵHf plots are commonly used to display Hf data, where:
 $\epsilon\text{Hf}_{(0)} = \left\{ \left[\frac{(^{176}\text{Hf}/^{177}\text{Hf})^0_{\text{sample}}}{(^{176}\text{Hf}/^{177}\text{Hf})^0_{\text{CHUR}}} \right] - 1 \right\} \times 10^4$ & $\epsilon\text{Hf}_{(t)} = \left\{ \left[\frac{(^{176}\text{Hf}/^{177}\text{Hf})^t_{\text{sample}}}{(^{176}\text{Hf}/^{177}\text{Hf})^t_{\text{CHUR}}} \right] - 1 \right\} \times 10^4$

$(^{176}\text{Hf}/^{177}\text{Hf})_{\text{CHUR}}^t / (^{176}\text{Hf}/^{177}\text{Hf})_{\text{CHUR}} - 1 \} \times 10^4$ (e.g., Vervoort, 2014). The $\varepsilon\text{Hf}(t)$ notation indicates the $^{176}\text{Hf}/^{177}\text{Hf}$ ratio at the time of crystallization based upon the evolution of the chondritic uniform reservoir (CHUR) at that time. Measurement precision is expressed as a 2σ average uncertainty. Furthermore external precision is approximately $\pm 2 \varepsilon$ units, as indicated by the distribution of reference material analyses (e.g., Bahlburg et al., 2009), with a predicted ~ 3.1 epsilon unit reproducibility based on 2σ uncertainties. We define εHf arrays according to Bahlburg et al., (2011), who define εHf values within 5 units of the depleted mantle (DM) as juvenile, values between 5 and 12 ε units below the depleted mantle as intermediate and anything $> 12 \varepsilon$ units below the depleted mantle as evolved.

6. Lu-Hf Results

In the following section samples are described from oldest to youngest (i.e., Mesozoic and Cenozoic) irrespective of their present geographic location. Age clusters within single samples are also described from oldest to youngest in terms of positive ϵ_{Hf} vs. age trends (ϵ_{Hf} pull-ups; increase in ϵ_{Hf} over time), negative ϵ_{Hf} vs. age trends (ϵ_{Hf} pull-downs; decrease in ϵ_{Hf} over time), and vertical ϵ_{Hf} vs. age trends (ϵ_{Hf} vertical arrays; no trend), where applicable. Positive ϵ_{Hf} vs. age trends (ϵ_{Hf} pull-ups) are significant of melting of a juvenile reservoir and are often interpreted to represent crustal thinning. Negative ϵ_{Hf} vs. age trends (ϵ_{Hf} pull-downs) are significant of melting of an intermediate or evolved reservoir and are often interpreted as crustal thickening or melting of ancient (evolved) crust. Vertical ϵ_{Hf} vs. age trends (ϵ_{Hf} vertical arrays) are significant of melting of a heterogeneous reservoir and are often interpreted to be a result of melts mixing with a highly age-variable upper plate (e.g., Ji et al., 2009). Results specific to individual spots are located in appendix 7.

Sample 15YP12 contains a single major zircon U-Pb age cluster and several minor age clusters, which evolve from [-6, -10] ϵ_{Hf} units from 360-345 Ma followed by ϵ_{Hf} evolution from [-10, -2.5] units from 345-310 Ma interpreted as a small ϵ_{Hf} pull-down followed by an ϵ_{Hf} pull-up (Fig. 9).

Sample 15KZ01 contains two major zircon age clusters, which evolve from [-7.5, -2.5] from 365-310 Ma and from [2.5, -2.5] from 260-220 Ma, interpreted as an ϵ_{Hf} pull-up followed by a pull-down. A single zircon plots at -15 ϵ_{Hf} units and is likely sourced from a different arc (Fig. 9).

Sample 15YP04 shows a single major cluster of zircon ages from 345-320 Ma which are characterized by ϵ_{Hf} values from [-10,-2] with a vertical ϵ_{Hf} -age trend, interpreted as a vertical array (Fig. 9).

Sample 15YP13 exhibits a dominant Late Cretaceous cluster of zircon ages and many older isolated single analyses. Older analyses plot between [-6, 8] ϵ_{Hf} units and are too disparate to identify meaningful trends. Zircons with 115-90 Ma crystallization ages exhibit ϵ_{Hf} values that evolve from [8, 2], followed by 80-75 Ma zircons with ϵ_{Hf} values that evolve from [-5, 5]. A single concordant zircon U-Pb age at ~66 Ma is defined by an ϵ_{Hf} value of [-2.5] (Fig. 9).

Sample 15G001 was collected from a Late Cretaceous tuff. A single zircon age cluster is observed from 84-75 Ma exhibiting ϵ_{Hf} values between [7.5, 0] (Fig. 9).

Sample 15G002 contains a cluster of zircon ages from 350-300 Ma which exhibit ϵ_{Hf} values of [0, -7.5], from 300-230 Ma ϵ_{Hf} values range from [-7.5, 2.5] followed by a decrease in ϵ_{Hf} values to [0] from 230-200 Ma. Zircons with crystallization ages from 85-75 Ma exhibit ϵ_{Hf} values that range from [5, -7] (Fig. 9).

Sample 15YP11 was collected from an Eocene Tuff and exhibits a single zircon age cluster from 55-47 Ma, which exhibit ϵ_{Hf} values from [2.5, 8]. Sample 15YP07 was collected from a stratigraphically higher Eocene tuff whose zircon ages clustered between 52-46 Ma and exhibit ϵ_{Hf} values from [4, 7.5] (Fig. 10).

Sample 15YP08 was collected from Eocene terrestrial sandstone and exhibits a complex zircon age distribution. Four zircons with crystallization ages between 350-330 Ma plot from [10, -6] ϵ_{Hf} units. Two zircons with crystallization ages of ~275 and ~245 Ma exhibit ϵ_{Hf} values of [-2] and [-3.5] (Fig. 10).

Sample 15YP09 collected from a stratigraphically higher Eocene terrestrial sandstone and also exhibits a complex zircon age distribution. Three zircons with crystallization ages ranging from 315-210 Ma exhibit ϵ_{Hf} values that range from [-5, 0]. Zircons with crystallization ages between 90-80 Ma exhibit ϵ_{Hf} values of [-12, -5] (Fig. 10).

Sample 15YP14 was collected from an Eocene terrestrial sandstone and exhibits a complex zircon age distribution. Five zircons with crystallization ages between 350-300 Ma exhibit ϵ_{Hf} values of [2, -2.5]. Three zircons with crystallization ages from 270-250 Ma exhibit ϵ_{Hf} values of [5, -5]. At 100 Ma three zircons with overlapping crystallization ages exhibit ϵ_{Hf} values of [5, 12.5], from 90-75 Ma zircons exhibit ϵ_{Hf} values of [-10, 6] (Fig. 10).

7. CUMULATIVE PLOTS

Under the assumption that zircons within detrital samples from the southern Saricakaya Basin, the northern Saricakaya Basin, the Murdunu-Göynük Basin, and the Orhaniye Basin formed by similar orogenic processes (i.e., Variscan, Cimmerian and Alpine orogenies), cumulative probability density and ϵ_{Hf} plots are constructed to describe the onset and duration of arc magmatism, as well as characterize changes in the contributing melt reservoir (i.e., crustal vs. mantle sources) during the closure of the Tethyan oceans (Fig. 11).

7.1 Cumulative Zircon PDP

Crystallization ages of 518/812 detrital zircons (64%) fall between 0-416 Ma, which brackets the orogenic events of interest. The Variscan Orogeny occurred from the Devonian-Carboniferous and yields 346/518 (66.8%) analyses, which are characterized by a minor Devonian (59/346; 17%) and major Carboniferous (287/346; 83%) age clusters. Permian dates are characterized by an increase in magmatism (30/518; 6%) prior to the Cimmerian Orogeny. In this study we loosely bracket the Cimmerian Orogeny as a Triassic event, however strictly speaking this orogeny lasted from 220-200 Ma (Okay et al., 2002); using this latter definition our samples only yield 3/518 analyses (0.6%). A broader Triassic definition however, (250-200 Ma) yields 34/518 grains (6.6%). From 200-115 Ma, a single analysis is observed (1/518; 0.2%). Zircons from the Alpine Orogeny yielded of 107/518 analyses (20.7%), which defines an increase in the abundance of zircons from 120-90 Ma (11/107; 10.3%), followed by a major age cluster (95/107; 88.8%) from 90-70 Ma. A single concordant U-Pb age is observed at ~66 Ma (1/107; 0.9%) (Fig. 11).

7.2 Cumulative Lu-Hf Plot

The shapes and colors of data points are based on their tectonic setting (Orange: Cenozoic Foreland Basin, Green: Late Mesozoic Forearc Basin, Blue: Middle Mesozoic Passive Margin, Purple: Early Mesozoic-Late Paleozoic Forearc Basin) and their lithology (Circle: Detrital, Triangle: Volcanic, Diamond: Basement). From 400-340 Ma an evolved horizontal trend at -7.5ϵ units is observed, detrital grains in Cenozoic sediments exhibit observable deviations from this trend between 380-360 Ma. From 340-300 Ma vertical arrays are observed, followed by an ϵ_{Hf} pull-up, which remains in the evolved regime from 300-250 Ma. From 120-80 Ma, an intermediate to evolved ϵ_{Hf} pull-down is observed. Grains from Cenozoic strata with overlapping crystallization ages exhibit similar trends, however deviate towards more juvenile ϵ_{Hf} values at 100 Ma and more evolved ϵ_{Hf} values between 85-80 Ma. From 80-75 Ma, ϵ_{Hf} values from Cretaceous and Eocene strata exhibit a sharp pull-up from evolved to intermediate. A single concordant detrital zircon plots in the evolved regime at ca. 66 Ma. Volcanogenic sediments with crystallization ages ranging from 55-45 Ma plot in the intermediate ϵ_{Hf} domains and exhibit a slight pull-up from 55-50 Ma followed by a minor pull-down from 50-45 Ma (Fig. 11).

8. SYNTHESIS

8.1 350-250 Ma

The Variscan Orogeny resulted in abundant calc-alkaline plutonism within the Sakarya Zone from 350-300 Ma, characterized by evolved ϵHf pull-ups and vertical arrays (Fig. 12 A). Zircon U-Pb and Hf data are consistent with a north dipping subduction zone along the southern margin of the Sakarya Zone (Fig. 12 B). Evolved ϵHf pull-ups and vertical arrays (Fig. 12 A) are interpreted to be either a result of granitoid emplacement into a heterogeneous basement consisting of metamorphosed marginal sediments of Gondwanan affinity; a mixture of accretionary sediments, exotic micro-terranes, and Devonian plutons, or the intrinsic nature of the detrital zircons which sampled a long lived cordillera (i.e., Chapman et al., 2017). Variscan shortening and regional metamorphism is also observed in the İstanbul Zone, however to a lesser degree (Okay and Tüysüz, 1999), suggesting inter-terrane proximity. An ϵHf pull-up from 300-250 Ma is observed in samples located within the Saricakaya and Murdunu-Göynük basins (Fig. 12 A). This weakly defined ϵHf pull-up may be significant of lithospheric and crustal thinning driven by slab roll-back, which resulted in the opening of the Intra-Pontide Ocean (Fig. 12 B).

8.2 250-200 Ma

Sample 15KZ01, collected from the Orhaniye Basin is spatially and chronologically unique to this study in that Cretaceous and older samples from near and around the Sakarya River Valley (Fig. 3) analyzed in this study do not yield similar zircon age dates. Triassic zircon U-Pb age clusters exhibit an ϵHf pull-down from 250-230 Ma, followed by a magmatic gap from 220-200 Ma (Fig. 12 A), interpreted as crustal thickening and flat-slab tectonism (Fig. 12 C), which resulted in arc shut-down related to underthrusting of the Karakaya Complex (Okay et al., 2002). The Triassic magmatic gap (250-200 Ma) observed in the Saricakaya and Murdunu-

Göynük basins also suggests down-going slab segmentation (e.g., ridge subduction; Ramos, 2009). Triassic metamorphism and shortening are also observed within the İstanbul Zone (Okay and Tüysüz, 1999), suggesting continued inter-terrane proximity.

8.3 200-115 Ma

Detrital zircon U-Pb data reveal a period of regional magmatic quiescence from >200-115 Ma (Fig. 12 A), consistent with a passive margin, flat slab subduction, a transform plate boundary, or some combination of these scenarios. Analysis of a Jurassic sandstone (15YP04) from the Saricakaya Basin (Fig. 8) unconformably overlying Sakarya Zone basement (Fig. 3) yields a unimodal age peak at ~325 Ma, with very few Precambrian grains. Zircon U-Pb data from samples collected from the underlying Karakaya Complex proximal to our study area by P. Ustaömer et al., (2011) and T. Ustaömer et al., (2016) yield abundant Triassic dates, which are absent in our Jurassic sample. This, and the presence of a regional transgression (Okay and Tüysüz, 1999) indicates that during the Jurassic-Early Cretaceous the Karakaya Complex and overlying Jurassic-Early Cretaceous sediments of the Central Sakarya Basin were still submerged and significant topography had yet to develop (Fig 12 C). Thus, our data suggests magmatic quiescence driven by any type of subduction and associated orogenesis is unlikely.

8.4 115-80 Ma

Late Cretaceous granitoids are located along the northern margin of the İstanbul Zone (~150 km north of the İAS; Fig. 2 inset) and absent within the Sakarya Zone as well as the Moesian and Scythian platforms (e.g., Banks and Robertson, 1997). The distribution of these granitoids is consistent with a north-dipping Late Cretaceous subduction zone along the southern margin of the Sakarya Zone and not the İstanbul Zone (c.f., Akbayram et al., 2016), implying these terranes sutured during or prior to pluton emplacement (i.e., closure of the Intra-Pontide

Ocean \geq 115 Ma; Fig. 12). Detrital zircon U-Pb data indicate magmatism re-initiated at \sim 115 Ma, and until 100 Ma is characterized by an intermediate to minimally evolved ϵ_{Hf} pull-down (Fig. 12 A), interpreted as crustal thickening of the Sakarya Zone. At 100 Ma a major deviation from this trend towards more juvenile ϵ_{Hf} values is observed, interpreted as initiation of an intra-oceanic subduction zone to the south (Fig. 12 D).

Blueschists of the Tavşanlı Zone contain arc detritus (Okay et al., 1996), experienced HP-LT metamorphism between 90-80 Ma (Okay et al., 1998; Sherlock et al., 1999; Sherlock and Kelly, 2002) and are overthrust by ophiolites with \sim 95 Ma metamorphic soles (van Hinsbergen et al., 2016). These data serve as evidence that from 100-80 Ma the Tavşanlı Zone was part of the down-going plate of an intra-oceanic subduction zone. The timing of these independent observations coincides with increasing magmatism and an ϵ_{Hf} pull-down to highly evolved ϵ_{Hf} values only observed in Late Cretaceous zircons analyzed from within Paleogene terrigenous units of the Sarıcakaya foreland basin (Fig. 12 A), in support of our interpretation that parts of the Tavşanlı Zone were incorporated into the mantle wedge at this time (Fig. 12 D). Zircons of similar age from within the northerly Murdunu-Göynük Basin exhibit a more subdued pull-down (Fig. 12 A), interpreted as continued crustal thickening along the northern subduction zone (Fig. 12 D).

8.5 80-66 Ma

From 80-66 Ma magmatism peaks, wanes, and ceases. After synchronous pull-downs of varying magnitudes, an ϵ_{Hf} pull-up is observed within Cretaceous units of the northern Murdunu-Göynük Basin (Fig. 12 A), interpreted as crustal thinning, a function of rapid slab roll-back which drove back-arc extension, opened the final portion of the Western Black Sea and subsequently translated the sutured Sakarya-İstanbul Zone (i.e., Western Pontides) to the south

(Fig. 12 E). A vertical array, observed in similar aged grains from the Saricakaya Basin is interpreted to represent intra-oceanic slab break-off, whose melts were sourced from both crustal and mantle reservoirs (Fig. 12 E). Vertical arrays produced from melt migration through heterogeneous continental crust can be ruled out due to the oceanic nature of the upper plate. A single zircon analyzed from a volcanoclastic horizon within the Saricakaya Basin (15YP13) yields a concordant U-Pb age of ~66 Ma, defines a small ϵ_{Hf} pull-down, and precedes total arc shut-off (Fig. 12 A). We interpret the 66 Ma ϵ_{Hf} pull-down followed by complete absence of zircon U-Pb ages to represent crustal thickening and total arc shut-off respectively, a result of transition to low angle subduction, and incipient collision between the Tavşanlı Zone and Western Pontides (Figs. 12 E).

8.6 < 65 Ma

From 65-55 Ma arc magmatism ceases (Fig. 12 A), interpreted as mantle wedge shut down within both subduction zones, a result of low angle subduction (Fig 12 F), which ultimately drove exhumation of basement units (i.e. Karakaya Complex \pm Variscan Granitoids). Interbedded tuffaceous horizons of the Saricakaya Basin yield maximum depositional ages of ~52 and 48 Ma (Fig. 10), serving as a maximum constraint to the age for overlying sediments. Maximum depositional ages of terrestrial strata within the Saricakaya Basin are notably unrepresentative of their true depositional age (Fig. 8), serving as further evidence for arc shut-off and syn-collisional tectonism (e.g., Gehrels 2014).

Zircon U-Pb coupled with Lu-Hf data enable discrimination of sources contributing to the Saricakaya basin fill, which include Carboniferous zircons that exhibit a range of evolved ϵ_{Hf} values from the Söğüt Granite (P. Ustaömer et al., 2011; this study), sporadic Jurassic zircons from the Murdunu Formation of the Central Sakarya Basin (e.g., Altiner et al., 1991) or possibly

the Central Pontides (Gücer et al., 2016), Campanian zircons that exhibit highly evolved ϵ_{Hf} values from the Tavşanlı Zone, and moderately evolved-intermediate ϵ_{Hf} values from the Central Sakarya Basin. Precambrian and older grains are likely recycled from ancient Laurasian passive margin strata that mantled the Pontides prior to orogenesis, whose primary sources are the İstanbul Zone (P. Ustaömer et al., 2005) and the Eastern European Craton (Okay et al., 2013), which were deposited into the Central Sakarya Basin and reworked into the Sarıcakaya Basin during collision (Fig. 12 F). It is also likely that a portion of Precambrian grains within the Sarıcakaya basin are sourced from Gondwanan passive margin strata whose primary sources are Pan African terranes and older African cratons (e.g., Kröner and Şengör, 1990).

Volcaniclastic samples collected from the Sarıcakaya Basin exhibit zircon crystallization ages ranging between 52-48 Ma, which overlap with ages from granitoids of the Tavşanlı Zone (Harris et al., 1994; Okay et al., 1998) and may be genetically related to Paleogene plutonism within the Sakarya and İstanbul Zones (Fig 2; inset). The older of the two samples (52 Ma) exhibits a jump defined by the youngest forearc detrital grain (66 Ma; 15YP13) from evolved to minimally intermediate followed by a small pull-down from 52-48 Ma, which we interpret as a second episode of slab break-off followed by renewed underthrusting and crustal thickening (e.g., DeCelles et al. 2011; Fig 12 F). Return to underthrusting is also supported by the presence of the southeast directed northern Söğüt thrust that juxtaposes Sakarya Zone basement structurally above Paleogene foreland basin sediments (Fig. 3). The Neogene southward sweep of basic magmatism (e.g., Dilek and Altunkaynak, 2009) was likely a result of this syn-collisional crustal thickening, which ultimately lead to lithospheric delamination (Fig. 12 F).

9. CONCLUSIONS

Detrital zircon U-Pb geochronology in conjunction with Lu-Hf isotopes serve as a streamlined approach for testing and refining tectonic models and complements paleomagnetic, geophysical, petrologic, and field based datasets, all of which must ultimately be employed in order to understand the geology of a region. Our findings suggest that an Andean-style subduction zone located on the southern margin of the Sakarya Zone along with a southern intra-oceanic subduction zone synchronously facilitated the closure of the İzmir-Ankara Ocean from at least 100 Ma to at least 75 Ma. Elements of previous models are integral to the tectonic history of the region, but cannot independently explain NW Turkey's tectonic evolution. In light of our U-Pb and Lu-Hf datasets and synthesis, a viable Alpine tectonic model involves the following:

120-100 Ma:

- Initiation of Andean-style subduction along the southern margin of the Pontides.
- Suturing of the İstanbul and Sakarya Zones (Western Pontides)
- Initiation of İzmir-Ankara intra-oceanic subduction

100-80 Ma:

- South-directed obduction of İzmir-Ankara oceanic lithosphere
- HP-LT metamorphism of the Tavşanlı Zone
- Melting of the Tavşanlı Zone

80-65 Ma:

- Slab roll-back of the marginal Sakarya subduction zone
- Opening of the Western Black Sea
- Slab break-off within the İzmir Ankara intra-oceanic subduction zone
- Incipient collision

55 Ma-45 Ma:

- Collision of the Tavşanlı and Sakarya Zones
- Slab break-off within the marginal Sakarya Zone subduction zone
- Emplacement of Early Eocene calc-alkaline plutons within the Tavşanlı Zone ±Sakarya and İstanbul Zones
- Sakarya Zone crustal thickening

References:

- Açıkalm, S. Vellekoop, J. Ocakoğlu, F. Yılmaz, I. Ö. Smit, J. Altner, S. Ö. Goderis, S. Vonhof, H. Speijer, R.P. Woelders, L. and Fornaciari, E. (2015). Geochemical and palaeontological characterization of a new K-Pg Boundary locality from the Northern branch of the Neo-Tethys: Mudurnu–Göynük Basin, NW Turkey. *Cretaceous Research*, v. 52, p. 251-267.
- Akbayram, K. Okay, A. I. and Satır, M. (2013). Early Cretaceous closure of the intra-Pontide Ocean in western Pontides (northwestern Turkey). *Journal of Geodynamics*, v. 65, p. 38-55.
- Akbayram, K. Şengör, A. C. & Özcan, E. (2016). The evolution of the Intra-Pontide suture: implications of the discovery of late Cretaceous–early Tertiary melanges. *Geological Society of America Special Papers*, v. 525, SPE525-18.
- Altner, D. Koçyiğit, A. Farinacci, A. Nicosia, U. and Conti, M. A. (1991). Jurassic, Lower Cretaceous stratigraphy and paleogeographic evolution of the southern part of north-western Anatolia. *Geologica Romana*, v. 28, p. 13-80.
- Aydin, Y. (1974). Etude petrographique et geochemique de la partie centrale du Massif d'Istranca (Turquie) (Doctoral dissertation).
- Aydinçakir, E. Şen, C. (2013). Petrogenesis of the post-collisional volcanic rocks from the Borçka (Artvin) area: implications for the evolution of the Eocene magmatism in the Eastern Pontides (NE Turkey). *Lithos*, v. 172–173, p. 98–117.
- Bahlburg, H. Vervoort, J.D. DuFrane, S.A. Bock, B. Augustsson, C. and Reimann, C. (2009). Timing of crust formation and recycling in accretionary orogens: Insights learned from the western margin of South America. *Earth-Science Reviews*, v. 97, p. 215–241.
- Bahlburg, H. Vervoort, J.D. DuFrane, S.A. Carlotto, V. Reimann, C. and Cardenas, J. (2011). The U–Pb and Hf isotope evidence of detrital zircons of the Ordovician Ollantaytambo Formation, southern Peru, and the Ordovician provenance and paleogeography of southern Peru and northern Bolivia. *Journal of South American Earth Sciences*, v. 32, p. 196–209
- Banks, C. J. & Robinson, A. G. (1997). Mesozoic strike-slip back-arc basins of the western Black Sea region. *Regional and petroleum, geology of the Black Sea and surrounding region: AAPG Memoir 68*, p. 53-62.
- Bozkurt, E. Winchester, J. A. and Satır, M. (2013). The Çele mafic complex: evidence for Triassic collision between the Sakarya and İstanbul Zones, NW Turkey. *Tectonophysics*, v. 595, p. 198-214.
- Candan, O. Çetinkaplan, M. Oberhänsli, R. Rimmelé, G. and Akal, C. (2005). Alpine high-P/low-T metamorphism of the Afyon Zone and implications for the metamorphic evolution of Western Anatolia, Turkey. *Lithos*, v. 84, p. 102-124.
- Çelik, Ö. F. Delaloye, M. and Feraud, G. (2006). Precise ^{40}Ar – ^{39}Ar ages from the metamorphic sole rocks of the Tauride Belt Ophiolites, southern Turkey: implications for the rapid cooling history. *Geological Magazine*, v. 143, p. 213-227.
- Chapman, J. B. Ducea, M. N. Kapp, P. Gehrels, G. E., and DeCelles, P. G. (2017). Spatial and temporal radiogenic isotopic trends of magmatism in Cordilleran orogens, *Gondwana Research*.
- Coney, P. J. Jones, D. L. and Monger, J. W. (1980). Cordilleran suspect terranes. *Nature*, v. 28, p. 329-333.

- Daşçı, H. T. O. Parlak, N. Nurlu, and Z. Billor (2014). Geochemical characteristics and age of metamorphic sole rocks within a Neotethyan ophiolitic mélangé from Konya region (central southern Turkey), *Geodinamica Acta*, v. 27, p. 223-243.
- DeCelles, P. G. Kapp, P. Quade, J. & Gehrels, G. E. (2011). Oligocene–Miocene Kailas basin, southwestern Tibet: Record of postcollisional upper-plate extension in the Indus-Yarlung suture zone. *Geological Society of America Bulletin*, v. 123, p. 1337-1362.
- Dickinson, W. R. and Seely, D. R. (1979). Structure and stratigraphy of forearc regions. *AAPG Bulletin*, v. 63, p. 02-31.
- Dilek, Y. and Altunkaynak, Ş. (2009). Geochemical and temporal evolution of Cenozoic magmatism in western Turkey: mantle response to collision, slab break-off, and lithospheric tearing in an orogenic belt. *Geological Society of London Special Publications*, v. 31, p. 213-233.
- Dilek, Y. and Sandvol, E. (2009). Seismic structure, crustal architecture and tectonic evolution of the Anatolian-African plate boundary and the Cenozoic orogenic belts in the Eastern Mediterranean region. *Geological Society, London, Special Publications*, v. 327, p. 127-160.
- Elmas, A. and Yiğitbaş, E. 2001, Ophiolite emplacement by strike-slip tectonics between the Pontide Zone and the Sakarya Zone in northwestern Anatolia, Turkey. *International Journal of Earth Sciences*, v. 90, p. 257–269.
- Elmas, A. and Yiğitbaş, E. 2005, Comment on Tectonic evolution of the Intra- Pontide suture zone in the Armutlu Peninsula, NW Turkey, by Robertson and Ustaömer. *Tectonophysics*, v. 405, p. 213–221,
- Ersoy, E. Y. and Palmer, M. R. (2013). Eocene-Quaternary magmatic activity in the Aegean: implications for mantle metasomatism and magma genesis in an evolving orogeny. *Lithos*, v. 180, p. 05-24.
- Fedo, C. M., Sircombe, K. N. & Rainbird, R. H. (2003). Detrital zircon analysis of the sedimentary record. *Reviews in Mineralogy and Geochemistry*, v. 53, p. 277-303.
- Gehrels, G. (2014). Detrital zircon U-Pb geochronology applied to tectonics. *Annual Review of Earth and Planetary Sciences*, v. 42, p.127-149.
- Gehrels, G. and Pecha, M. (2014). Detrital zircon U-Pb geochronology and Hf isotope geochemistry of Paleozoic and Triassic passive margin strata of western North America. *Geosphere*, v. 10, p. 49-65.
- Genç, C. Ş. And Tüysüz, O. (2010). Tectonic setting of the Jurassic bimodal magmatism in the Sakarya Zone (Central and Western Pontides), Northern Turkey: a geochemical and isotopic approach. *Lithos*, v. 118, p. 005–111.
- Göncüoğlu, M.C. and Erendil, M. (1990). Pre–late Cretaceous tectonic units of Armutlu Peninsula, in Proceedings of the 8th Petroleum Congress: Ankara, *Turkish Association of Petroleum Geologists, Chamber of Petroleum Engineers*, v. 1, p. 161–168 [in Turkish].
- Göncüoğlu, M. C., Turhan, N. Şentürk, K. Özcan, A. Uysal, Ş. & Yaliniz, M. K. (2000). A geotraverse across northwestern Turkey: tectonic units of the Central Sakarya region and their tectonic evolution. *Geological Society of London Special Publications*, v. 173, p. 139-161.
- Göncüoğlu, M.C. Gürsu, S. Tekin, U.K. and Köksal, S. (2008). New data on the evolution of the Neotethyan oceanic branches in Turkey: Late Triassic ridge spreading in the Intra-Pontide branch: *Ophioliti*, v. 33, p. 153–164.
- Görür, N. and Okay, A. I. (1996). A fore-arc origin for the Thrace Basin, NW Turkey. *Geologische Rundschau*, v. 85, p. 662-668.

- Görür, N. (1997). Cretaceous syn- to postrift sedimentation on the southern continental margin of the western Black Sea Basin. *Regional and petroleum, geology of the Black Sea and surrounding region: AAPG Memoir 68*, p. 227–240.
- Gücer, M. A. Arslan, M. Sherlock, S. and Heaman, L. M. (2016). Permo-Carboniferous granitoids with Jurassic high temperature metamorphism in Central Pontides, Northern Turkey. *Mineralogy and Petrology*, v. 110, p. 943-964.
- Harris, N. B. Kelley, S. & Okay, A. I. (1994). Post-collision magmatism and tectonics in northwest Anatolia. *Contributions to Mineralogy and Petrology*, v. 117, p. 241-252.
- Hawkesworth, C. J., & Kemp, A. I. S. (2006). Using hafnium and oxygen isotopes in zircons to unravel the record of crustal evolution. *Chemical Geology*, v. 226, p. 144-162.
- Jackson, S. E. Pearson, N. J. Griffin, W. L. and Belousova, E. A. (2004). The application of laser ablation-inductively coupled plasma-mass spectrometry to in situ U–Pb zircon geochronology. *Chemical Geology*, v. 211, p. 47-69.
- Ji, W. Q. Wu, F. Y. Chung, S. L. Li, J. X. and Liu, C. Z. (2009). Zircon U–Pb geochronology and Hf isotopic constraints on petrogenesis of the Gangdese batholith, southern Tibet. *Chemical Geology*, v. 262, p. 229-245.
- Ketin, I. (1966). Tectonic units of Anatolia. *Bulletin of Mineralogical Resources*, v. 66, p. 23-34.
- Koçyiğit, A. Özkan, S. Rojay, B. (1988). Examples from the fore arc basin remnant at the active margin of Northern Neo-Tethys: emplacement age of the Anatolian Nappe. *METU Journal of Pure and Applied Sciences*, v.21, p. 183–210.
- Koçyiğit, A. (1991). An example of an accretionary forearc basin from northern Central Anatolia and its implications for the history of subduction of Neo-Tethys in Turkey. *Geological Society of America Bulletin*, v. 103, p. 22–36.
- Kröner, A. and Şengör, A. M. C. (1990). Archean and Proterozoic ancestry in late Precambrian to early Paleozoic crustal elements of southern Turkey as revealed by single-zircon dating. *Geology*, v. 18, p. 1186-1190.
- Licht, A. Coster, P., Ocakoğlu, F. Campbell, C. Métais, G. Mulch, A. Taylor, M. Beard, K. C. (2017). Tectono-stratigraphy of the Orhaniye Basin, Turkey: Implications for collision chronology and Paleogene biogeography of central Anatolia. *Journal of Asian Earth Sciences*.
- Maffione, M. Hinsbergen, D. J. Gelder, G. I. Goes, F. C. and Morris, A. (2017). Kinematics of Late Cretaceous subduction initiation in the Neo-Tethys Ocean reconstructed from ophiolites of Turkey, Cyprus, and Syria. *Journal of Geophysical Research: Solid Earth*.
- McLean, N. M. Bowering, J. F. and Gehrels, G. (2016). Algorithms and software for U-Pb geochronology by LA-ICPMS. *Geochemistry, Geophysics, Geosystems*, v. 17, p. 2480-2496.
- Moix, P. Beccalotto, L. Kozur, H. W. Hochard, C. Rosselet, F. and Stampfli, G. M. (2008). A new classification of the Turkish terranes and sutures and its implication for the paleotectonic history of the region. *Tectonophysics*, v. 451, p. 7-39.
- Nairn, S. P. Robertson, A. H. Ünlügenç, U. C. Tasli, K. and İnan, N. (2013). Tectonostratigraphic evolution of the Upper Cretaceous–Cenozoic central Anatolian basins: an integrated study of diachronous ocean basin closure and continental collision. *Geological Society of London Special Publications*, v. 372, p. 343-384.

- Oczlon, M. S. (2006). Terrane map of Europe. Geologisch-Paläontologisches Institut Ruprecht-Karls-Universität.
- Okay, A. İ. (1984a). Distribution and characteristics of the north-west Turkish blueschists. *Geological Society of London Special Publications*, v. 17, p. 455-466.
- Okay, A. İ. (1986). High-pressure/low-temperature metamorphic rocks of Turkey. *Geological Society of America Memoirs*, v. 164, p. 333-347.
- Okay, A. İ. Şengör, A. C. and Görür, N. (1994). Kinematic history of the opening of the Black Sea and its effect on the surrounding regions. *Geology*, V. 22, p. 267-270.
- Okay, A. İ. Satir, M. Maluski, H. Siyako, M. Monie, P. Metzger, R. and Akyüz, S. (1996). Paleo- and Neo-Tethyan events in northwestern Turkey: geologic and geochronologic constraints. *World and Regional Geology*, v.1, p. 420-441.
- Okay, A. İ. Harris, N. B. and Kelley, S. P. (1998). Exhumation of blueschists along a Tethyan suture in northwest Turkey. *Tectonophysics*, v. 285, p. 275-299.
- Okay, A. İ., and Tüysüz, O. (1999). Tethyan sutures of northern Turkey. Geological Society, London, Special Publications, 156(1), 475-515.
- Okay, A. İ. (2000). Was the Late Triassic orogeny in Turkey caused by the collision of an oceanic plateau? *Geological Society, of London Special Publications*, 173(1), 25-41.
- Okay, A. İ. Tansel, İ. and Tüysüz, O. (2001). Obduction, subduction and collision as reflected in the Upper Cretaceous–Lower Eocene sedimentary record of western Turkey. *Geological Magazine*, v. 138, p. 117-142.
- Okay, A. İ. Monod, O. & Monié, P. (2002). Triassic blueschists and eclogites from northwest Turkey: vestiges of the Paleo-Tethyan subduction. *Lithos*, v. 64, p. 155-178.
- Okay, A. İ. and Satir, M. (2006). Geochronology of Eocene plutonism and metamorphism in northwest. *Geodinamica Acta*, v. 19, p. 251-266.
- Okay, A. İ. Tüysüz, O. Satir, M. Özkan-Altiner, S. Altiner, D. Sherlock, S. and Eren, R. H. (2006). Cretaceous and Triassic subduction-accretion, high-pressure–low-temperature metamorphism, and continental growth in the Central Pontides, Turkey. *Geological Society of America Bulletin*, v. 118, p. 1247-1269.
- Okay, A. İ. (2008). Geology of Turkey: a synopsis. *Anschnitt*, v. 21, p. 19-42.
- Okay, A. İ. and Whitney, D. L. (2010). Blueschists, eclogites, ophiolites and suture zones in northwest Turkey: a review and a field excursion guide. *Ophioliti*, v. 35, p. 131-172.
- Okay, A. İ. Sunal, G. Sherlock, S. Altiner, D. Tüysüz, O. Kylander–Clark, A. R. and Aygül, M. (2013). Early Cretaceous sedimentation and orogeny on the active margin of Eurasia: Southern Central Pontides, Turkey. *Tectonics*, v. 32, p.1247-1271.
- Önen, A. P. and Hall, R. (1993). Ophiolites and related metamorphic rocks from the Kütahya region, north-west Turkey. *Geological Journal*, v. 28, p. 399-412.
- Önen, A. P. (1993). Ophiolites and related metamorphic rocks from the Kütahya region, NW Turkey. PhD thesis, University of London.

- Önen, A. P. (2003). Neotethyan ophiolitic rocks of the Anatolides of NW Turkey and comparison with Tauride ophiolites. *Journal of the Geological Society*, v. 160, p. 947-962.
- Özcan, Z. Okay, A. Özcan, E. Hakyemez, A. and Altiner, S. (2012). Late Cretaceous-Eocene geological evolution of the Pontides based on new stratigraphic and palaeontologic data between the Black Sea coast and Bursa (NW Turkey). *Turkish Journal of Earth Sciences*, v. 21, p. 933-960.
- Öztürk, Y. Y. Helvacı, C. and Satir, M. (2012). Geochemical and isotopic constraints on petrogenesis of the Beypazarı granitoid, NW Ankara, Western Central Anatolia, Turkey. *Turkish Journal of Earth Sciences*, v. 21, p. 53-77.
- Patchett, P. J. and Tatsumoto, M. (1980). Hafnium isotope variations in oceanic basalts. *Geophysical Research Letters*, v. 7, p. 1077-1080.
- Pecha, M. E. Gehrels, G. E. McClelland, W. C. Giesler, D. White, C. and Yokelson, I. (2016). Detrital zircon U-Pb geochronology and Hf isotope geochemistry of the Yukon-Tanana terrane, Coast Mountains, southeast Alaska. *Geosphere*, v.12, p. 1556-1574.
- Pickett, E. A. and Robertson, A. H. (1996). Formation of the Late Palaeozoic–Early Mesozoic Karakaya Complex and related ophiolites in NW Turkey by Palaeotethyan subduction–accretion. *Journal of the Geological Society*, v.153, p. 995-1009.
- Pourteau, A. Sudo, M. Candan, O. Lanari, P. Vidal, O. Oberhänsli, R. (2013), Neotethys closure history of Anatolia: insight from ^{40}Ar – ^{39}Ar geochronology and P–T estimation in high-pressure metasediments. *Journal of Metamorphic Geology*.
- Pourteau, A. Oberhänsli, R. Candan, O. Barrier, E. and Vrielynck, B. (2015). Neotethyan closure history of western Anatolia: a geodynamic discussion. *International Journal of Earth Science*, v. 105, p. 203-224.
- Ramos, V.A. (2009). Anatomy and global context of the Andes: main geologic features and the Andean orogenic cycle. *Geological Society of America Memoirs*, v. 204, p. 31–65.
- Robertson, A. H. F. Dixon, J. E. Brown, S. Collins, A. Morris, A. Pickett, E. Sharp, I. and Ustaömer, T. (1996). Alternative tectonic models for the Late Palaeozoic–Early Tertiary development of Tethys in the Eastern Mediterranean region. *Geological Society of London Special Publications*, v. 105, p. 239-263.
- Robertson, A. H. Ustaömer, T. Pickett, E. A. Collins, A. S. Andrew, T. and Dixon, J. E. (2004). Testing models of Late Palaeozoic–Early Mesozoic orogeny in Western Turkey: support for an evolving open-Tethys model. *Journal of the Geological Society*, v. 161, p. 501-511
- Robertson, A.H.F. and Ustaömer, T. (2000). Tectonic evolution of the Intra-Pontide suture zone in the Armutlu Peninsula, NW Turkey: *Tectonophysics*, v. 381, p. 175–209.
- Robertson, A. H. Parlak, O., & Ustaömer, T. (2012). Overview of the Palaeozoic–Neogene evolution of neotethys in the Eastern Mediterranean region (southern turkey, cyprus, Syria). *Petroleum Geoscience*, v. 18, p. 381-404.
- Salaün, G. Pedersen, H.A. Paul, A. Farra, V. Karabulut, H., Hatzfeld, D., Papazachos, C., Childs, D.M. and Pequegnat, C. (2012). High-resolution surface wave tomography beneath the Aegean-Anatolia region: constraints on upper-mantle structure. *Geophysical Journal International*, v. 190, p.406-420.
- Şengör, C. and Yilmaz, Y. (1981). Tethyan evolution of Turkey: a plate tectonic approach: *Tectonophysics*, v. 75.3 p. 181-241.
- Şengör, A. C. (1984a). The Cimmeride orogenic system and the tectonics of Eurasia. *Geological Society of America Special Papers*, v. 195, p. 1-74.

- Şengör, A. M. C. Altner, D. Cin, A. Ustaömer, T. and Hsü, K. J. (1988). Origin an assembly of the Tethyside orogenic collage at the expense of Gondwana Land. *Geological Society of London Special Publications*, v. 37, p. 119-181.
- Sguigna, A. P. Larabee, A. J. and Waddington, J. C. (1982). The half-life of ^{176}Lu by a γ - γ coincidence measurement. *Canadian Journal of Physics*, v. 60, p. 361-364.
- Sircombe, K. N. and Stern, R. A. (2002). An investigation of artificial biasing in detrital zircon U-Pb geochronology due to magnetic separation in sample preparation. *Geochimica et Cosmochimica Acta*, v. 66, p. 2379-2397.
- Sláma, J. Košler, J. Condon, D. J. Crowley, J. L. Gerdes, A. Hanchar, J.M. Horstwood, M.S. Morris, G.A. Nasdala, L. Norberg, N. and Schaltegger, U. (2008). Plešovice zircon—a new natural reference material for U–Pb and Hf isotopic microanalysis. *Chemical Geology*, v. 249, p. 01-35.
- Sherlock, S. Kelley, S. Inger, S. Harris, N. and Okay, A. (1999). 40 Ar-39 Ar and Rb-Sr geochronology of high-pressure metamorphism and exhumation history of the Tavşanlı Zone, NW Turkey. *Contributions to Mineralogy and Petrology*, v. 137, p. 46-58.
- Sherlock, S. and Kelley, S. (2002). Excess argon evolution in HP–LT rocks: a UVLAMP study of phengite and K-free minerals, NW Turkey. *Chemical Geology*, v. 182, p. 619-636.
- Shin, T. A. Catlos, E. J. Jacob, L. and Black, K. (2013). Relationships between very high pressure subduction complex assemblages and intrusive granitoids in the Tavşanlı Zone, Sivrihisar Massif, central Anatolia. *Tectonophysics*, v. 595, p. 183-197.
- Speciale, P. A. Catlos, E. J. Yıldız, G. O. Shin, T. A. and Black, K. N. (2012). Zircon ages from the Beypazarı granitoid pluton (north central Turkey): tectonic implications. *Geodinamica Acta*, v. 25, p. 162-182.
- Stampfli, G. M. (2000). Tethyan oceans. *Geological Society of London Special Publications*, v. 173, p. 1- 23.
- Stampfli, G., and Borel, G., 2002, A plate tectonic model for the Paleozoic and Mesozoic constrained by dynamic plate boundaries and restored synthetic oceanic isochrones: *Earth and Planetary Science Letters*, v. 196.1 p. 17-33.
- Stampfli, G. M. and Kozur, H. (2006). Europe from the Variscan to the Alpine cycles. *Geological Society of London Special Publications*, v. 32, p. 57-82.
- Tüysüz, O. (1999). Geology of the Cretaceous sedimentary basins of the Western Pontides. *Geological Journal*, v. 34, p. 75-93.
- Ustaömer, P.A. Mundil, R. and Renne, P. R. (2005). U/Pb and Pb/Pb zircon ages for arc-related intrusions of the Bolu Massif (W Pontides, NW Turkey): evidence for Late Precambrian (Cadomian) age. *Terra Nova*, v. 17, p. 215-223.
- Ustaömer, P. A. Ustaömer, T. Gerdes, A. and Zulauf, G. (2011). Detrital zircon ages from a Lower Ordovician quartzite of the Istanbul exotic terrane (NW Turkey): evidence for Amazonian affinity. *International Journal of Earth Sciences*, v. 100, p. 23-41.
- Ustaömer, P. A. Ustaömer, T. & Robertson, A. (2012). Ion probe U-Pb dating of the Central Sakarya basement: a peri-Gondwana terrane intruded by late Lower Carboniferous subduction/collision-related granitic rocks. *Turkish Journal of Earth Sciences*, v. 21, p. 905-932.

- Ustaömer, T. and Robertson, A. H. F. (1994). Late Palaeozoic marginal basin and subduction-accretion: the Palaeotethyan Küre complex, central Pontides, northern Turkey. *Journal of the Geological Society*, v. 15, p. 291-305.
- Ustaömer, T. Ustaömer, P. A. Robertson, A. H. and Gerdes, A. (2016). Implications of U–Pb and Lu–Hf isotopic analysis of detrital zircons for the depositional age, provenance and tectonic setting of the Permian–Triassic Palaeotethyan Karakaya Complex, NW Turkey. *International Journal of Earth Sciences*, v. 105, p. 7-38.
- van Hinsbergen, D. J. Kaymakci, N. Spakman, W. and Torsvik, T. H. (2010b). Reconciling the geological history of western Turkey with plate circuits and mantle tomography. *Earth and Planetary Science Letters*, v. 297, p. 674-686.
- van Hinsbergen, D. J. Maffione, M. Plunder, A. Kaymakçı, N. Ganerød, M. Hendriks B. W. Hendriks, B.W. Corfu, F. Gürer, D. Gelder, G.I. Peters, K. and McPhee, P. J. (2016). Tectonic evolution and paleogeography of the Kırşehir Block and the Central Anatolian Ophiolites, Turkey. *Tectonics*, v. 35, p. 983-1014.
- Vermeesch, P. (2012). On the visualisation of detrital age distributions. *Chemical Geology*, v.312-313, p. 190-194.
- Vervoort, J. (2013). Lu-Hf Dating: The Lu-Hf Isotope System. *Encyclopedia of Scientific Dating Methods*, p. 1-20.
- White, W. M. (2013). Geochemistry (1st edition, v.1). Retrieved from <https://www.imwa.info/geochemistry/Chapters/Chapter07.pdf>
- Wotzlaw, J.F., Schaltegger, U., Frick, D.A., Dungan, M.A., Gerdes, A., and Günther, D., 2013, Tracking the evolution of large-volume silicic magma reservoirs from assembly to supereruption: *Geology*, v. 41, p. 867-870.
- Wu, F. Y. Ji, W. Q. Liu, C. Z. and Chung, S. L. (2010). Detrital zircon U–Pb and Hf isotopic data from the Xigaze fore-arc basin: constraints on Transhimalayan magmatic evolution in southern Tibet. *Chemical Geology*, v. 271, p. 13-25.
- Yılmaz, Y. Genç, Ş.C. Yiğitbaş, E. Bozcu, M. and Yılmaz, K. (1995), Geological evolution of the late Mesozoic continental margin of northwestern Anatolia. *Tectonophysics*, v. 243, p. 155–171.
- Yılmaz, Y. Tuysuz, O. Yigitbas, E. Genc, S. C. and Şengör, A. M. C. (1997). Geology and Tectonic Evolution of the Pontides. *Regional and Petroleum Geology of the Black Sea and Surrounding Region, AAPG Memoir 68*, p. 183-226.
- Yılmaz, Y. Tüysüz, O. Yigitbas, E. Can Genç, S. and Şengör, A. M. C. (1998). Geology and tectonic evolution of the Pontides. *Memoirs-American Association of Petroleum Geologists*, p. 183-226.
- Zepf, V. (2013). Rare Earth Elements: What and where they are. In *Rare Earth Elements. SpringerBerlin Heidelberg*, p. 11-39.

Figure Captions:

Figure 1.

Terrane map of the Eastern Mediterranean. Pontide terranes include the Strandja Zone, the İstanbul Zone, the Sakarya Zone, and the Eastern Pontides. Anatolides include the Tavşanlı Zone, Central Anatolian Crystalline Complex, Afyon Zone and the Menderes Massif. The Taurides are located to the south and east. Major suture zones include the Intra-Pontide suture, the İzmir Ankara Erzincan suture, and the Bitlis suture. Red lines indicate active structures, the white box indicates the mapping area, yellow ellipses represent sample locations and dark green shapes indicate the approximate locations of ophiolites. The bottom right inset represents the approximate locations of volcanic rocks (modified from Okay and Tüysüz, 1999; Ozclon, 2006; van Hinsbergen et al. 2016 & maps from ITU).

Figure 2.

Conceptual illustration of models describing the Alpine closure history of the Neotethyan oceans in NW Turkey. TB: Tauride Block, AFZ: Afyon Zone, TVZ: Tavşanlı Zone, SZ: Sakarya Zone, L: Lithosphere, OC: Oceanic Crust. See text for details.

Figure 3.

Geologic map (modified from Okay et al. 2002), synthetic stratigraphic column (modified from Moix et al. 2008 and Yilmaz et al. 1997), and schematic cross-section of the Sakarya of the Sakarya River Valley.

Figure 4.

Concordia plots and probability density plots (PDP's) super-imposed on histograms from samples collected within the footwall of the Söğüt Thrust, where the x-axis is age in millions of years (log-scale) and the y-axis is number of analyses. Maximum depositional ages are indicated within concordia plots when applicable. Large black ellipses and red circles indicate areas that have been enlarged in order to facilitate qualitative data evaluation.

Figure 5.

Concordia plots and probability density plots (PDP's) super-imposed on histograms from samples collected within the hanging-wall of the Söğüt Thrust, where the x-axis is age in millions of years (log-scale) and the y-axis is number of analyses. Maximum depositional ages are indicated within concordia plots when applicable. Large black ellipses and red circles indicate areas that have been enlarged in order to facilitate qualitative data evaluation.

Figure 6.

Concordia plots and probability density plots (PDP's) super-imposed on histograms from samples collected from north of the Sakarya River Valley near the town of Göynük, where the x-axis is age in millions of years (log-scale) and the y-axis is number of analyses. Maximum depositional ages are indicated within concordia plots when applicable. Large black ellipses and red circles indicate areas that have been enlarged in order to facilitate qualitative data evaluation.

Figure 7.

Concordia plots and probability density plots (PDP's) super-imposed on histograms from a sample collected from northwest of Ankara where the-x axis is age in millions (log-scale) of years and the y-axis is number of analyses. Maximum depositional ages are indicated within concordia plots when applicable. Large black ellipses and red circles indicate areas that have been enlarged in order to facilitate qualitative data evaluation.

Figure 8.

Zircon PDP's from samples collected from the Saricakaya, Murdunu-Göynük & Orhaniye Basins. Insets on detrital zircon plots with ages from 0-450 Ma and bracket magmatism during the opening and closure of the Tethyan Oceans. Major orogenies are indicated by colored columns (Blue: Cadomian, Red: Variscan, Green: Cimmerian, Yellow: Alpine). Tuffs analyzed along with maximum depositional ages (MDA's) in this study are in the right-hand corner.

Figure 9.

Age vs. Epsilon Hf plots for all Mesozoic samples. Vertical error bars represent estimated ~3 epsilon unit reproducibility (± 1.5) and horizontal errors bars represent estimated zircon U-Pb uncertainties at 2σ or $\pm 2.5\%$. See text for detailed descriptions.

Figure 10.

Age vs. Epsilon Hf plots for all Cenozoic samples. Vertical error bars represent estimated ~3 epsilon unit reproducibility (± 1.5) and horizontal errors bars represent estimated zircon U-Pb uncertainties at 2σ ($\pm 2.5\%$). See text for detailed descriptions.

Figure 11.

Cumulative detrital zircon U-Pb and Lu-Hf plots for data collected in the Saricakaya, Murdunu-Göynük and Orhaniye Basins. Color of data points indicate the depositional age of a sample; orange-Paleogene, green-Cretaceous, blue-Jurassic, and purple-Paleozoic. The shape of a data points indicates the lithology of the sample; circle-detrital, triangle-volcanic, and diamond-basement.

Figure 12.

Cumulative detrital zircon U-Pb and Lu-Hf plots and conceptual Variscan-Alpine models of the tectonic evolution of NW Turkey. Color of data points indicate the depositional age of a sample; orange-Paleogene, green-Cretaceous, blue-Jurassic, and purple-Paleozoic. The shape of a data points indicates the lithology of the sample; circle-detrital, triangle-volcanic, and diamond-basement. TB; Tauride Block, AFZ; Afyon Zone, TVZ; Tavşanlı Zone, LN; Lycian Nappes, KC; Karakaya Complex, SZ; Sakarya Zone, ISZ; İstanbul Zone, SKB; Saricakaya Basin, GB; Göynük Basin, L; Lithosphere, OC; Oceanic Crust, Eop; Eocene plutons, Pp; Permian plutons, GB; Göynük Basin, OB; Orhaniye Basin. See section 8 for details.

Figures

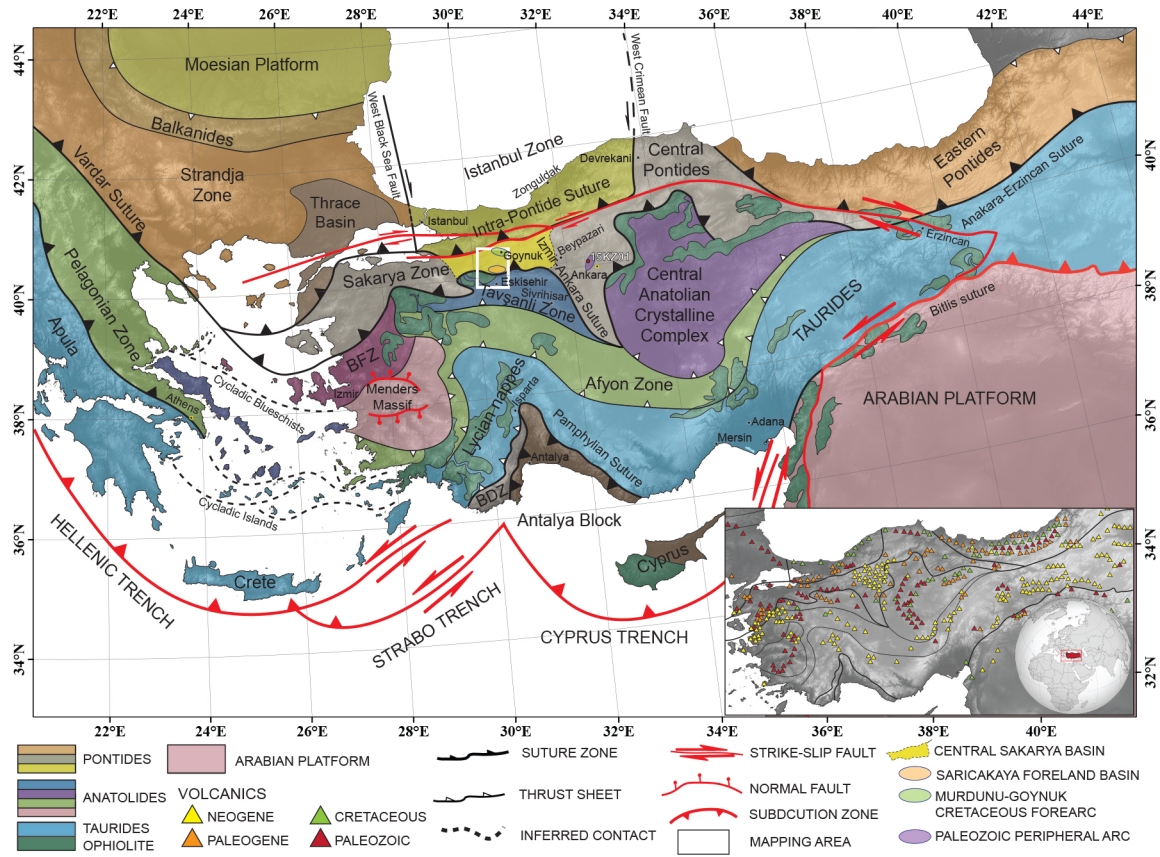


Figure 1

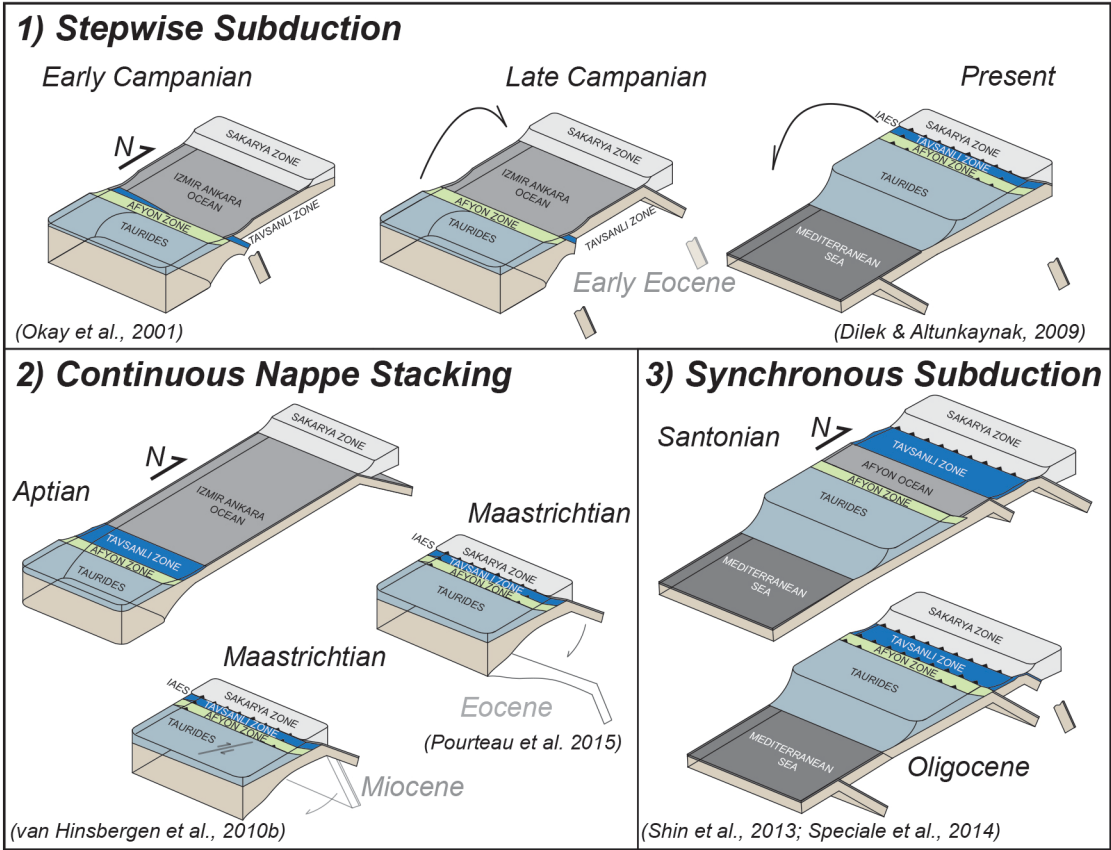


Figure 2

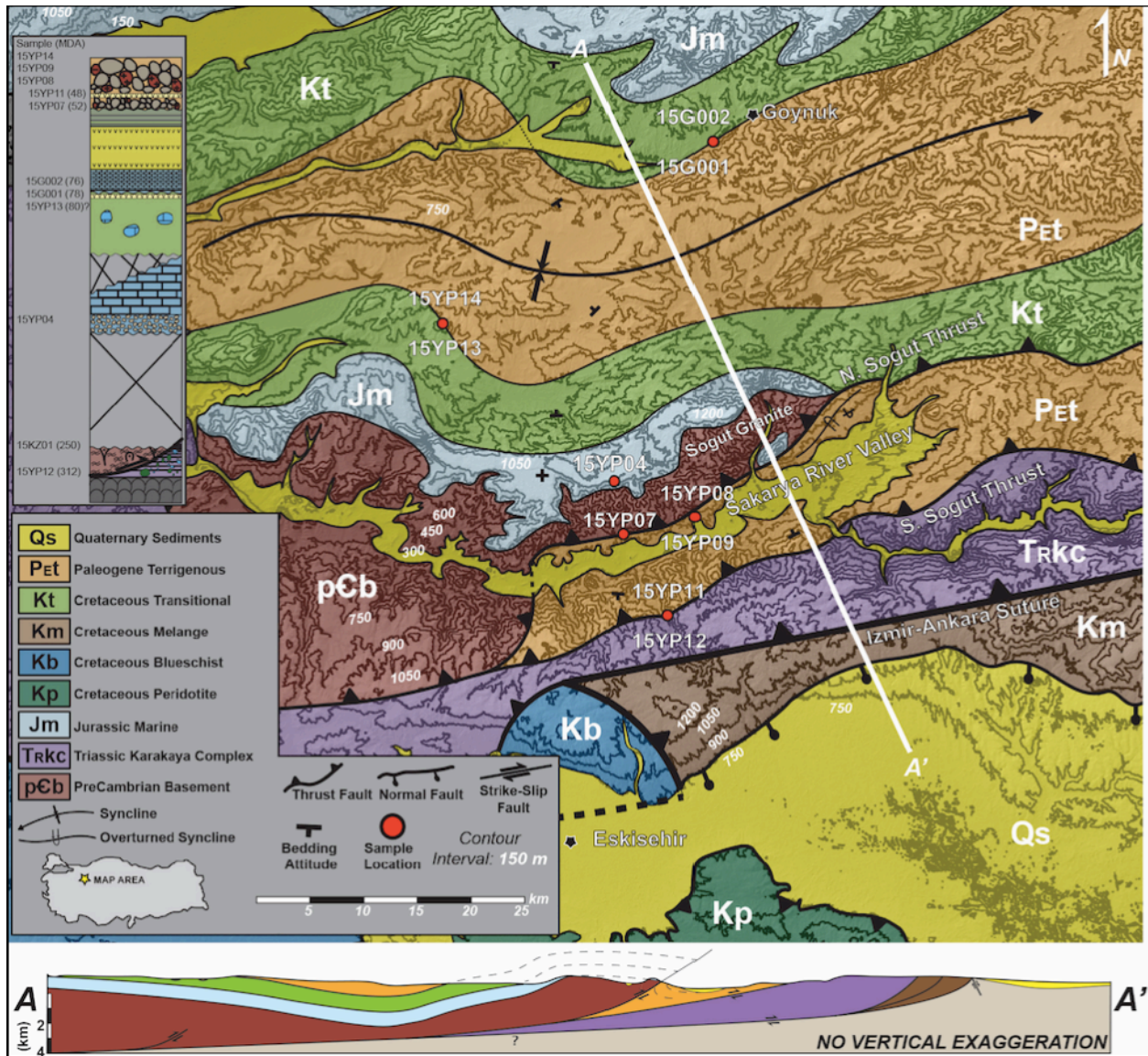
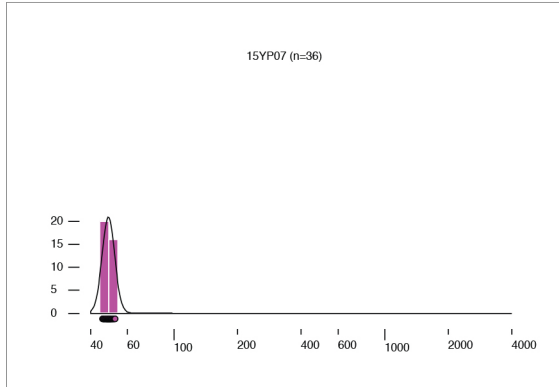
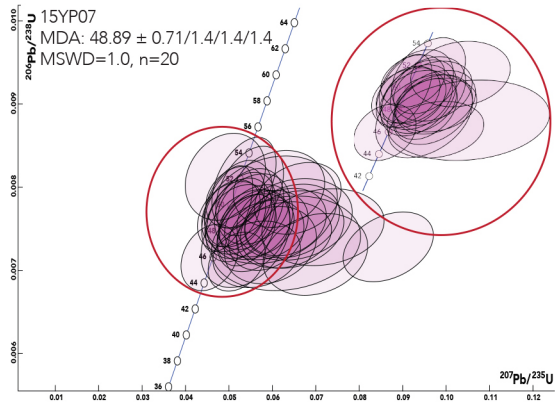
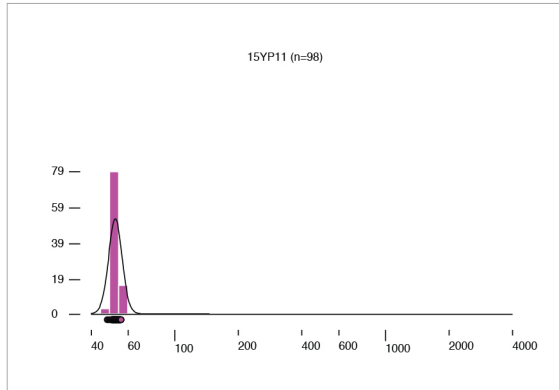
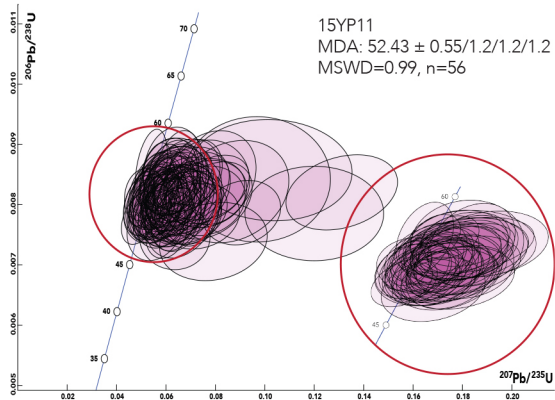
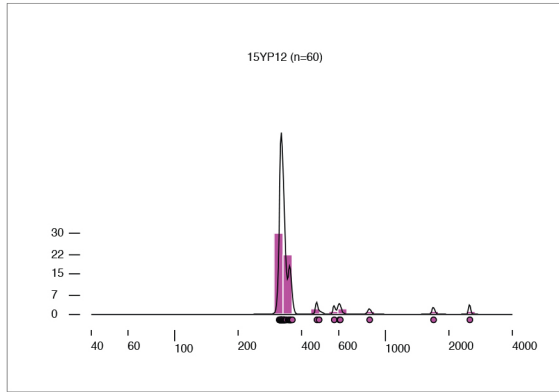
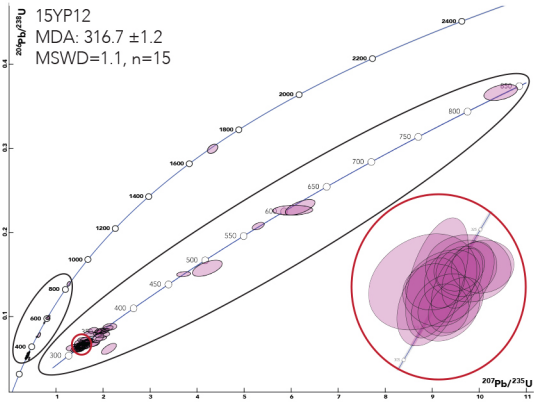


Figure 3



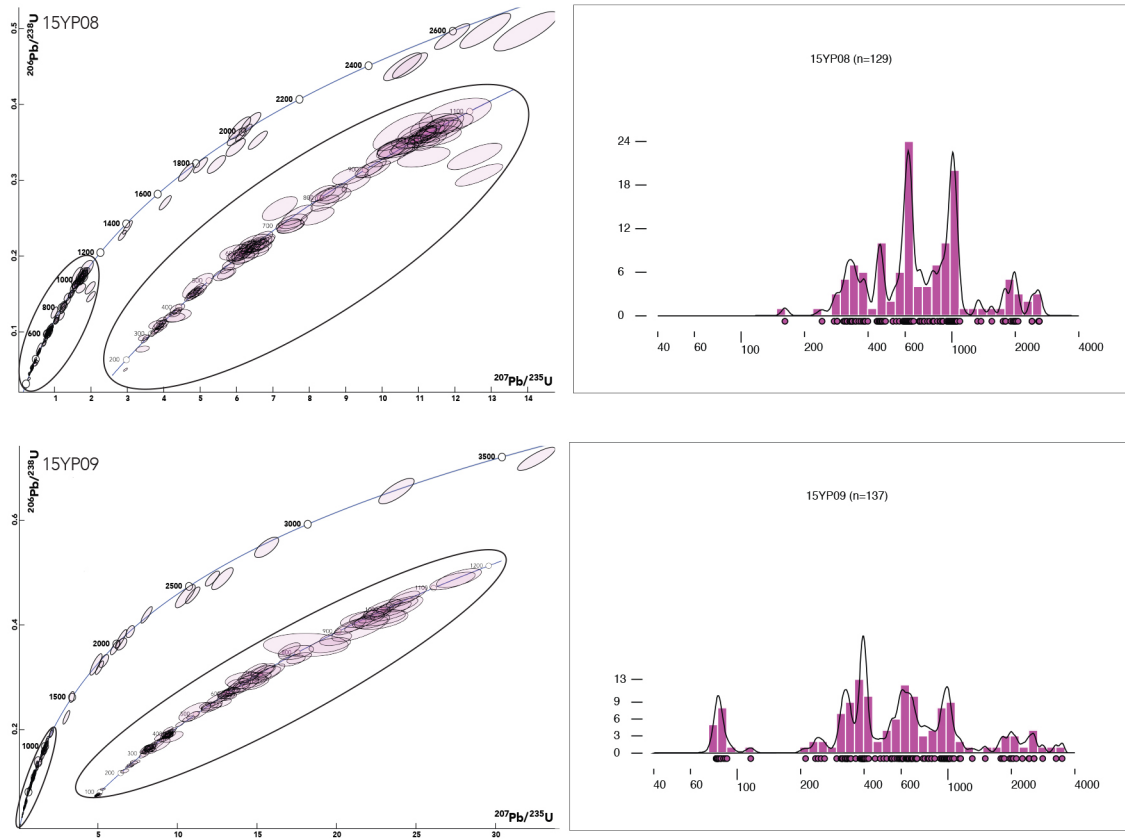


Figure 4

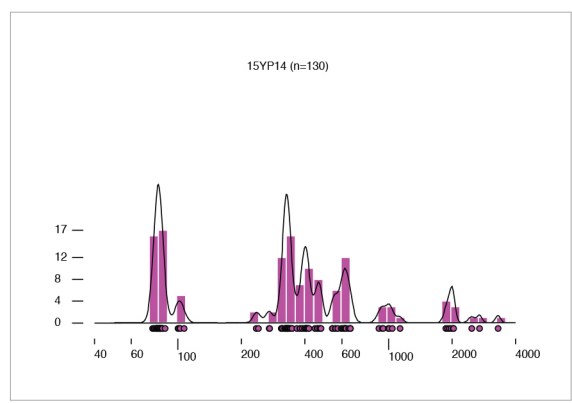
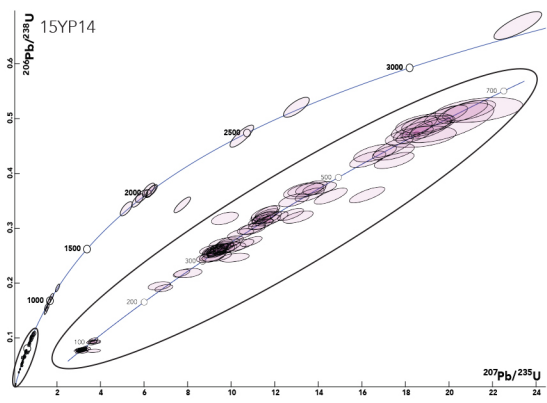
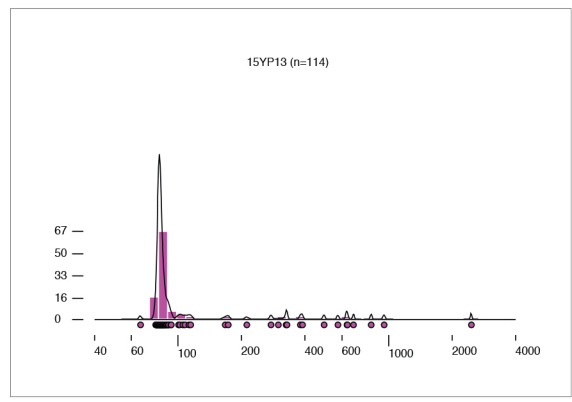
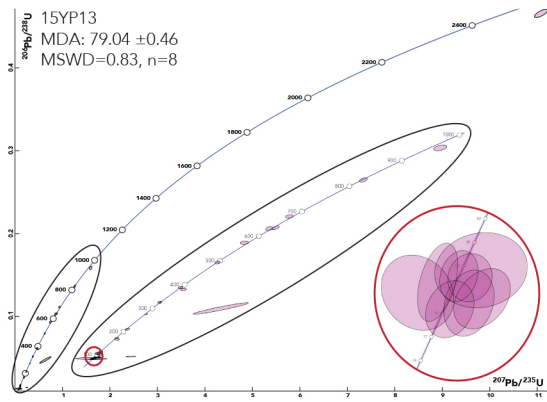
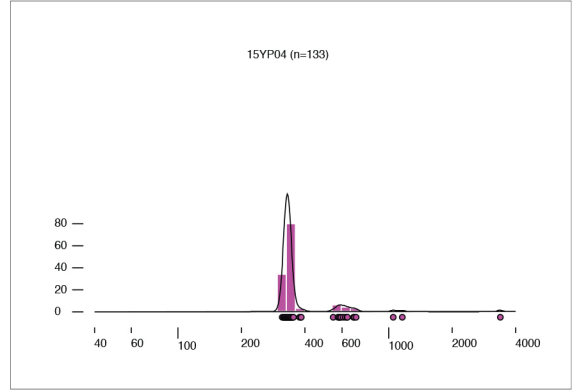
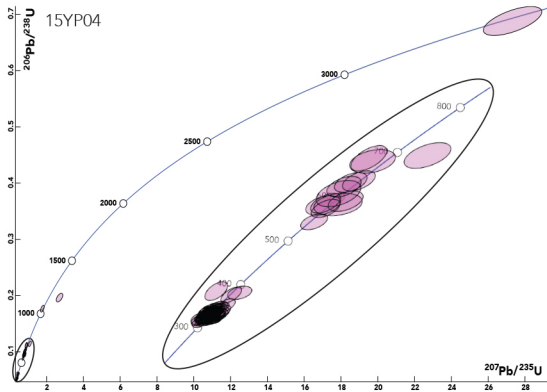


Figure 5

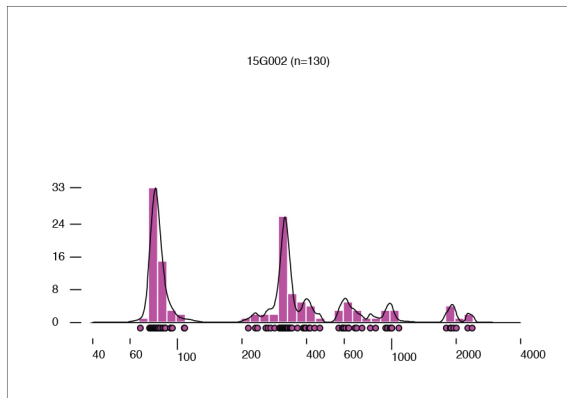
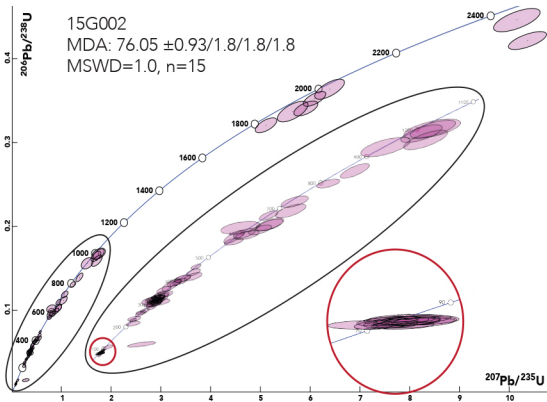
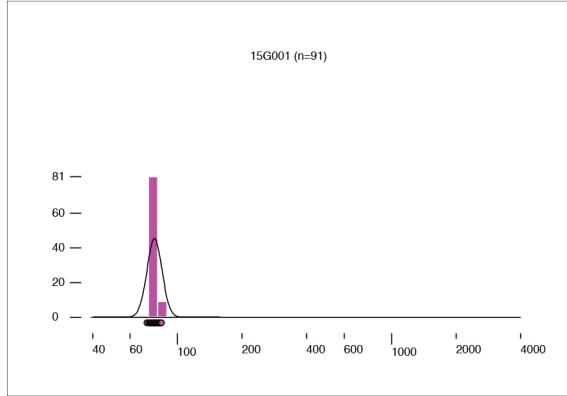
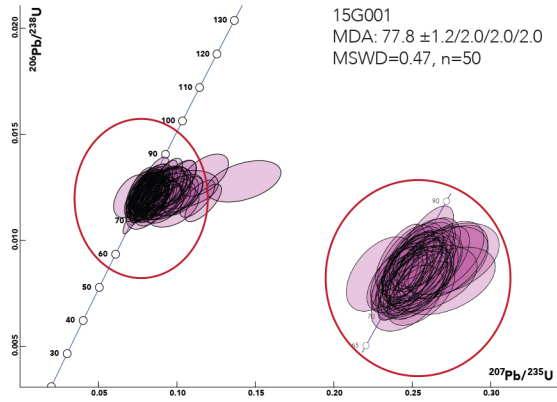


Figure 6

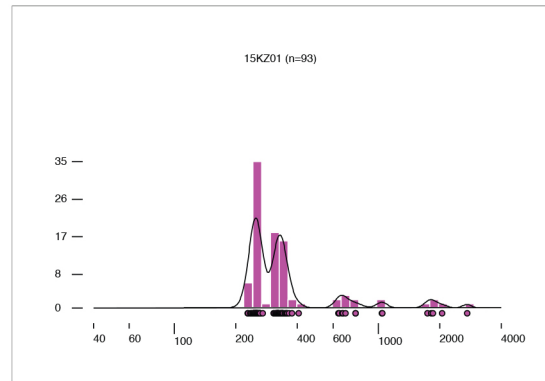
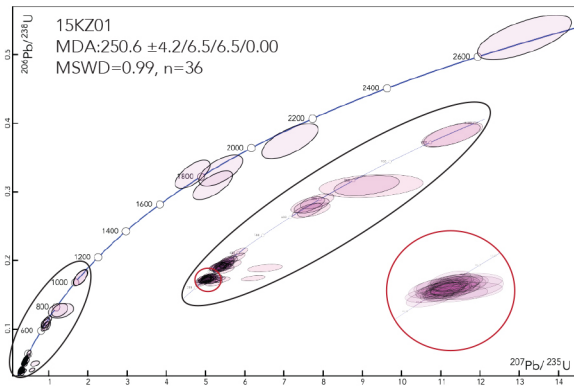


Figure 7

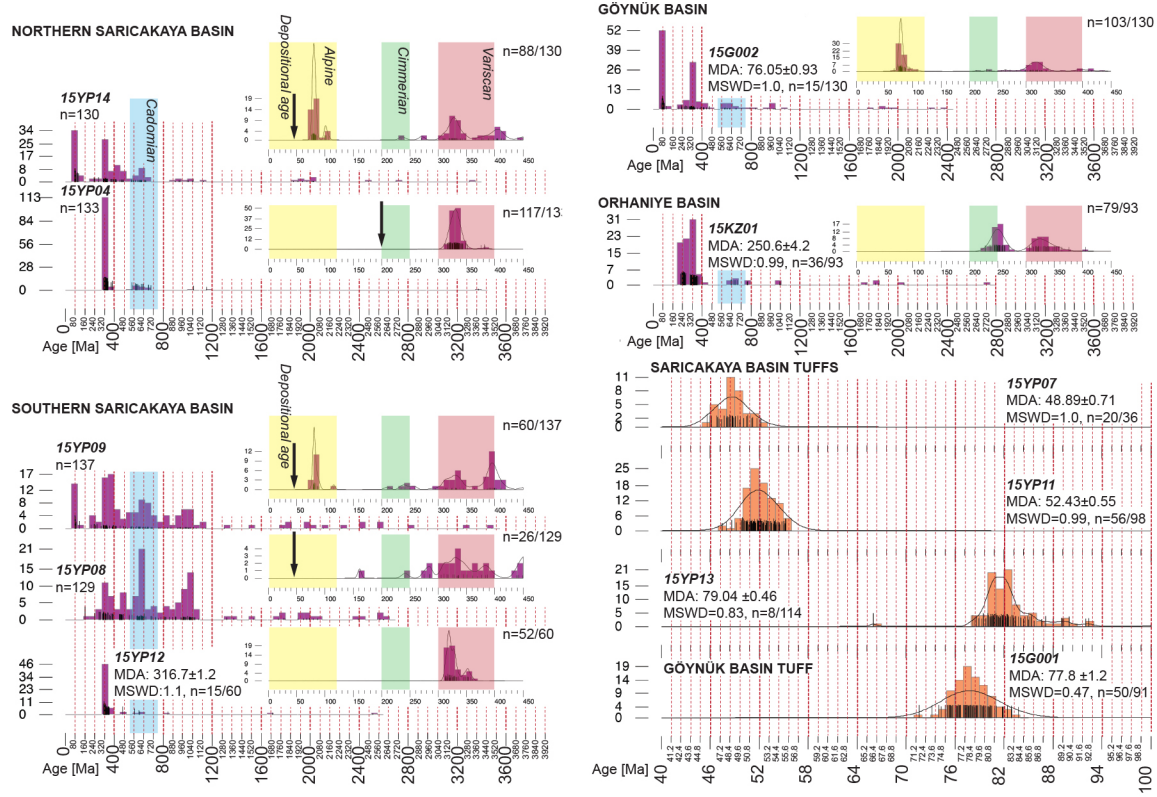


Figure 8

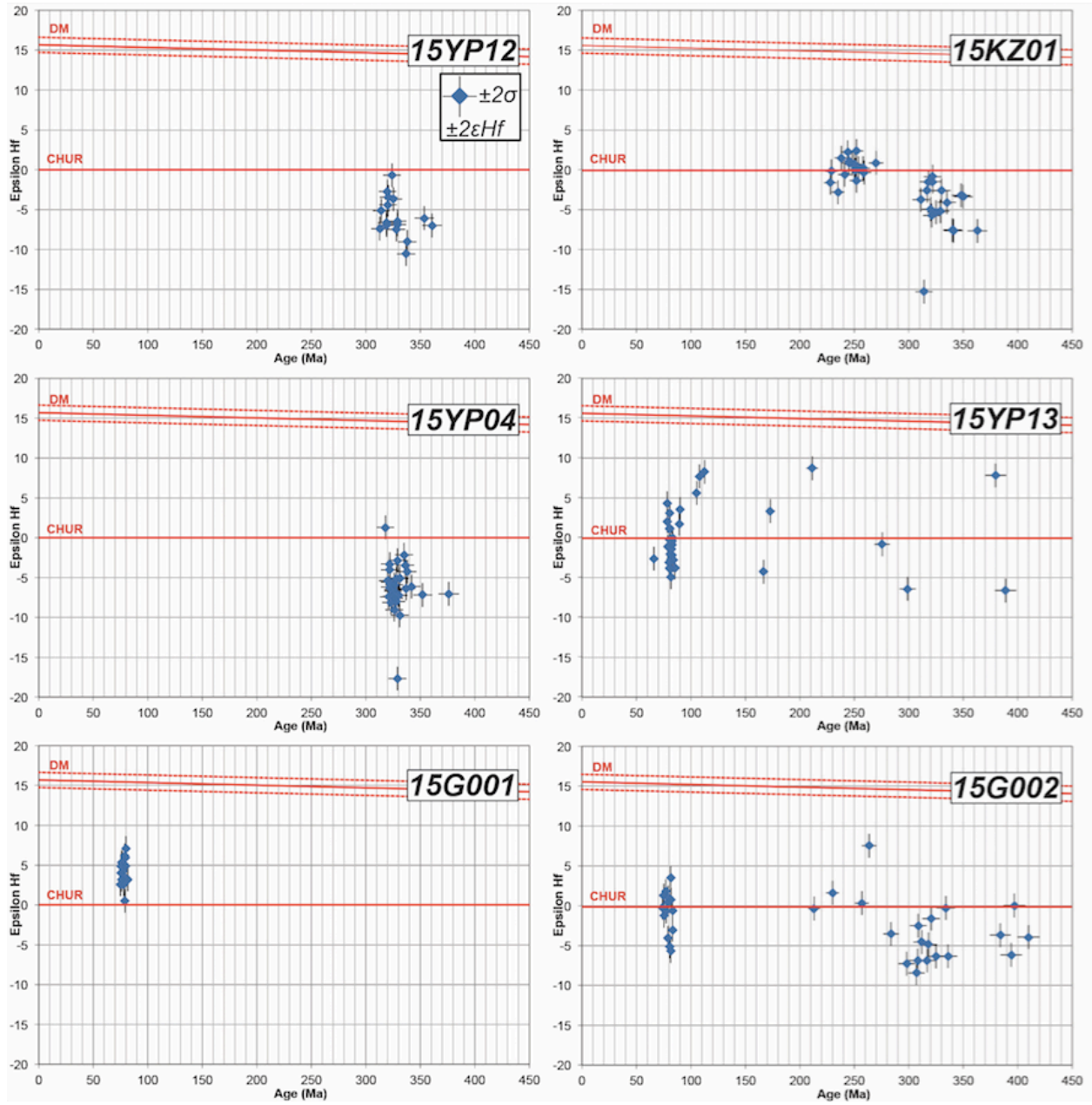


Figure 9

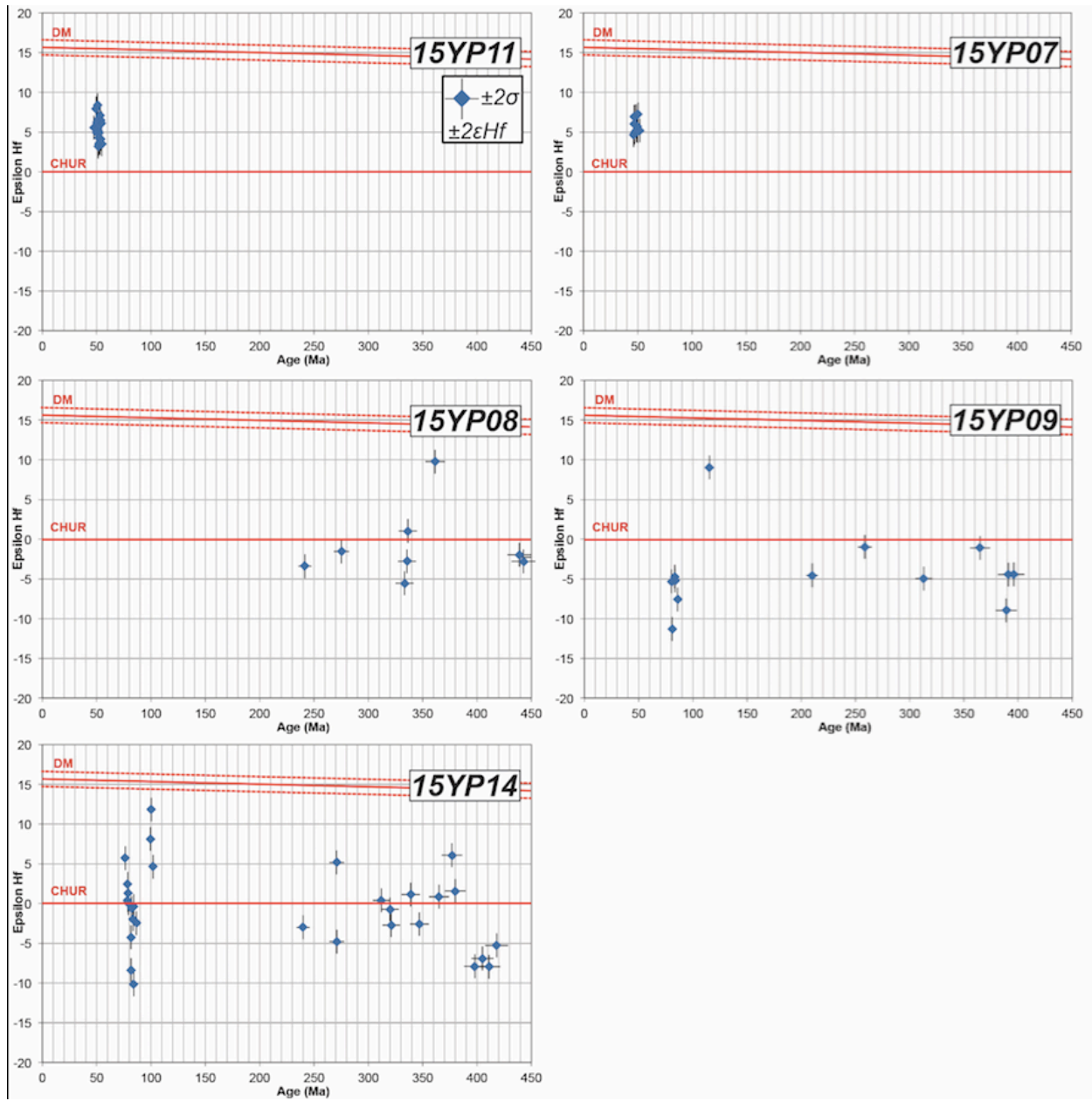


Figure 10

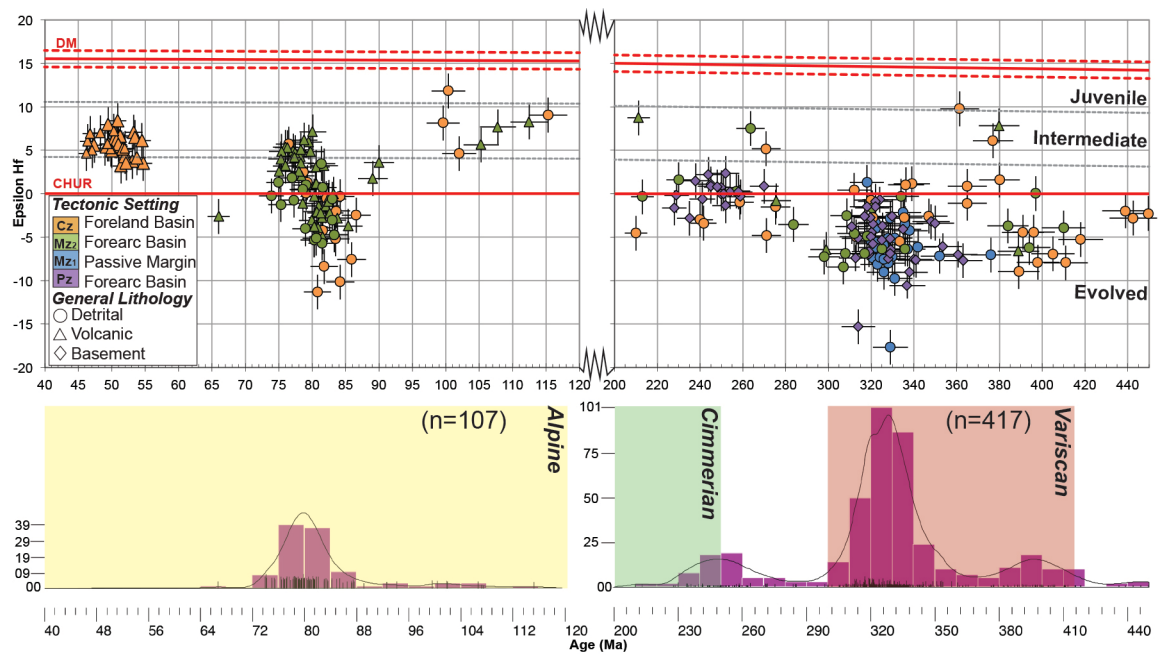


Figure 11

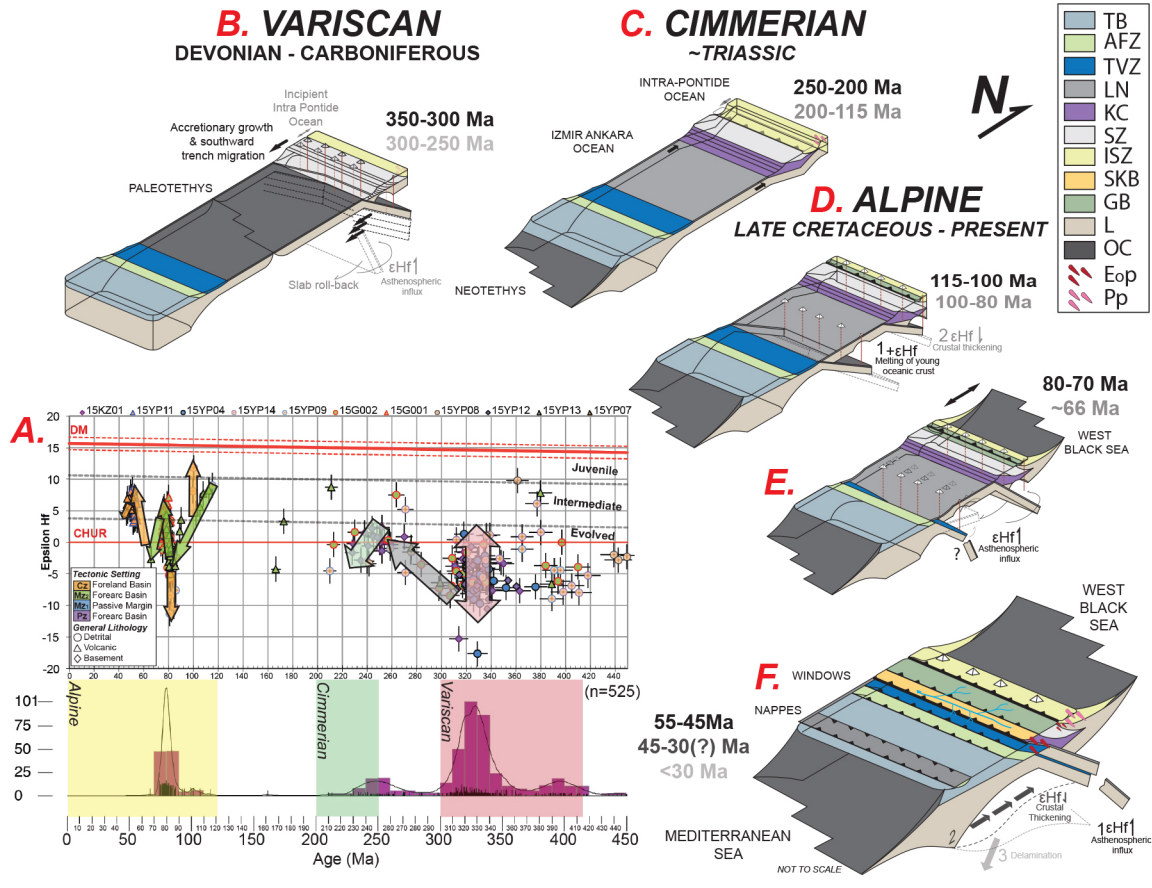


Figure 12

Appendices

Appendix 1: Detailed Terrane and Basin Descriptions

2.1 PONTIDES

2.1.1 Strandja Zone

The Strandja Zone, also known as the İstranca Massif (Aydin, 1974) is located in northwesternmost Turkey (Fig. 1). The southern margin of the terrane is juxtaposed against the Sakarya Zone via the E/W striking Vardar Suture. To the west the Vardar Suture strikes northwest and wraps around the Strandja Zone, which in turn is in tectonic contact with the southerly Pelagonian Zone. To the east, the Strandja Zone is truncated by the north striking, dextral West Black Sea Fault. To the southeast, its contact with the Istanbul Zone is covered by a thick, greater than ~20 km wide sequence of undisturbed Middle Eocene carbonates (Okay et al., 1996) (Fig. 2).

The basement of the Strandja Zone consists of felsic gneisses and migmatites intruded by Carboniferous - Permian granitoids emplaced during the Variscan orogeny (Okay and Tüysüz, 1999). Basement units are in turn unconformably overlain by Paleozoic and Early Mesozoic continental clastic sequences, volcanic rocks, and shallow marine carbonates, all of which have been subjected to latest Jurassic-earliest Cretaceous greenschist metamorphism based on K-Ar biotite cooling ages (Okay 1986; Okay et al., 1996). Paleozoic and Mesozoic sedimentary cover rocks are intruded by Late Cretaceous calc-alkaline, andesitic plutons emplaced during the progressive closure of the Vardar Ocean, which culminated by ~115 Ma based on hornblende Ar-Ar cooling ages of the metamorphic soles of suture zone peridotites near the Biga Peninsula (Okay et al., 1996). The most southeasterly portion of the terrane consists of a greater than 9 km thick sequence of Eocene and younger clastic sediments, collectively known as the Thrace Basin (e.g., Görür and Okay, 1996).

2.1.2 İstanbul Zone

The İstanbul Zone, also known as the İstanbul Nappe (Şengör et al. 1984a) is located along the southwestern lobe of the Black Sea and extends approximately 400 km E-W by 70 km N-S (Okay and Tüysüz, 1999). This terrane is juxtaposed against the Strandja Zone to the west via the dextral West Black Sea Fault. To the east, it is juxtaposed against the Central Pontides of the Sakarya Zone via the sinistral West Crimean Fault (Okay et al., 1994). To the south, the İstanbul Zone is in tectonic contact with the Sakarya Zone via the Late Triassic (Bozkurt et al., 2013), Early Cretaceous (Akbayram et al., 2013), pre-Santonian (Özcan et al., 2012), middle Late Cretaceous (Göncüoğlu et al., 2008), Turonian (Robertson and Ustaömer, 2004), pre-Cenomanian (Göncüoğlu and Erendil, 1990) Cenomanian (Tüysüz, 1999), Coniacian - Santonian (Yılmaz et al., 1995; Elmas and Yiğitbaş, 2001, 2005), Paleocene-Lutetian (Şengör and Yılmaz, 1981), Early Eocene (Okay et al., 1994; Akbayram et al., 2016), or Early Eocene-Oligocene (Görür and Okay, 1996) Intra-Pontide Suture (see Akbayram et al., 2016 for a detailed discussion). The İstanbul Zone is comprised of Cadomian (Pan-African) (P. Ustaömer et al., 2005) amphibolite-facies basement with intercalated tectonic lenses of micaschist and metadiorite (Şengör et al., 1984a). Basement rocks are in turn overlain by a sequence of transgressive Ordovician-Carboniferous clastic rocks, interpreted as passive margin sediments, resembling similar aged sedimentary packages of the Moesian Platform and are therefore interpreted to be part of the southern flank of Baltica prior to the opening of the Paleotethys (Okay et al., 1996). During the Early Devonian-Late Carboniferous (\pm Permian) Variscan Orogeny (Stampfli, 2000), marginal sediments were deformed, exhumed, faulted and folded diachronously from west to east (Okay and Tüysüz, 1999). Triassic transgressive sediments unconformably overlie Ordovician-Carboniferous tectonised units (Okay et al., 1996; Okay and

Tüysüz, 1999), which exhibit deformation related to the Cimmerian Orogeny. Triassic strata are unconformably overlain by Late Cretaceous sediments where Jurassic and Early Cretaceous sedimentary horizons are notably absent (Altiner et al., 1991). Extrusive and intrusive Late Cretaceous volcanic rocks are locally observed along the northern margin of the İstanbul Zone (Okay and Tüysüz, 1999) (Fig. 2; inset).

2.1.3 Sakarya Zone

The Sakarya Zone, as described by Okay (1984a) combines Şengör and Yilmaz, (1981)'s Sakarya Continent and Eastern Pontides. However, in this study, we treat the Eastern Pontides as a separate tectonic unit due to its contrasting Paleozoic-Cenozoic volcanic history (Fig. 2; inset). To the northwest, the Sakarya Zone is in tectonic contact with the Strandja Zone and the İstanbul Zone via the Vardar and Intra-Pontide sutures. The northeastern portion of the Sakarya Zone is known as the Central Pontides, and is characterized by Jurassic plutonic rocks, which exhibit contemporaneous HT-LP metamorphism (Gücer et al., 2016). The Central Pontides are located east of the İstanbul Zone and West Crimean Fault, north of the Central Anatolian Crystalline Complex and the Ankara Erzincan suture zone, west of the Eastern Pontides and the dextral Northern Anatolian Fault, and south of the Black Sea (Fig. 2). The southern margin of the Sakarya Zone (*sensu-stricto* Şengör and Yilmaz, 1981) from west to east is in tectonic contact with the Bornova Flysch Zone (BFZ), The Tavşanlı Zone and the western margin of the Central Anatolian Crystalline Complex (Fig. 2).

The Basement of the Sakarya Zone is characterized by Early Paleozoic passive margin strata, which are metamorphosed, folded, faulted and intruded by Carboniferous ±Devonian granitoids emplaced during the Variscan Orogeny (Okay et al., 1996). Carboniferous plutons and basement gneisses yield zircon U-Pb ID-TIMS and U-Pb Ion Microprobe ages clustering around

~400 and ~310 Ma respectively (Okay et al., 1996; P. Ustaömer et al., 2011). The Karakaya Complex (Fig. 3) is located structurally below the Variscan basement (Okay et al., 2002) and consists of a ca. 3 km thick package of mafic Carboniferous, Permian and Triassic sediments (Okay and Tüysüz, 1999; Ustaömer et al., 2016) that underwent varying degrees of metamorphism during the Late Triassic Cimmerian Orogeny (Okay, 2000; Okay et al., 2002). The tectonic setting of the Karakaya Complex has been interpreted as an oceanic seamount (Pickett and Roberson, 1996), an oceanic plateau (Okay, 2000), an ensimatic fore-arc sequence (Göncüoğlu et al., 2000), or an oceanic intra-arc to fore-arc (Okay et al., 1996) (see Okay et al., 2002). Together, metamorphosed Early Paleozoic passive margin strata, Variscan basement, and the under-thrust Karakaya Complex describe the basal lithologies of the Sakarya Zone (Okay et al., 2002; T. Ustaömer et al., 2016). Jurassic-Neogene sediments rest unconformably above basement lithologies, where the western Sakarya Zone contains conglomeratic strata, deposited during the Early Jurassic, overlain by a ~2 km thick limestone package deposited during the Middle Jurassic-earliest Late Cretaceous (Okay and Tüysüz, 1999). Late Cretaceous-Neogene strata rest depositionally above this limestone sequence, marked by an angular unconformity, which coarsens upward into marine turbidites interbedded with volcanic horizons, which transition into lagoonal and deltaic deposits. In turn, this sequence is unconformably overlain by fluvial deposits, which also contain volcanogenic horizons. A final enigmatic feature of the Sakarya Zone are abundant Late Cretaceous volcanogenic strata and the absence of their plutonic counterparts (Okay et al., 1996).

2.2 THE ANATOLIDES

2.2.1 Tavşanlı Zone

The Tavşanlı Zone (Okay, 1984a) strikes E-W for 250 - 300 km, has an average N-S width of ~50 km (Okay, 2008) and is in tectonic contact with the more northern Sakarya Zone via the İAS, whose defining feature is a Late Cretaceous blueschist belt, with lesser amounts of Triassic blueschists (Okay et al., 2002). Metamorphosed sediments consist of Paleozoic-Mesozoic passive margin strata capped by platform carbonates, representative of the northern margin of the Anatolides. During the Late Cretaceous (90-80 Ma), as a result of intra-oceanic subduction (van Hinsbergen et al., 2016 and references within), this zone underwent high-pressure low-temperature (HP-LT) metamorphism at approximately 20-24 kbar and 430-500 °C (Okay et al., 1998; Sherlock et al., 1999; Sherlock and Kelly, 2002). This immediately post dates initial obduction of the Lycian Nappes (~95 Ma; Önen, 2003; Celik et al., 2006), which contain oceanic crust of the İzmir-Ankara Ocean in the hanging-wall. To the east, the contact between the Tavşanlı Zone and the Central Anatolian Crystalline Complex is obscured by Upper Cretaceous-Middle Eocene sediments of the Orhaniye (Fig 1.), Haymana-Polatli, and Tuz Gölü sedimentary basins (e.g., Nairn et al., 2013; Licht et al., 2017)

2.2.2 Afyon Zone

The Afyon Zone (Okay, 1984a), structurally beneath the Tavşanlı Zone is characterized by Barrovian-type metamorphism resulting in amphibolite-greenschist facies metamorphism, reaching peak pressures and temperatures of ~10 kbar and temperatures of 350-400°C during the Paleocene (Candan et al., 2005). This metamorphic unit is observed for over 600 km, in tectonic contact with the Menderes Massif and the Tavşanlı Zone to the west, the Central Anatolian Crystalline Complex to the east, and the Taurides to the south (Fig. 2).

The Afyon Zone is underlain by Pan-African basement mantled by low-grade, Late Paleozoic metamorphic sediments which fine up-section from Carboniferous conglomerates to Permian neritic platform-type sediments. Overlying Mesozoic sediments consist of Triassic-Late Cretaceous turbidites, which grade into sandstone beginning in the Paleocene and are interpreted to represent the proximal facies of the Anatolide-Tauride Blocks northern passive margin (Candan et al., 2005).

2.2.3 Nappe Sheets

Metamorphic soles of ophiolitic bodies thrust over the Tavşanlı Zone (Önen and Hall, 1993; Önen, 1993), Afyon Zone (Daşçi et al., 2014), and the Taurides (Çelik et al., 2006) (van Hinsbergen et al., 2016; Table 1) yield Cenomanian Ar/Ar apparent cooling ages of ~95 Ma. The most well known of these bodies are the Lycian Nappes, of southwestern Turkey, which are thrust over the SW Tauride block, between the Menderes Massif in the west and the Antalya Block in the east (Fig. 1). These ophiolitic units are related to obduction of a south-directed thrust sheet along an intra-oceanic subduction zone within the İzmir-Ankara Ocean that was active from the Aptian-latest Cretaceous/earliest Paleocene (e.g., van Hinsbergen et al., 2016). During Early Paleogene syn-collisional orogenesis, these ophiolites were translated southward in the hanging-wall of younger south-directed thrust sheets.

2.3 BASINS

2.3.1 Central Sakarya Basin

The Central Sakarya Basin is the primary basin in NW Turkey (Okay and Tüysüz, 1999). This basin is further divided into the north-central Murdunu-Göynük Basin, which consists primarily of Jurassic marine and Cretaceous shallow marine to transitional sediments (Altiner et al., 1991), where minor outcrops north of the Intra-Pontide Suture are also observed. The more

southern portion of the Central Sakarya Basin is known as the Saricakaya Basin, deposited on the southern margin of the Sakarya Zone, north of the İzmir-Ankara Suture. This basin primarily consists of Tertiary red beds unconformably overlying basement and Early-Middle Mesozoic sediments (Okay and Tüysüz, 1999).

2.3.2 Murdunu-Göynük Basin

Prior to closure of the Intra-Pontide Ocean, an eastward narrowing embayment (morphologically similar to the Gulf of California) existed between the İstanbul and Sakarya Zones (Okay et al., 1994; Okay et al., 1996; Görür, 1997). This embayment served as the primary depocenter for detritus shed from the Cretaceous arc of the Western Pontides (Fig. 1). Outcrops of this forearc basin are abundant in the northern Sakarya Zone and to a lesser extent in southern İstanbul Zone. In the Sakarya Zone, strata is exposed in a belt of alternating NE-SW trending anticlines and synclines (e.g., Açikalin et al., 2014), whereas in the İstanbul Zone only smaller lenses of the lowest members are observed within the Northern Anatolian Fault Zone (e.g., Genç and Tüysüz, 2010). The lowermost members of the Murdunu-Göynük Basin were deposited above a pre-Jurassic continental basement (Açikalin et al., 2014) and are characterized by Jurassic volcanic rocks which fine up-section to Early Cretaceous pelagic carbonates (Şengör and Yilmaz, 1981; Altiner et al., 1991; Okay and Tüysüz, 1999; Tüysüz, 1999). Late Cretaceous strata are observed throughout the basin and consist of a thick ~1000 m sequence of volcanogenic turbidites with Cenomanian-Campanian depositional ages (Okay and Tüysüz, 1999). In the latest Cretaceous a coarsening upward sequence is observed, which contains sandstones and conglomerates (Açikalin et al., 2014). The Murdunu-Göynük Basin likely represents more proximal facies of a Late Cretaceous forearc basin.

2.3.3 Saricakaya Basin

Sedimentary deposits from the southern portion of the Central Sakarya Basin are located in and to the north of the Sakarya River Valley near the town of Eskişehir. The northern margin of the Sakarya River Valley is characterized by a SSW directed thrust fault (the Northern Söğüt Thrust), which juxtaposes a Carboniferous pluton (Söğüt granite; ~325 Ma; Ustaömer et al., 2011) over terrigenous Paleogene red beds that are locally folded into an overturned SSE verging syncline. This basin is also incorporated into the hanging-wall of another SSE directed thrust fault containing Paleozoic and Mesozoic accretionary units in its footwall, such as the Permo-Triassic marbles of the Karakaya Complex (Ustaömer et al., 2011) as well as Triassic and Cretaceous Ophiolitic material (Okay et al., 2002). South of this imbricate thrust stack HP-LT blueschist rocks of the Tavşanlı Zone are observed (Fig. 3).

Here we subdivide the Saricakaya basin into the north and south Saricakaya basin based upon whether the location is in the hanging-wall or footwall of the Northern Söğüt Thrust. The southern Saricakaya Basin (i.e., footwall) consists of a metamorphosed greenschist(?) basement, overlain by Permo-Triassic marbles, which are in turn unconformably overlain by a sequence of carbonaceous Jurassic sandstone beds, above which Paleogene red beds are present, consisting of a sequence of coarsening up conglomerates with interbedded Early Eocene tuffaceous units. Here we sampled an outcrop of the basement in the southern portion of the basin, two finer grained conglomeratic beds, and two underlying volcanic tuffs (Fig. 3).

The northern Saricakaya Basin (hanging wall) is stratigraphically similar to the southern basin, however it contains Cretaceous shallow marine to transitional sediments between the Jurassic and Paleogene sections unlike the southern basin.

2.3.4 Orhaniye Basin

Part of the greater Haymana-Polatli-Orhaniye basin complex (e.g., Narin et al., 2013), located southeast of the Neogene Galatean volcanic arc and west of the Central Anatolian Crystalline Complex, within the south pointing horn of the Sakarya Zone, the Orhaniye basin is the most northerly depocenter of the complex and has been interpreted to represent a peripheral forearc sub-basin (Licht et al., 2017; Dickinson and Seely, 1979). A continuous record of Upper Cretaceous-Eocene strata is deposited above the Northern Anatolian Ophiolitic Mélange, which consists of Upper Jurassic-Lower Campanian turbidites, ophiolites, pillow basalts, olistostromes, carbonates and radiolarites. The lower member of the Orhaniye basin is known as the Dikmendede formation, which exhibits variable thickness ranging from 200-850 m and is dominated by deep marine turbidites deposits, which generally fine up section and are capped by coarser grained clastics, interpreted to represent a deltaic environment, which were deposited during the Maastrichtian to perhaps the Lower Paleocene. The Dikmendede formation represents a progradational sequence, which is intruded by dike complexes emplaced during the Paleocene. The top of the Dikmendede formation is defined by an unconformity, above which sandstone, pedogenic red mudstone, and carbonate rich clastic material is observed. Collectively this sedimentary sequence is interpreted to represent a Paleocene-Middle Eocene lagoonal or coastal environment, known as the Uzunçarşidere formation (Koçyigit et al., 1988; Koçyigit, 1991).

Appendix 2: Sample Descriptions and Locations

S. Saricakaya Basin

Samples	Description	Location
15YP09	Volcaniclastic sandstone in Paleogene series of Saricakaya, 15 m above the appearance of basement clasts in the Pg section	N40°04'09.6" E30°44'37.5"
15YP08	Volcaniclastic sandstone in Paleogene series of Saricakaya, 15 m below the appearance of basement clasts in the Pg section (unconformability)	N40°04'09.6" E30°44'37.5"
15YP11	Volcaniclastic sandstone in Paleogene series of Saricakaya, ~30 m above the base of the Pg section	N40°01'18.9" E30°39'22.9"
15YP07	Volcaniclastic sandstone in Paleogene series of Saricakaya, random stratigraphic location	N40°03'08.4" E30°37'13.2"
15YP12	Greenschist (?), basement of Pontides, below Pg section and next to the Suture	N40°01'18.9" E30°39'22.9"

N. Saricakaya Basin

Samples	Description	Location
15YP14	Paleogene sandstone, Yenipazar section, 10m above the disconformity with Maastrichian flysch	N40°10'01.7" E30°31'18.5"
15YP13	Volcaniclastic sandstone in Maastrichian (?) flysch, Yenipazar section, 5m below the disconformity	N40°10'01.7" E30°31'18.5"
15YP04	Lower Jurassic sandstone, base of the Tethyan series, South of Yenipazar	N40°06'06.0" E30°37'02.3"

Murdunu-Goynuk Basin

Samples	Description	Location
15GO02	First conglomeratic bed in late cretaceous flysch, Gojnuk section	N40°24'21.6" E30°47'00.5"
15GO01	First volcaniclastic bed in Campanian flysch, Gojnuk section	N40°23'46.2" E30°46'50.8"

Orhaniye Basin

Samples	Description	Location
15KZ01	Permian metasandstone, metamorphosed basement of Orhaniye area	N40°11'10.6" E32°33'32.7"

Appendix 3: U-Pb Analytical Parameters

Laboratory & Sample Preparation	
Laboratory name	KU Geology Isotope Geochemistry Laboratories
Sample type/mineral	Zircon
Sample preparation	Standard mineral separation & epoxy grain mount
Laser Ablation System	
Make, Model & type	ArF excimer 193 nm, Photon Machines Analyte G2, ATLEX 300
Ablation cell & volume	Hexel 2, two-volume cell
Laser Wavelength (nm)	193
Pulse width	5 ns
Fluence	2 J/cm ²
Repetition rate	10 Hz
Spot Diameter (nominal/actual)	20/20 µm
Sampling mode/pattern	Single spot
Carrier gas (l/min)	He, 1.01 (cell); Ar, 1.1
Ablation duration (secs)	26 (long method)

ICP-MS Instrument	
Make, Model & type	Thermo Element2 magnetic sector field ICP-MS
Sample introduction	Ablation aerosol
RF power	1100 W
Make-up gas flow	Ar, 1.1/min
Sampling depth	20 μm
Detection system	Single detector, counting & analog
Masses measured	^{206}Pb , ^{207}Pb , ^{208}Pb , ^{232}Th , ^{238}U
Integration time per peak (ms)	1-5 (long)
Total integration time per reading (secs)	23 (long)
Total method time (secs)	42 (long)
Sensitivity/Efficiency	$\sim 0.1\%$ U, GJ-1
IC Dead time (ns)	2 ns
UO+/U+(%)	< 0.01
$^{238}\text{U}+$ / $^{232}\text{Th}+$	> 0.6

Data Processing	
Gas blank (s)	21 (long)
Calibration strategy	Sample/ standard bracketing. GJ-1 used as primary calibration standard. Plešovice and Fish Canyon Tuff used as secondary reference materials.
Reference Material info	GJ-1 (Jackson et al., 2004) Plešovice (Sláma et al., 2008) Fish Canyon Tuff (Wotzlaw et al., 2013)
Data processing package used	ET_Redux-3.6.14, IGOR PRO, Iolite 2.5
Mass discrimination	Y-Intercept, Downhole
Common-Pb correction, composition and uncertainty	No common-Pb correction applied to the data
Uncertainty level & propagation	Age uncertainties at $\pm 2\sigma$ absolute, propagation is by quadratic addition following McLean et al., 2016, Paton et al., 2010
Reproducibility	See Appendix 2
Quality control/ Validation	Plešovice and Fish Canyon Tuff used as secondary reference materials.

Appendix 4: U-Pb Standard Values

Sample	Secondary Standard ₁	Secondary Standard ₂
	Plešovice	Fish Canyon Tuff
15YP08	341.2 ±3.2 Ma (MSWD=0.55)	28.85 ±0.65 Ma (MSWD=0.53)
15YP09	341.2 ±3.2 Ma (MSWD=0.55)	28.85 ±0.65 Ma (MSWD=0.53)
15G002	340.0 ±3.9 Ma (MSWD=1.3)	27.39 ±0.59 Ma (MSWD=1.6)
15YP04	347.2 ±3.4 Ma (MSWD=1.0)	28.66 ±0.50 Ma (MSWD=1.2)
15YP07	341.2 ±3.5 Ma (MSWD=0.40)	28.07 ±0.55 Ma (MSWD=0.88)
15YP11	341.2 ±3.5 Ma (MSWD=0.40)	28.07 ±0.55 Ma (MSWD=0.88)
15KZ01	341.1 ±8.5 Ma (MSWD=0.96)	29.4 ±1.2 Ma (MSWD=1.2)
15G001	337.2 ±8.5 Ma (MSWD=0.46)	28.29 ±0.97 Ma (MSWD=0.69)
15YP12	343.2 ±1.1 Ma (MSWD=1.3)	28.69 ±0.19 Ma (MSWD=2.6)
15YP13	343.2 ±1.1 Ma (MSWD=1.3)	28.69 ±0.19 Ma (MSWD=2.6)
15YP14	341.9 ±3.8 Ma (MSWD=0.65)	27.90 ±0.59 Ma (MSWD=1.8)
Reference age by CA-TIMS	337.2 ±0.13 Ma (Sláma et al., 2008)	28.642 ±0.025 Ma (Wotzlaw et al., 2013)

Appendix 5: LA-ICP-MS Zircon Data Tables

Table 1: LA-ICP-MS Zircon Isotope and Age Data Table: 15Y109 & 15Y108: SGT FW Terrigenous Clastics

Sample-Grain #	Dates (Ma)		207Pb/235U age		207Pb/206Pb age		Isotopic Ratios		207Pb/235U c		207Pb/206Pb c		208Pb/232Th c		± %	Rho (σ)	% disc b
	206Pb/238U	±2σ	207Pb/235U	±2σ	207Pb/206Pb	±2σ	206Pb/238U c	±2σ	207Pb/235U c	±2σ	207Pb/206Pb c	±2σ	208Pb/232Th c	±2 %			
15Y109-01	79.0681	3.6876	82.5657	2.2962	184.90085	175.77694	0.01234	4.64428	0.08711	0.22578	0.04981	0.79156	0.00366	8.95445	0.4771	57.23664	
15Y109-02	79.10375	3.73745	81.55198	7.9671	153.78833	139.04073	0.01235	4.75495	0.08363	0.10295	0.04915	0.79258	0.00371	11.08110	0.38377	45.85887	
15Y109-03	79.45905	7.83536	87.25577	10.05607	106.16338	97.92726	0.01240	9.92489	0.08973	19.34019	0.02450	16.69087	0.00371	13.85580	0.45005	74.04685	
15Y109-04	80.25241	8.07207	87.90638	7.40347	198.78289	182.32567	0.01253	4.22257	0.08113	10.32127	0.05048	9.42838	0.00065	15.20570	0.28768	65.34129	-110.20023
15Y109-05	80.27046	3.2065	85.18596	7.01225	225.24282	210.27039	0.01253	3.91287	0.08752	6.89656	0.05068	6.05068	0.00339	9.76220	0.35395	64.36270	
15Y109-06	80.55834	8.28414	89.96667	7.21527	147.30241	161.79646	0.01258	3.55002	0.09265	8.41032	0.03346	7.62347	0.00341	8.35138	0.33724	76.80456	
15Y109-07	80.55881	8.53687	85.73067	8.45057	222.24543	204.22567	0.01257	4.19933	0.08811	10.32127	0.05048	8.83070	0.00065	15.20570	0.28768	65.34129	
15Y109-08	80.84181	3.91900	86.41838	7.45572	243.34113	166.36880	0.01262	4.87470	0.08884	9.03294	0.05108	7.66649	0.00340	12.29168	0.47155	66.77840	
15Y109-09	81.83294	2.79335	80.65770	5.63425	45.98631	44.78736	0.01278	4.34593	0.08268	7.28669	0.04096	6.42575	0.00340	10.47997	0.39863	57.79505	
15Y109-10	81.27155	3.12969	86.53710	6.27017	177.58548	146.42575	0.01300	3.78566	0.08986	7.58218	0.04965	6.57604	0.00387	13.72617	0.44003	53.10903	
15Y109-11	81.48446	9.46139	86.05186	7.40347	322.68019	179.86915	0.01300	4.82959	0.08927	11.83975	0.04612	9.43706	0.00445	13.44486	0.51054	55.63812	
15Y109-12	81.85925	5.79016	90.08119	8.72872	201.81431	166.93194	0.01342	6.87621	0.09277	10.16967	0.05707	7.57337	0.00369	12.97931	0.64425	57.42708	
15Y109-13	87.27612	5.61618	97.07162	10.80145	344.91532	207.24030	0.01363	6.48144	0.10032	11.72995	0.05340	9.76765	0.00472	10.68551	0.51098	74.69036	
15Y109-14	80.08237	82.8287	89.25047	10.64198	220.92179	0.01392	7.18427	0.09188	12.52994	0.04791	10.25476	0.00604	17.33925	0.53528	4.93864		
15Y109-15	115.28631	6.52319	12.40888	87.17829	234.47318	0.01804	4.58196	0.11828	11.57828	0.04778	10.63305	0.00501	9.46004	0.31145	-32.24199		
15Y109-16	201.11249	10.58651	218.69387	18.36415	212.09267	171.00404	0.03313	5.08650	0.24033	9.41884	0.05264	7.92730	0.00933	19.25268	0.48447	32.67625	
15Y109-17	234.21423	8.88688	240.31443	18.40087	298.27598	168.34617	0.03763	3.84640	0.26702	8.67707	0.05232	7.77793	0.01334	7.38799	0.62762	3.86810	21.40798
15Y109-18	241.38813	8.81175	244.36253	15.71166	273.03455	137.64237	0.03816	3.72176	0.27209	7.29059	0.05174	6.26907	0.01150	8.36246	0.43830	11.59603	
15Y109-19	249.81822	10.21861	257.29586	17.60171	325.99308	132.35612	0.03951	4.90934	0.28840	7.81187	0.05296	6.07649	0.01132	7.30699	0.60286	23.36702	
15Y109-20	251.16319	9.46139	261.16319	12.16319	322.68019	151.99919	0.04093	3.71443	0.29287	8.16719	0.05287	8.32228	0.01334	7.38799	0.31426	21.40798	
15Y109-21	284.95622	17.22313	302.98201	26.25973	465.25973	122.03455	0.04682	5.98181	0.34769	8.21044	0.05389	5.62400	0.01132	10.38964	0.60237	19.24754	
15Y109-22	309.80309	10.87427	309.63447	15.28033	308.37335	90.65400	0.04023	3.59626	0.35655	5.77229	0.05255	4.51352	0.01300	9.43538	0.58533	-40.46344	
15Y109-23	314.34298	15.42040	321.74637	31.64626	382.31423	220.33198	0.04982	5.04676	0.37283	11.65811	0.05430	10.59133	0.01573	15.43012	0.34653	18.66610	
15Y109-24	314.20000	15.42040	315.76049	15.42040	314.69929	0.04906	3.37445	0.46716	6.47626	0.05278	6.81184	0.01384	9.28805	0.38574	3.83924		
15Y109-25	315.91013	11.54265	326.97994	20.15335	406.55225	133.95911	0.05023	3.74739	0.37992	7.28107	0.05249	6.42648	0.01480	5.76749	0.46564	24.29532	
15Y109-26	323.74517	13.36309	321.70359	17.16623	306.94974	102.27951	0.05150	4.23719	0.37277	6.27994	0.05252	4.63507	0.01480	5.76749	0.46564	-24.47172	
15Y109-27	324.18413	13.36309	323.66072	21.36097	315.98239	105.98239	0.05150	4.23719	0.37277	6.27994	0.05252	4.63507	0.01480	5.76749	0.46564	-24.47172	
15Y109-28	324.36518	11.90604	325.80044	23.51900	335.85196	0.05165	3.76392	0.37829	8.53774	0.05134	7.66238	0.01276	7.88403	0.34670	2.75571		
15Y109-29	330.05994	12.28097	328.00974	18.96667	269.16054	127.21818	0.05262	3.81457	0.37461	6.91797	0.05166	5.77126	0.01268	9.45742	0.50185	-22.82623	
15Y109-30	331.00000	12.28097	325.12452	22.12452	325.12452	127.21818	0.05262	3.81457	0.37461	6.91797	0.05166	5.77126	0.01268	9.45742	0.50185	-22.82623	
15Y109-31	331.29946	13.88130	332.95268	19.50154	344.56182	118.68091	0.05274	4.30325	0.38806	6.93624	0.05339	5.94999	0.01519	11.48252	0.58688	3.85979	
15Y109-32	332.52739	14.89168	332.14552	17.71382	247.78933	101.80179	0.05294	4.60021	0.37337	6.47996	0.05118	4.56376	0.01456	7.13027	0.60928	-34.19560	
15Y109-33	332.90973	15.46139	332.22723	20.15335	344.56182	118.68091	0.05274	4.30325	0.38806	6.93624	0.05339	5.94999	0.01519	11.48252	0.58688	3.85979	
15Y109-34	332.90973	15.46139	332.22723	20.15335	344.56182	118.68091	0.05274	4.30325	0.38806	6.93624	0.05339	5.94999	0.01519	11.48252	0.58688	3.85979	
15Y109-35	332.90973	15.46139	332.22723	20.15335	344.56182	118.68091	0.05274	4.30325	0.38806	6.93624	0.05339	5.94999	0.01519	11.48252	0.58688	3.85979	
15Y109-36	332.90973	15.46139	332.22723	20.15335	344.56182	118.68091	0.05274	4.30325	0.38806	6.93624	0.05339	5.94999	0.01519	11.48252	0.58688	3.85979	
15Y109-37	332.90973	15.46139	332.22723	20.15335	344.56182	118.68091	0.05274	4.30325	0.38806	6.93624	0.05339	5.94999	0.01519	11.48252	0.58688	3.85979	
15Y109-38	332.90973	15.46139	332.22723	20.15335	344.56182	118.68091	0.05274	4.30325	0.38806	6.93624	0.05339	5.94999	0.01519	11.48252	0.58688	3.85979	
15Y109-39	332.90973	15.46139	332.22723	20.15335	344.56182	118.68091	0.05274	4.30325	0.38806	6.93624	0.05339	5.94999	0.01519	11.48252	0.58688	3.85979	
15Y109-40	332.90973	15.46139	332.22723	20.15335	344.56182	118.68091	0.05274	4.30325	0.38806	6.93624	0.05339	5.94999	0.01519	11.48252	0.58688	3.85979	
15Y109-41	332.90973	15.46139	332.22723	20.15335	344.56182	118.68091	0.05274	4.30325	0.38806	6.93624	0.05339	5.94999	0.01519	11.48252	0.58688	3.85979	
15Y109-42	332.90973	15.46139	332.22723	20.15335	344.56182	118.68091	0.05274	4.30325	0.38806	6.93624	0.05339	5.94999	0.01519	11.48252	0.58688	3.85979	
15Y109-43	332.90973	15.46139	332.22723	20.15335	344.56182	118.68091	0.05274	4.30325	0.38806	6.93624	0.05339	5.94999	0.01519	11.48252	0.58688	3.85979	
15Y109-44	332.90973	15.46139	332.22723	20.15335	344.56182	118.68091	0.05274	4.30325	0.38806	6.93624	0.05339	5.94999	0.01519	11.48252	0.58688	3.85979	
15Y109-45	332.90973	15.46139	332.22723	20.15335	344.56182	118.68091	0.05274	4.30325	0.38806	6.93624	0.05339	5.94999	0.01519	11.48252	0.58688	3.85979	
15Y109-46	332.90973	15.46139	332.22723	20.15335	344.56182	118.68091	0.05274	4.30325	0.38806	6.93624	0.05339	5.94999	0.01519	11.48252	0.58688	3.85979	
15Y109-47	332.90973	15.46139	332.22723	20.15335	344.56182	118.68091	0.05274	4.30325	0.38806	6.93624	0.05339	5.94999	0.01519	11.48252	0.58688	3.85979	
15Y109-48	332.90973	15.46139	332.22723	20.15335	344.56182	118.68091	0.05274	4.30325	0.38806	6.93624	0.05339	5.94999	0.01519	11.48252	0.58688	3.85979	
15Y109-49	332.90973	15.46139	332.22723	20.15335	344.56182	118.68091											

Table 1 cont: LA-ICP-MS Zircon Isotopic and Age Data Table: 15YP09 & 15YP08: SGT FW Terrestrial Clastics

Sample-Grain #	Dates (Ma)		Isotopic Ratios				208Pb/232Th c	±2e	Rho (ρ)	% disc b					
	200Pb/238U age	±2e	207Pb/235U age	±2e	207Pb/206Pb age	±2e					207Pb/235U c	±2e	207Pb/206Pb c	±2e	
15YP09															
15YP09-090	161.10542	6.20448	196.28314	8.78691	63.98589	0.02551	3.90139	0.21326	4.94464	0.06115	3.03785	0.00671	6.17077	0.76833	74.96089
15YP09-091	245.22699	12.06067	266.45178	26.28841	490.74034	0.03819	5.90028	0.30007	11.36407	0.05700	10.16027	0.01018	11.84539	0.35909	50.76221
15YP09-094	275.54817	10.78742	274.20799	13.19245	264.47954	0.04364	4.00535	0.31003	5.52578	0.05155	3.80675	0.01173	5.05514	0.71192	-4.10944
15YP09-143	285.03048	11.26910	270.02185	20.19730	141.81935	0.04521	4.06525	0.29465	8.60376	0.04890	7.50347	0.01207	12.59813	0.37960	-100.98137
15YP09-088	285.28249	10.65885	280.60326	13.36007	88.28352	0.04825	3.81982	0.31831	5.48535	0.05104	3.93676	0.01248	5.12332	0.67185	-17.99147
15YP09-049	305.24907	13.40924	313.36643	374.19321	80.77106	0.04849	4.50239	0.36154	5.81509	0.05410	3.68018	0.01248	9.94625	0.76154	18.24274
15YP09-017	309.94517	10.39736	314.46357	15.61316	348.08845	0.04925	3.43864	0.36302	5.81808	0.05348	4.69317	0.01388	8.14189	0.55731	10.95793
15YP09-055	315.30836	11.55210	318.75928	16.17876	425.10678	0.05013	3.75744	0.38234	5.80869	0.05354	4.42737	0.01315	8.02385	0.68664	25.82843
15YP09-015	317.79495	12.48146	325.31254	14.21696	379.46735	0.05053	4.02903	0.37766	5.14357	0.05423	3.19738	0.01379	6.53257	0.77262	16.25237
15YP09-112	326.36683	12.51611	339.70613	18.45028	432.02938	0.05193	3.93670	0.39732	6.44876	0.05552	5.10773	0.01530	8.03460	0.57574	24.45726
15YP09-019	328.53804	12.01895	333.66128	15.01905	369.53431	0.05229	3.75883	0.38903	5.32055	0.05399	3.76855	0.01367	6.36742	0.67843	11.09404
15YP09-036	333.44809	19.16390	328.56750	22.94248	294.13889	0.05309	5.50589	0.38208	8.26618	0.05222	5.78362	0.01630	8.95130	0.69705	-13.36417
15YP09-032	335.02939	15.82327	316.61006	25.58134	184.92572	0.05335	4.82509	0.36618	9.51901	0.04981	8.19119	0.01408	9.09550	0.42270	-81.16971
15YP09-042	335.57089	16.34776	336.41034	18.68480	342.21733	0.05343	5.05887	0.42984	6.58538	0.05434	4.23884	0.01547	7.21406	0.75117	1.94217
15YP09-077	336.30005	15.29538	337.37716	25.47046	344.80758	0.05355	4.67334	0.39412	8.98533	0.05340	7.67438	0.01345	13.72064	0.48261	2.46733
15YP09-140	344.77569	11.48308	343.55223	14.23668	332.28474	0.05494	3.42350	0.40263	4.91887	0.05318	3.51199	0.01586	6.23416	0.67169	-2.83071
15YP09-142	351.24544	12.81936	337.52739	17.23980	244.06768	0.05600	3.75735	0.39433	6.05481	0.05109	4.79079	0.01531	7.03367	0.59128	-43.91133
15YP09-061	361.35606	17.09102	384.17807	37.69408	524.07799	0.05766	4.80994	0.45989	12.00601	0.05788	10.97397	0.02422	29.04843	0.29335	31.04918
15YP09-081	369.03141	23.70519	396.91433	45.31533	562.69984	0.05892	6.62143	0.47831	14.10580	0.05891	12.45513	0.03111	19.90680	0.41098	34.41794
15YP09-006	377.34028	13.02322	386.48565	20.39503	441.61169	0.06028	3.58402	0.40906	6.06321	0.05575	5.32980	0.01714	10.21024	0.49764	14.55383
15YP09-056	384.12261	14.41041	386.01301	15.19777	397.36106	0.06140	3.86872	0.46253	4.76839	0.05466	2.78758	0.01719	8.97353	0.80248	3.31519
15YP09-087	387.25862	12.22812	395.11394	16.49776	441.33987	0.06191	3.25649	0.47549	5.08156	0.05575	3.90096	0.01636	6.57972	0.61093	12.25388
15YP09-104	397.43717	16.48467	395.76360	25.26178	386.13632	0.06359	4.28239	0.47667	7.80396	0.05439	6.52403	0.01681	8.45385	0.51584	-2.92665
15YP09-065	438.98375	15.33406	438.92699	18.48526	438.66493	0.07047	3.61767	0.54077	5.23455	0.05568	3.78326	0.01767	7.57429	0.67268	-0.07268
15YP09-070	442.62967	15.20462	445.26123	20.97899	458.88125	0.07108	3.58854	0.55040	5.87818	0.05619	4.67865	0.01922	7.90428	0.58814	3.54156
15YP09-145	449.56648	16.09789	451.24185	16.09789	451.24185	0.07223	3.71170	0.57956	6.04128	0.05621	4.78658	0.01958	8.64105	0.55504	2.27275
15YP09-024	459.91354	16.46295	444.97392	19.12754	412.42421	0.07246	3.78489	0.54951	5.36224	0.05943	3.78484	0.02191	7.94031	0.60918	-9.33683
15YP09-135	453.54303	14.47148	458.99992	18.22162	486.22888	0.07289	3.38084	0.57148	4.97930	0.05689	3.72161	0.01873	6.25229	0.63480	6.72232
15YP09-082	455.53925	16.32929	458.73103	25.60616	474.74951	0.07322	3.71746	0.57111	7.02570	0.05659	5.96163	0.01857	15.41278	0.47845	4.06440
15YP09-093	457.62707	16.25067	452.70080	18.06230	427.78802	0.07337	3.68325	0.56180	4.98945	0.05541	3.36576	0.01875	7.34693	0.72337	-6.98270
15YP09-125	462.40185	15.44238	454.05459	17.10858	411.71121	0.07447	3.46496	0.56381	4.71300	0.05501	3.19475	0.01936	7.69380	0.71819	-12.31164
15YP09-133	466.42604	17.69574	471.00888	21.46017	493.40553	0.07504	3.95231	0.59022	5.75497	0.05707	4.19645	0.01854	8.43408	0.65801	5.46706
15YP09-010	475.45616	14.51310	467.06668	15.73406	426.03654	0.07654	3.17396	0.58406	4.23540	0.05537	2.80439	0.02251	11.59147	0.73002	-11.59985
15YP09-107	482.23935	45.87039	463.61260	48.33627	372.48388	0.07768	3.90738	0.57871	13.30033	0.05406	8.87369	0.02453	17.92021	0.73920	-29.46583
15YP09-083	524.61598	18.20475	524.80186	24.80186	662.25386	0.07878	3.61833	0.72078	5.90236	0.06169	4.66435	0.02779	8.98349	0.51723	20.78235
15YP09-109	524.70584	23.81797	547.31674	33.18643	642.59279	0.08440	4.35259	0.71433	7.97336	0.06112	4.41494	0.02717	7.59202	0.53376	18.34555
15YP09-121	544.86722	17.79773	556.13682	20.36993	602.54114	0.08820	3.41113	0.72929	4.80497	0.06000	3.38407	0.02508	5.13193	0.68669	9.57178
15YP09-074	561.91351	22.01952	573.78275	32.10240	621.08213	0.09108	4.09893	0.75961	7.44077	0.06052	6.20998	0.02308	7.58632	0.49449	9.52760
15YP09-003	583.56976	22.59185	602.68811	31.19899	675.26758	0.09475	4.05629	0.81042	6.97059	0.06206	5.66883	0.02644	10.07870	0.54784	13.57948
15YP09-146	588.38871	19.29702	594.79234	22.99786	636.0011	0.09557	3.43673	0.77879	5.23227	0.05913	3.94531	0.02474	7.66627	0.61121	-3.07179
15YP09-043	592.79911	27.20359	600.31604	44.55944	628.80983	0.09632	4.81339	0.80619	10.05077	0.06073	8.82322	0.03035	10.81054	0.36960	5.72681
15YP09-062	594.45423	21.86702	601.54600	23.96360	628.36448	0.09660	3.87525	0.80838	5.34233	0.06072	3.69622	0.02650	6.23454	0.70489	5.39659
15YP09-094	596.81479	23.97652	591.57804	32.22088	571.54177	0.09700	4.21408	0.79072	7.30148	0.05915	5.96288	0.02666	6.95994	0.50594	-4.42190
15YP09-114	599.60169	26.20271	599.61559	29.80061	590.65110	0.09748	4.58569	0.80495	6.67853	0.05992	4.85333	0.02775	6.55448	0.66649	0.00749
15YP09-101	604.56083	29.13905	580.91444	46.24963	489.50418	0.09882	5.06083	0.77201	10.06922	0.05997	9.42379	0.02587	8.28282	0.41225	-23.50460
15YP09-085	604.78816	21.48252	624.24666	24.67358	495.40707	0.09836	3.72751	0.84926	5.35607	0.06265	3.84618	0.02760	5.24859	0.66942	13.03106
15YP09-084	608.10220	24.42974	631.67758	40.32909	716.99099	0.09892	4.21782	0.86285	8.74751	0.06239	7.82248	0.02636	5.89856	0.39856	15.18691
15YP09-122	609.69174	23.89460	599.96121	22.96184	563.36042	0.09920	6.25402	0.80556	5.12637	0.05893	3.05718	0.02568	5.64978	0.79629	-8.22410
15YP09-037	610.94526	34.75840	602.50078	32.20776	570.85525	0.09941	5.97924	0.81008	4.24847	0.05913	4.40085	0.02812	8.03458	0.80179	-7.22280
15YP09-089	615.98771	18.38756	603.77554	19.25907	62.06134	0.10027	3.13441	0.81236	4.27196	0.05879	2.90261	0.02537	7.42916	0.71703	-10.35403
15YP09-030	618.36194	21.34063	616.94370	16.174283	63.79050	0.10067	3.62532	0.83601	4.71350	0.06025	3.01233	0.03037	14.38222	0.76700	-1.80201
15YP09-002	619.39169	26.80096	611.63156	37.54515	582.99789	0.10085	4.54763	0.82643	8.32480	0.05946	6.97290	0.02831	6.49480	0.48745	-6.24253
15YP09-124	621.45689	21.91839	649.50009	30.51212	748.21225	0.10200	3.78997	0.89584	4.65589	0.06423	5.28624	0.02855	8.09735	0.49961	16.94143
15YP09-033	622.06822	21.61770	619.26174	21.70507	609.48348	0.10143	3.65162	0.84039	4.93162	0.06019	3.08097	0.02789	4.17324	0.76462	-2.96482
15YP09-009	622.84676	20.57386	668.07275	20.92579	668.07275	0.10144	3.47088	0.86473	4.49025	0.06185	2.84874	0.02692	5.75222	0.76727	6.79962
15YP09-060	626.63080	22.94219	640.61287	25.97654	690.23482	0.10209	3.84887	0.87932	5.53826	0.06250	3.98228	0.02765	7.62995	0.67150	9.21484
15YP09-126	627.94881	22.73602	625.86696	22.86696	631.80545	0.10231	3.80660	0.85756	4.86808	0.06082	3.03447	0.02696	6.30198	0.77116	0.61042
15YP09-105	628.36707	22.03211	611.46222	21.96469	549.32879	0.10238	3.68621	0.82813</							

Table 1 cont: LA-ICP-MS Zircon Isotopic and Age Data Table: 15YP09 & 15YP08: SCT FW Terrigenous Clastics

Sample/Grain #	Dates (Ma)		207Pb/235U age		207Pb/206Pb age		Isotopic Ratios		207Pb/235U c		207Pb/206Pb c		208Pb/232Th c		Rho (ρ)	% disc b
	206Pb/238U	±2σ	±2σ	±2σ	±2σ	±2σ	206Pb/238U c	±2σ	±2σ	±2σ	±2σ	±2σ	±2σ			
15YP08																
15YP08-069	781.99205	28.72264	810.86543	32.01951	890.97322	86.69773	0.12897	3.91036	1.22238	5.82454	0.06877	4.31676	0.03171	8.36991	0.63821	12.23170
15YP08-044	807.33573	35.08878	819.59945	39.46015	853.02930	109.32956	0.13342	4.63690	1.24158	7.15068	0.06752	5.49074	0.03708	11.32903	0.61228	5.35662
15YP08-014	809.21764	27.85421	829.45309	40.02884	884.06723	123.15216	0.13375	3.67600	1.26344	7.20354	0.06854	6.19819	0.03675	9.49526	0.42624	8.46650
15YP08-031	816.51790	28.62368	804.60557	30.72386	771.77323	85.71951	0.13503	3.74058	1.20873	5.61367	0.06495	4.18586	0.03619	6.07641	0.64467	-5.79765
15YP08-128	820.76457	31.08509	830.68657	30.56211	857.23272	74.64781	0.13578	4.04429	1.26619	5.46897	0.06766	3.68258	0.03463	6.14807	0.72339	4.26433
15YP08-102	831.53754	30.98516	800.44251	30.28417	953.91946	70.62470	0.14122	3.84457	1.38001	5.22126	0.07091	5.33382	0.04186	5.73079	0.72722	10.72340
15YP08-141	877.48672	30.70510	867.78928	38.35490	843.11153	111.44535	0.14582	3.75169	1.35053	6.70009	0.06720	5.55121	0.03628	9.64845	0.51739	-4.07718
15YP08-078	881.33826	38.76246	1116.12918	39.91007	1607.24947	67.84325	0.14650	4.71981	2.00182	6.01139	0.09914	3.72293	0.05114	4.88137	0.78180	45.16481
15YP08-013	900.10403	27.49628	907.24421	28.37206	924.66553	70.28751	0.14985	3.28001	1.44367	4.79643	0.06991	3.49661	0.02414	7.78988	0.65314	2.65626
15YP08-086	900.92701	29.25859	26.14890	26.14890	985.13490	52.09037	0.14989	3.49969	1.48845	4.36136	0.07200	2.60263	0.02792	10.49947	0.79441	8.54785
15YP08-040	904.26657	33.09102	913.00602	30.51547	933.92538	66.03286	0.15061	3.93177	1.45757	5.14409	0.07022	3.31705	0.04367	5.20601	0.75066	3.16783
15YP08-127	941.55882	34.60341	1016.64963	48.57531	1177.60464	126.39747	0.15762	3.95287	1.72167	7.74641	0.07925	6.64196	0.04108	6.12084	0.47529	19.87474
15YP08-108	945.96621	45.60117	1108.51528	46.06347	1442.99995	86.24565	0.15806	5.20577	1.97940	6.98571	0.09087	4.68333	0.10154	6.76248	0.73675	34.44447
15YP08-039	959.18540	48.85525	952.46579	48.00046	936.97314	113.52421	0.16043	5.50256	1.55496	7.95401	0.07033	5.74533	0.05052	6.17871	0.67440	-2.37064
15YP08-079	962.83472	27.46267	936.83321	26.34738	936.83321	60.81706	0.16109	3.07417	1.56122	4.31258	0.07032	3.02454	0.04408	7.26855	0.60391	-2.77547
15YP08-067	965.78345	31.27702	955.44122	31.27702	926.67150	78.51279	0.16202	3.30878	1.56246	5.13939	0.06997	3.92082	0.04005	6.05802	0.62324	-4.45808
15YP08-011	972.17288	39.71682	967.10459	39.71682	955.60319	108.17226	0.16277	3.48691	1.59206	6.49459	0.07097	5.47915	0.04246	5.24133	0.45804	-1.73395
15YP08-076	976.38870	33.27284	967.75448	36.70074	931.74479	94.51708	0.16353	3.68182	1.58098	6.00863	0.07015	4.74846	0.04182	8.69707	0.51012	-4.79143
15YP08-117	983.48007	33.39803	983.80770	32.02567	984.53882	72.22464	0.16482	3.67103	1.63505	5.16408	0.07198	3.63197	0.03864	8.41051	0.68889	0.10754
15YP08-147	986.78123	33.82238	989.37308	33.95021	995.12570	79.44737	0.16541	3.70633	1.64953	5.46137	0.07236	4.01114	0.04444	8.52451	0.65263	0.83853
15YP08-118	997.02770	21.99522	1001.07469	45.22646	1009.94735	133.25320	0.16727	2.38514	1.68025	7.26562	0.07289	6.86296	0.04897	11.14104	0.30229	1.27928
15YP08-149	998.01409	31.62346	1029.56764	29.81221	1097.22995	62.33408	0.16744	3.42863	1.75652	4.67604	0.07612	3.17852	0.04308	5.74967	0.76194	9.04239
15YP08-103	1011.15675	39.66238	982.85989	37.85518	1002.26229	85.39599	0.16983	4.25121	1.68338	6.05903	0.07192	4.31167	0.04823	8.32096	0.67539	-2.87903
15YP08-020	1015.48463	39.04603	1020.85183	34.84629	1032.37822	71.04068	0.17061	4.16847	1.73296	5.50611	0.07370	3.97376	0.04511	5.92524	0.73828	1.63638
15YP08-054	1016.23306	47.18866	1038.24253	47.18866	1084.87929	123.98573	0.17075	3.70487	1.78017	7.42930	0.07565	6.43960	0.04542	8.42379	0.40152	6.32754
15YP08-004	1016.78629	27.28478	1018.97323	26.46560	1023.67669	59.31339	0.17085	2.90677	1.72791	4.16869	0.07338	2.98809	0.04432	5.81482	0.66999	0.67310
15YP08-073	1017.58485	30.78998	1011.22239	29.87282	997.63801	67.87879	0.17098	3.27995	1.70717	4.73467	0.07245	3.41549	0.04379	5.48275	0.67956	-1.99139
15YP08-134	1021.83657	31.35808	1044.37992	26.41081	998.31540	50.29578	0.17177	3.32652	1.71560	4.17121	0.07247	2.51659	0.04102	5.42408	0.79056	-2.35609
15YP08-072	1027.99927	36.29950	1007.93041	39.80313	964.55644	100.14731	0.17289	3.83089	1.69840	6.35175	0.07128	5.06646	0.04371	7.16249	0.54555	-6.57741
15YP08-025	1031.27826	64.33482	976.32739	56.68053	854.67190	126.66335	0.17348	6.78445	1.92941	6.16571	0.06758	6.32520	0.04057	11.95917	0.69320	-20.66364
15YP08-053	1032.18699	38.29319	1047.20344	39.80601	1078.66364	92.15350	0.17365	4.02679	1.80482	6.21342	0.07541	4.73197	0.04517	6.21106	0.60520	4.30873
15YP08-099	1033.84444	37.17312	1031.74513	31.67500	1027.29763	60.89448	0.17395	3.90289	1.76244	4.96625	0.07352	3.97101	0.04611	6.03299	0.75125	-0.63728
15YP08-021	1038.72947	38.80665	1041.45488	30.22555	1047.17866	53.59004	0.17484	3.85098	1.78098	4.71062	0.07424	2.79428	0.04536	6.76840	0.81150	0.80685
15YP08-063	1039.70880	32.90294	1027.74733	27.22811	1002.37585	50.62628	0.17502	3.43546	1.75158	4.26948	0.07262	2.54548	0.04316	5.32865	0.79558	-3.72425
15YP08-106	1041.97212	49.80660	1044.99800	49.80660	1049.78853	93.07274	0.17543	5.16088	1.79736	7.04710	0.07434	4.79792	0.04344	6.07434	0.72684	0.74457
15YP08-018	1044.25722	34.69071	1046.49980	37.33839	1052.60339	89.41329	0.17585	3.60808	1.80414	5.82189	0.07444	4.56905	0.04624	8.01278	0.56062	0.79291
15YP08-115	1052.84876	39.58771	1036.36469	43.30099	1001.75091	106.83566	0.17742	4.08800	1.77804	6.81118	0.07259	5.44798	0.04625	8.86065	0.53826	-5.10085
15YP08-068	1059.05182	34.60642	1064.38149	41.86271	1075.32248	103.15911	0.17855	3.55297	1.85567	6.48088	0.07529	5.42017	0.04192	10.19276	0.48507	1.51310
15YP08-137	1087.20306	58.09473	1074.57456	62.53728	1049.04218	149.47704	0.18371	5.83300	1.88145	9.72904	0.07431	7.78654	0.04045	12.09730	0.56699	-6.63769
15YP08-132	1320.73366	35.81819	1372.19932	28.44540	1453.27377	44.94996	0.22738	2.99079	2.86287	3.83343	0.09136	6.29257	0.06925	6.29257	0.90173	9.11783
15YP08-096	1375.24033	46.39066	1409.04849	33.02339	1400.55551	140.02968	0.23780	3.75983	3.00663	4.40563	0.09171	2.29637	0.06223	5.47522	0.84811	5.84115
15YP08-136	1542.11765	47.85545	1642.62876	33.02082	1773.76212	39.20377	0.27026	3.50218	4.04170	4.12337	0.10851	1.21644	0.08949	7.92442	0.84436	13.05950
15YP08-130	1742.85289	57.83547	1752.31548	37.80169	1765.58476	46.98703	0.31044	3.80419	4.61683	4.61664	0.10791	2.61209	0.07537	6.68746	0.81783	1.17385
15YP08-123	1788.61257	49.30204	1821.38828	32.25602	1859.07980	39.65185	0.31977	3.16860	5.01222	3.87170	0.11373	2.22487	0.08181	7.98636	0.81316	3.79044
15YP08-139	1794.31199	57.23471	1892.93105	38.93414	2002.85657	49.16676	0.32094	3.67052	5.45112	4.62597	0.12324	2.81548	0.08776	6.04140	0.78507	10.41136
15YP08-066	1901.92473	55.98067	1972.74703	37.99529	2007.84956	49.60107	0.34317	3.41369	5.97868	4.45060	0.12641	2.85562	0.08407	6.12031	0.74915	7.12576
15YP08-080	1947.86556	57.42139	2057.56002	34.59179	2169.32351	35.12514	0.35278	3.43094	6.58663	3.99160	0.13547	2.03999	0.08185	5.96749	0.85646	10.20862
15YP08-029	1969.71912	55.37053	1975.27682	35.80103	1981.10145	45.70203	0.35737	3.27644	5.99609	4.18728	0.12174	2.60734	0.08708	5.77801	0.76502	0.57455
15YP08-150	1994.74109	53.92537	2004.76351	31.44577	2015.48600	32.22170	0.36258	3.15885	6.20223	3.65253	0.12412	1.83719	0.08622	5.51466	0.85962	1.04748
15YP08-046	2024.19992	69.14321	1989.19326	42.20532	1953.02942	50.87006	0.36889	4.00160	6.09264	4.94808	0.11984	2.89805	0.08775	5.67879	0.80190	-3.64508
15YP08-032	2059.47997	61.17356	2031.66482	36.77672	2003.52126	42.98579	0.37641	3.48656	6.39560	4.26505	0.12329	2.05663	0.09378	8.10091	0.80779	-2.79246
15YP08-119	2394.21390	81.05184	2485.13338	44.68161	2485.13338	45.46396	0.44977	4.07839	10.55922	4.92477	0.17035	2.46454	0.11759	5.42066	0.82468	6.48771
15YP08-047	2400.70746	74.34884	2503.32410	40.84431	2587.64522	40.97334	0.45123	3.73981	10.76817	4.48573	0.17316	2.49055	0.11702	6.48392	0.82635	7.22424
15YP08-016	2568.93830	73.42761	2598.57479	37.27028	2621.75854	33.97915	0.48960	3.48335	11.92556							

Table 2. LA-ICP-MS Zircon isotopic and Age Data Table 155002: Murudun-Goyukc classic

Sample-Grain #	Dates (Ma)		207Pb/235U age		207Pb/206Pb age		Isotopic Ratios		207Pb/235U c		207Pb/206Pb c		208Pb/232Th c		ε ₂	Rho (g)	% disc b
	z10	z20	z10	z20	z10	z20	z10	z20	z10	z20	z10	z20	z10	z20			
155002-001	66.6932	4.8018	75.6478	78.5943	488.0487	154.1393	0.0140	7.23743	0.08160	10.29377	0.05694	7.32780	0.00028	791.58821	0.00083	86.33483	
155002-005	73.8762	2.7937	78.4893	75.7222	221.39007	200.8400	0.0153	3.80522	0.08037	9.93996	0.04000	9.24335	0.00123	790.47900	0.00054	66.62287	
155002-011	74.04646	5.4027	76.0214	8.4027	5.4027	14.04646	0.0158	6.40909	0.08164	10.29377	0.05694	7.32780	0.00028	791.58821	0.00083	86.33483	
155002-016	74.20378	2.0413	8.4012	68.2113	110.2571	274.0655	0.0158	4.11355	0.07024	12.80055	0.04422	12.12355	0.00141	791.78889	0.00164	107.0585	
155002-019	75.05208	6.5818	95.2621	5.00127	6.5818	10.0137	0.0170	4.09137	0.07733	9.0428	0.04258	8.05551	0.00193	800.87051	0.00204	201.2596	
155002-018	75.02021	4.0656	74.5310	74.9091	58.6035	207.0093	0.0171	5.44658	0.07616	10.74297	0.04721	9.25992	0.00198	856.87750	0.00622	-28.02887	
155002-017	75.83728	8.0261	85.8864	65.1786	462.1230	139.2577	0.0176	4.97375	0.07707	7.70700	0.04643	6.56421	0.00189	805.50147	0.00520	63.69378	
155002-004	75.54587	3.6019	81.5306	9.5064	260.7463	238.8877	0.0179	4.79638	0.08361	12.18327	0.05147	11.19942	0.00160	811.79515	0.00265	70.27500	
155002-078	76.38603	7.2939	76.0044	204.0236	40.1828	383.1618	0.0187	3.67887	0.08250	10.55808	0.05022	8.38450	0.00150	795.86492	0.00180	62.55814	
155002-028	76.7064	2.9310	81.9590	5.7285	229.12018	177.8597	0.0197	3.84480	0.08374	7.32128	0.04076	6.23046	0.00180	841.20816	0.00117	66.52209	
155002-011	79.0062	9.3167	80.9241	79.0062	162.20032	206.9009	0.0222	3.37628	0.08428	14.88822	0.04622	9.40597	0.00211	831.08309	0.00653	51.58651	
155002-030	79.9758	3.3958	7.93957	9.05209	209.9553	101.101	0.0249	4.45949	0.07955	10.28501	0.04624	9.27898	0.00190	804.37900	0.00140	-75.83517	
155002-073	77.15804	3.2125	8.2322	219.8032	247.6240	102.104	0.0240	4.1952	0.08393	11.68933	0.05167	11.56673	0.00157	794.62935	0.00286	64.89630	
155002-090	77.2448	3.8105	91.3808	446.9976	209.4278	209.4278	0.0205	4.2565	0.07583	10.96204	0.05588	10.07911	0.00151	801.15373	0.02566	82.70415	
155002-075	77.27278	2.8274	77.0033	68.52106	218.7384	192.2577	0.0206	3.87955	0.08798	10.94346	0.04740	9.81729	0.00158	795.34951	0.00238	-42.73708	
155002-010	77.62808	2.8941	80.3037	3.75454	166.58031	158.79075	0.0211	3.75454	0.08230	8.08580	0.04929	7.13042	0.00175	820.47873	0.00384	51.65847	
155002-022	77.88119	3.7364	81.9240	178.7499	282.18189	102.215	0.0215	4.82702	0.08314	14.00939	0.04963	13.12319	0.00190	801.92005	0.00278	55.93584	
155002-080	79.70480	2.8932	82.4834	79.70480	162.20032	206.9009	0.0222	3.37628	0.08428	14.88822	0.04622	9.40597	0.00211	831.08309	0.00653	51.58651	
155002-083	79.38081	2.5497	71.3931	6.45888	38.84319	182.40746	0.0223	3.37628	0.07993	8.72280	0.04642	8.80824	0.00163	798.50212	0.00279	-81.39778	
155002-065	78.55925	2.8104	81.6557	171.70424	158.6712	102.216	0.0226	3.59971	0.08369	7.98674	0.04786	7.12953	0.00167	793.09220	0.00856	54.24719	
155002-024	78.58000	3.4179	82.8589	7.2745	207.92216	176.5005	0.0226	4.3717	0.08052	9.17429	0.05030	8.06275	0.00162	804.78352	0.00782	62.20701	
155002-077	78.83500	3.0764	80.8026	8.37679	156.62857	102.8038	0.0230	3.52495	0.08238	10.46858	0.04858	10.15312	0.00182	795.42889	0.00540	37.74551	
155002-036	78.96110	6.2743	82.8279	7.40959	209.04539	165.8188	0.0232	4.62344	0.08458	8.8363	0.05074	7.50204	0.00173	854.55842	0.00789	62.22777	
155002-021	79.00800	2.8072	80.7634	5.7240	121.57651	146.19570	0.0233	3.57631	0.08239	7.47403	0.04848	6.50103	0.00154	801.50304	0.03766	30.02244	
155002-020	79.12439	8.0362	81.6557	11.23093	157.10965	125.5962	0.0235	4.08125	0.08125	12.18743	0.05022	12.18743	0.00202	852.72862	0.00354	55.86522	
155002-044	79.24277	4.6352	88.2030	15.9145	337.9571	348.2864	0.0237	8.11438	0.09075	18.99272	0.05324	17.17209	0.00204	887.14162	0.03259	76.55232	
155002-023	79.38755	3.7493	82.5405	6.2396	174.75935	47.5334	0.0239	4.08469	0.08469	6.93359	0.04749	73.79412	0.00174	797.94112	0.01529	54.57322	
155002-043	79.57111	4.6357	82.9085	12.8326	188.83547	118.95169	0.0242	5.77320	0.08514	16.13264	0.04974	15.12884	0.00157	797.65545	0.02052	56.23847	
155002-075	79.79142	8.1343	83.5453	8.28645	138.67907	155.8363	0.0245	6.00523	0.08484	9.9986	0.04984	7.9921	0.00139	799.12139	0.02764	57.25688	
155002-085	79.86470	3.2642	81.5230	9.0636	217.49602	127.4147	0.0247	4.1185	0.08320	11.59886	0.05006	10.03067	0.00167	800.67376	0.03855	42.35500	
155002-076	79.95993	4.7601	75.8083	11.3277	139.31708	102.148	0.0248	5.82358	0.08422	10.51027	0.05077	14.77354	0.00148	797.78303	0.02719	250.24201	
155002-031	79.96480	7.3280	84.9636	7.2715	227.89004	166.2042	0.0248	4.60239	0.08728	8.81070	0.04704	7.75715	0.00204	846.63000	0.04836	64.91272	
155002-026	79.97782	8.1460	81.6557	7.1024	114.04508	144.3156	0.0248	4.31536	0.08438	9.41113	0.04838	8.47296	0.00174	798.42786	0.01277	76.21777	
155002-043	80.55022	4.4275	86.2638	10.8354	246.96793	255.8707	0.0257	5.5298	0.08842	13.22818	0.05109	12.01544	0.00212	846.96635	0.03688	66.2222	
155002-074	80.94700	8.48835	85.8885	9.78789	225.52348	433.768	0.0264	4.33768	0.08827	11.54222	0.05030	11.12608	0.00158	795.41334	0.02453	48.57004	
155002-019	81.05584	8.0804	84.5880	81.05584	81.05584	197.2495	0.0265	4.5297	0.08903	10.06662	0.04962	8.99327	0.00174	798.43296	0.03709	53.94913	
155002-082	81.29365	2.6357	80.9241	81.29365	472.0022	174.37840	0.0266	3.98464	0.08924	8.95224	0.05024	8.01626	0.00169	801.62766	0.00294	80.77761	
155002-003	81.32860	8.19423	80.9241	203.4566	166.46231	439.829	0.0269	4.84497	0.08624	10.26933	0.04983	10.26933	0.00161	816.48601	0.04138	49.34607	
155002-013	81.42205	3.10480	84.1838	7.7320	160.87652	174.37840	0.0271	3.8828	0.08935	9.61655	0.04930	8.81735	0.00181	805.01653	0.03384	48.38785	
155002-002	81.54025	8.0809	80.9241	81.54025	206.83104	194.2782	0.0272	4.58224	0.08923	10.26933	0.04983	10.26933	0.00161	801.62766	0.00294	80.77761	
155002-003	81.55504	4.25945	80.2767	37.40789	327.17461	127.17461	0.0273	5.25744	0.08228	12.45229	0.04989	11.28800	0.00180	801.62766	0.00294	75.08978	
155002-024	82.08093	4.48991	78.1149	168.14004	187.75834	101.296	0.0296	4.24487	0.08829	9.51162	0.04945	8.08829	0.00168	797.77903	0.00956	50.64772	
155002-013	83.08817	4.67889	84.2385	12.18532	123.0342	101.34814	0.0296	5.6677	0.08660	15.14889	0.04847	14.00461	0.00217	838.90000	0.02731	33.19179	
155002-018	84.94249	3.26357	84.2385	7.15231	161.706	128.6127	0.0302	6.7999	0.09125	12.18532	0.05126	12.18532	0.00217	838.90000	0.02731	33.19179	
155002-072	85.39083	3.2451	82.2493	5.21814	185.5962	190.9044	0.0333	3.85738	0.09077	6.91115	0.04940	4.96742	0.00177	791.08036	0.03500	48.43350	
155002-045	87.19488	4.3548	88.9842	18.41717	127.2984	188.41717	0.0362	5.08413	0.09159	12.47260	0.04880	11.41514	0.00250	848.6225	0.03866	38.48384	
155002-087	87.49398	3.54281	87.7478	7.7082	83.74608	188.2702	0.0367	4.07761	0.08985	9.34084	0.04771	8.40939	0.00200	800.50756	0.03570	-44.9511	
155002-016	87.58427	3.51884	80.9241	87.58427	80.9241	188.2702	0.0368	4.08469	0.09125	12.18532	0.05126	12.18532	0.00217	838.90000	0.02731	33.19179	
155002-007	87.58470	5.0667	86.6446	8.6474	203.54779	147.447	0.037	5.10010	0.09404	10.00000	0.05011	7.0725	0.00200	792.56456	0.03570	54.15451	
155002-004	92.64675	5.1717	102.0578	92.64675	102.0578	137.2487	0.0448	5.62380	0								

Table 3.1A-ICP/MS Zircon Isotope and Age Data Table 15YPO6-16YHM Trans-Marine

Sample-Grain #	Dates (Ma)				Isotopic Ratios											
	206Pb/238U age	±2σ	207Pb/235U age	±2σ	207Pb/206Pb age	±2σ	206Pb/238U c	±2σ	207Pb/235U c	±2σ	207Pb/206Pb c	±2σ	208Pb/232Th c	±2σ	‰	‰
15YPO6																
15YPO4-030	312.12882	11.35522	304.21488	19.17850	243.95184	140.07285	0.60961	3.73006	0.34933	7.36509	0.05109	6.35068	0.00991	270.45543	0.45822	-17.84600
15YPO4-019	316.08069	11.52337	312.79275	19.50599	288.32097	137.49374	0.60205	3.73909	0.36077	7.31999	0.05209	6.28999	0.00842	269.77785	0.48148	-6.62993
15YPO4-028	316.47949	11.74864	312.77006	21.21458	307.78545	146.21288	0.60522	3.81421	0.37145	7.37992	0.05371	6.30633	0.00962	270.78997	0.44524	-11.54900
15YPO4-028	316.47949	12.43104	302.73144	19.76732	195.82886	143.94540	0.60507	4.02552	0.34736	7.62533	0.05004	6.47630	0.00881	270.47441	0.48593	-61.76185
15YPO4-004	318.41891	11.11992	290.82160	20.29460	280.82160	145.96660	0.60563	3.58228	0.36390	7.56654	0.05215	6.68482	0.00814	269.52088	0.41811	-9.48843
15YPO4-011	313.54714	11.30981	325.13601	20.01867	365.35092	135.98139	0.60582	3.63095	0.37742	7.26670	0.05389	6.29453	0.00897	269.61226	0.46025	12.53993
15YPO4-025	319.98847	11.86122	321.87726	20.23617	302.23617	142.70704	0.60589	3.80262	0.37748	7.52826	0.05311	6.49756	0.00957	270.59499	0.49594	-3.71219
15YPO4-027	320.17517	11.57871	337.34913	18.85555	457.48571	117.74182	0.60592	3.71025	0.35048	6.64116	0.05615	6.50809	0.00932	270.13121	0.53265	30.01417
15YPO4-026	320.22355	10.74115	321.86664	18.11030	329.65931	123.70566	0.60593	3.44113	0.37323	6.63314	0.05304	5.67073	0.00899	270.04597	0.47292	2.86228
15YPO4-073	320.53003	10.66742	338.82888	21.57325	447.79035	142.21235	0.60598	3.41431	0.37966	7.57474	0.05631	6.76160	0.01003	273.34082	0.39484	30.88903
15YPO4-039	320.60895	11.85715	305.57179	21.39787	300.39788	172.80217	0.60599	4.05268	0.35080	8.97520	0.04995	7.82026	0.00966	272.71037	0.46027	-48.38807
15YPO4-016	320.61762	12.00372	320.86334	20.86334	286.48888	147.02249	0.60599	3.84139	0.36078	7.75142	0.05205	6.71923	0.00822	270.19192	0.44500	-40.01224
15YPO4-055	320.90446	12.30709	329.44933	23.52473	390.22091	156.12544	0.60594	4.23200	0.36827	8.49328	0.05499	7.12967	0.01137	272.18993	0.45327	17.76319
15YPO4-119	321.01773	11.67266	319.29574	19.29574	254.67211	136.40300	0.60596	3.73081	0.36120	7.22996	0.05133	6.13901	0.00908	277.89106	0.48916	-26.95139
15YPO4-017	321.26329	10.64540	322.94111	19.39179	335.09005	135.74256	0.60510	3.32296	0.37442	7.07747	0.05317	6.24888	0.00896	269.89435	0.41685	-41.21628
15YPO4-033	321.55714	11.94313	324.22219	21.05233	343.40545	147.03809	0.60515	3.49171	0.37618	7.64678	0.05337	6.80302	0.00962	270.45006	0.39549	6.36235
15YPO4-020	321.59475	12.00372	310.69475	17.74020	229.67897	126.97815	0.60515	3.46614	0.35797	6.68883	0.05078	5.71835	0.00862	269.80136	0.48925	-40.01224
15YPO4-081	322.03903	11.37912	333.95884	25.31946	417.89556	142.21235	0.60522	3.62574	0.38944	9.00848	0.05516	8.24661	0.00970	273.99620	0.32180	22.93988
15YPO4-012	322.05663	10.75007	309.47401	18.79048	215.84444	138.25044	0.60522	3.47295	0.35933	7.11264	0.05047	6.23027	0.00854	269.56662	0.40113	-49.19487
15YPO4-015	322.07427	11.21298	314.54767	17.55636	259.03601	122.36519	0.60523	3.57400	0.36111	6.54721	0.05143	5.48547	0.00888	269.89039	0.51460	-44.33571
15YPO4-071	322.39025	12.30141	328.80049	22.27327	371.05656	147.88828	0.60528	4.20240	0.38183	8.02628	0.05402	6.83820	0.01034	273.22958	0.49343	13.11560
15YPO4-041	322.56344	12.72556	323.25007	20.78007	328.37305	139.13865	0.60531	4.08706	0.37487	7.93810	0.05301	6.41285	0.00938	270.67941	0.50607	1.79329
15YPO4-027	322.65337	12.12038	317.20862	18.61552	271.39989	123.96168	0.60531	3.68621	0.36170	6.91281	0.05090	6.18016	0.00909	272.82272	0.49452	-45.31616
15YPO4-047	322.96537	11.73771	336.04186	21.47591	394.06186	145.50436	0.60538	3.72957	0.37664	7.61300	0.05337	6.86337	0.00967	271.44818	0.42978	3.89332
15YPO4-067	324.01840	12.77539	328.15559	23.72832	357.28192	124.45754	0.60555	4.04672	0.36472	8.10508	0.05370	5.71797	0.01061	272.25545	0.54745	9.31016
15YPO4-009	324.16271	11.50109	327.22648	18.38849	349.07778	123.42797	0.60529	3.64377	0.38026	6.61343	0.05300	5.54436	0.00855	269.37901	0.51865	7.13740
15YPO4-079	324.16271	12.12038	322.94111	20.68681	271.39989	123.96168	0.60529	3.47847	0.36170	6.91281	0.05090	6.18016	0.00909	272.82272	0.49452	-45.31616
15YPO4-018	324.51072	13.84942	333.41416	21.10810	396.00817	122.04248	0.60516	3.48081	0.38889	7.54055	0.05463	6.13771	0.00963	270.03126	0.54386	18.05544
15YPO4-061	325.26178	11.83891	314.18802	18.52115	134.18802	122.04248	0.60517	3.73584	0.37974	6.79974	0.05268	5.60960	0.00964	271.99417	0.53453	-3.52457
15YPO4-034	325.52415	10.94044	324.60672	18.23979	318.03151	123.42797	0.60529	3.65060	0.37670	6.62211	0.05277	5.62026	0.00894	270.37905	0.48764	-2.35594
15YPO4-111	325.58010	12.58113	321.86107	20.68681	271.39989	123.96168	0.60529	3.47847	0.36170	6.91281	0.05090	6.18016	0.00909	272.82272	0.49452	-45.31616
15YPO4-039	326.23029	11.31167	318.43567	18.48323	117.43567	135.55979	0.60519	3.58989	0.37744	6.70398	0.05276	5.68128	0.00908	270.67941	0.50607	-2.77052
15YPO4-006	326.31644	12.92908	330.01838	19.84668	356.20417	126.98822	0.60532	4.08733	0.38403	7.12700	0.05343	6.09594	0.00954	275.15968	0.54029	3.99682
15YPO4-005	326.41029	12.28594	324.31339	19.81479	339.28951	122.90506	0.60534	3.86973	0.37630	7.20745	0.05267	6.08432	0.00927	269.13701	0.51185	-5.53722
15YPO4-012	326.41029	12.92908	330.01838	19.84668	356.20417	126.98822	0.60534	4.08733	0.38403	7.12700	0.05343	6.09594	0.00954	275.15968	0.54029	3.99682
15YPO4-006	327.69705	10.83053	323.15221	17.90097	290.52982	122.56406	0.60515	3.39261	0.37473	6.52500	0.05214	5.57387	0.00924	269.45680	0.48934	-41.72921
15YPO4-077	327.75036	12.54213	346.75229	20.02903	476.10212	124.03811	0.60516	3.61514	0.40706	6.86219	0.05663	5.86091	0.01069	271.45482	0.48064	31.15985
15YPO4-032	327.86612	10.72425	336.73983	19.61478	338.49588	129.82886	0.60528	3.36019	0.39325	6.91061	0.05489	6.03888	0.00929	270.28748	0.45127	17.72959
15YPO4-017	327.88140	12.44687	317.20862	18.61552	271.39989	123.96168	0.60528	3.47847	0.36170	6.91281	0.05090	6.18016	0.00909	272.82272	0.49452	-45.31616
15YPO4-027	328.02543	10.75483	315.80798	18.39798	185.80798	127.48507	0.60520	3.36559	0.38607	6.59636	0.05306	5.63610	0.00908	270.67941	0.47852	7.81361
15YPO4-047	328.22423	11.94800	326.58455	19.26768	314.91196	131.44443	0.60523	3.50295	0.37938	6.95519	0.05270	6.02082	0.00958	271.85547	0.47926	-4.22730
15YPO4-070	328.29753	10.54411	323.62819	17.92575	290.45198	122.79341	0.60524	3.39732	0.37537	6.52995	0.05214	5.61627	0.00932	272.26445	0.47471	-11.01611
15YPO4-109	328.46445	10.73022	319.29574	19.44201	254.45193	139.00508	0.60527	3.46869	0.37608	7.12713	0.05137	6.11816	0.00959	273.68730	0.43120	-18.30840
15YPO4-126	328.81477	11.85011	346.74684	22.57091	468.70361	144.23748	0.60533	3.69998	0.40705	7.26995	0.05644	6.81345	0.00956	271.97466	0.43365	29.84931
15YPO4-115	328.83208	12.05337	312.90904	17.29006	188.84216	118.61368	0.60523	3.76311	0.35883	6.98219	0.05285	5.28760	0.00949	271.45776	0.56120	-19.13065
15YPO4-100	328.87129	12.74970	333.18398	24.78355	363.39130	158.44405	0.60524	3.98045	0.38839	8.83271	0.05384	7.88497	0.00992	276.19253	0.40129	9.49885
15YPO4-128	329.09796	11.65660	328.86688	19.04535	327.47713	126.28797	0.60528	3.44287	0.38251	6.84925	0.05295	5.91866	0.01004	279.29065	0.46067	-4.04862
15YPO4-004	329.21751	11.06880	329.79550	18.50588	333.87587	123.41893	0.60540	3.45732	0.38375	6.63093	0.05314	5.65829	0.01002	275.01755	0.49029	1.95254
15YPO4-008	329.34177	10.99804	322.58581	17.06002	292.19639	115.81386	0.60542	3.42853	0.37365	6.22891	0.05172	5.20555	0.00864	269.37905	0.52520	-39.99417
15YPO4-127	329.59894	11.73476	331.88146	19.12667	348.71217	125.14246	0.60546	3.65548	0.38673	6.81846	0.05349	5.75880	0.00981	279.29756	0.50814	5.48109
15YPO4-068	329.67395	12.84487	317.20862	18.61552	271.39989	123.96168	0.60547	3.48025	0.38423	6.84774	0.05453	5.48827	0.00881	272.42079	0.59416	-15.90122
15YPO4-045	329.79348	11.83310	319.38644	19.30704	284.15613	133.51544	0.60549	3.68988	0.38664	7.07575	0.05110	6.04207	0.00979	271.02598	0.48735	-35.07483
15YPO4-021	329.84012	12.28242	327.10869	19.33205	348.22189	127.48507	0.60550	3.82347	0.38018	6.97907	0.05255	5.83734	0.00942	275.65505	0.51928	-7.01385
15YPO4-085	329.95314	11.82198	325.90655	20.72086	306.81233	117.41937	0.60552	4.02180	0.41561	7.02223						

Table 3 cont: LA-ICP-MS Zircon isotopic and Age Data Table 15VP07 & 15VP11, SGTW volcanic

Sample-Grain #	Dates (Ma)		207Pb/235U age		207Pb/206Pb age		Isotopic Ratios		207Pb/235U c		207Pb/206Pb c		δ ² ‰	Rho (g)	% disc b	
	207Pb/235U age	z	z	z	z	z	z	z	z	z	z	z				
15VP11-001	47.45103	4.15216	77.86612	20.29293	1339.72756	446.41474	0.07939	8.78548	0.07917	27.51574	0.07776	26.07549	0.00399	35.71389	0.14856	95.83800
15VP11-002	47.98008	3.51600	62.53335	13.50997	662.58742	400.44584	0.07447	7.35721	0.06352	22.52543	0.06149	21.92027	0.00379	19.88044	0.00000	92.75854
15VP11-003	48.03249	2.91337	58.47466	14.24749	521.25251	319.27387	0.07857	6.13441	0.06002	14.60995	0.05629	12.31931	0.00068	12.22029	0.00000	95.66991
15VP11-004	49.14442	7.94747	55.26256	17.38829	389.80365	389.80365	0.07566	7.68576	0.05943	20.98021	0.05299	19.44434	0.00259	19.44434	0.23277	84.97650
15VP11-005	49.78620	3.31117	63.09214	9.48958	602.51089	276.65288	0.07755	6.67821	0.06411	15.58501	0.06000	14.08170	0.00206	17.08142	0.29357	91.73688
15VP11-006	49.84220	2.94711	60.82960	9.85386	517.96116	316.61595	0.07775	5.93712	0.06411	16.76700	0.05771	15.84661	0.00316	17.68408	0.13827	90.37723
15VP11-007	49.94335	2.97443	48.98388	9.21489	2.33055	338.01885	0.07878	5.62321	0.04942	15.42322	0.04611	14.62637	0.00222	9.43318	0.39985	26.023071
15VP11-008	49.94680	2.13800	50.76555	4.37553	89.59826	169.41600	0.07878	4.65978	0.05237	8.85632	0.04783	7.52131	0.00249	7.87463	0.46407	44.25272
15VP11-009	50.13504	2.51603	54.86037	6.62273	266.40327	241.95459	0.07881	5.03903	0.05552	12.44556	0.05159	11.37543	0.00242	11.61859	0.32609	81.18077
15VP11-010	50.14615	3.48490	71.36336	16.07512	850.81262	409.05483	0.07881	6.97958	0.07260	23.57599	0.06746	22.51948	0.00335	22.56660	0.11982	94.10738
15VP11-011	50.20221	5.01100	115.09620	25.13401	1833.49048	341.47515	0.07885	9.98128	0.12003	33.86668	0.11090	31.49715	0.00261	28.97396	0.00000	97.23236
15VP11-012	50.21887	3.01469	62.94147	9.89722	578.80689	298.76078	0.07881	6.03223	0.06395	16.28417	0.05937	15.33661	0.00258	13.89594	0.20551	93.24613
15VP11-013	50.40999	3.27989	67.78540	12.77039	734.72224	349.15170	0.07885	6.53473	0.06904	19.59827	0.06382	18.47527	0.00374	17.52111	0.11121	93.14013
15VP11-014	50.40935	4.01304	63.72210	10.49566	597.64455	297.01305	0.07885	7.99455	0.06477	17.07481	0.05986	15.08762	0.00285	19.14019	0.28386	91.56561
15VP11-015	50.41594	3.10434	54.29027	9.48075	228.78813	350.10496	0.07885	6.18205	0.05492	18.01808	0.05076	16.92398	0.00265	23.28280	0.16189	97.96392
15VP11-016	50.42621	5.01100	115.09620	25.13401	1833.49048	341.47515	0.07885	9.98128	0.12003	33.86668	0.11090	31.49715	0.00261	28.97396	0.00000	97.23236
15VP11-017	50.50281	3.63295	60.65109	12.02640	482.18008	378.62284	0.07887	7.22567	0.04355	20.66183	0.04678	19.35794	0.00254	17.98986	0.21808	89.52594
15VP11-018	50.51423	8.42123	88.10822	28.13819	1282.63129	283.88819	0.07887	8.80137	0.10962	17.37826	0.08861	16.95012	0.00247	28.65500	0.14945	96.06467
15VP11-019	50.52918	3.97971	68.55685	11.78102	754.05739	315.55394	0.07887	6.71664	0.06985	17.87458	0.06441	16.46444	0.00377	23.86395	0.18977	93.29898
15VP11-020	50.61630	2.98442	53.62022	7.34668	189.73936	273.73261	0.07888	5.91535	0.05422	14.11599	0.04991	12.61678	0.00247	13.55586	0.30555	92.33362
15VP11-021	50.73048	5.02843	65.75557	13.73724	390.36532	390.36532	0.07900	9.95460	0.06980	22.92662	0.06444	20.63275	0.00383	25.45805	0.30659	92.23962
15VP11-022	50.79094	3.65542	16.10174	6.7734221	446.67546	607.0791	0.07901	7.03800	0.06212	25.20108	0.06212	24.20052	0.00400	22.17099	0.15943	92.50144
15VP11-023	50.85823	2.96610	59.46589	9.97966	421.46546	328.59102	0.0792	5.85647	0.06031	17.83656	0.05325	16.34810	0.00292	18.23804	0.22225	97.92829
15VP11-024	50.88988	3.97912	58.97900	9.49567	602.04217	290.98822	0.07939	7.85163	0.06456	16.92088	0.06031	16.48248	0.00291	24.97614	0.36848	97.26527
15VP11-025	50.95971	3.67878	56.27659	11.94270	388.97800	434.69817	0.0794	7.26778	0.05699	21.94375	0.05210	20.79236	0.00281	20.48049	0.29998	82.35900
15VP11-026	50.97509	3.21888	59.55210	9.45201	419.64747	308.10078	0.0794	6.34119	0.06040	16.49793	0.05721	15.19796	0.00251	19.27601	0.20405	87.82588
15VP11-027	51.09559	4.06925	68.38988	11.14723	727.38827	288.27026	0.0795	8.00686	0.06967	19.54699	0.06360	18.29986	0.00368	17.54951	0.02801	92.28318
15VP11-028	51.11786	3.21786	61.70759	11.66682	587.39684	322.12802	0.0796	7.42594	0.06512	18.02512	0.06041	16.94968	0.00341	19.31559	0.13754	93.48344
15VP11-029	51.08688	2.86287	57.57125	6.69203	220.40439	376.62744	0.0796	5.62741	0.05430	11.84714	0.05310	10.43203	0.00217	10.43203	0.14173	84.81349
15VP11-030	51.14308	3.48643	11.79254	3.665023	380.34002	607.997	0.0797	6.60789	0.05919	20.95556	0.05919	19.05116	0.00334	21.36203	0.27206	86.04578
15VP11-031	51.25225	3.76789	66.76032	11.84200	665.37958	325.59368	0.0798	7.38249	0.06796	18.43521	0.06178	16.88248	0.00329	20.04816	0.20987	92.29729
15VP11-032	51.32338	3.52338	54.09255	6.72056	179.30203	213.68795	0.0798	6.64656	0.05712	12.79959	0.04969	10.92265	0.00218	10.92265	0.44454	97.99735
15VP11-033	51.32277	4.05346	54.17158	11.51938	182.05223	438.10461	0.0799	7.93196	0.05480	18.19624	0.04974	16.20797	0.00312	20.53015	0.22738	71.80876
15VP11-034	51.32392	3.82159	31.15491	5.14288	54.14288	311.5491	0.0799	6.42100	0.05191	15.74469	0.04712	14.34493	0.00210	14.91764	0.10173	93.20651
15VP11-035	51.36952	3.42723	63.62268	9.30288	539.12007	274.44379	0.0800	6.69133	0.06425	15.24471	0.06027	13.97791	0.00295	15.28255	0.28654	90.47160
15VP11-036	51.38841	3.12786	61.84259	11.66682	587.39684	322.12802	0.0800	7.42594	0.06512	18.02512	0.06041	16.94968	0.00341	19.31559	0.13754	93.48344
15VP11-037	51.38811	2.92373	60.20321	10.85197	354.90647	354.90647	0.0800	5.71516	0.06108	17.82419	0.05538	16.74429	0.00267	18.95928	0.21642	87.95183
15VP11-038	51.40643	2.66613	56.05753	5.51279	259.62808	197.05256	0.0801	5.20815	0.05676	10.50437	0.05043	9.14238	0.00231	8.84978	0.14547	80.19486
15VP11-039	51.42097	3.16226	57.23596	8.90959	308.34786	306.79544	0.0801	6.18289	0.05799	16.69791	0.05255	14.84448	0.00309	14.94252	0.22950	83.32588
15VP11-040	51.48648	3.42446	66.39385	12.28627	640.68666	402.20964	0.0802	6.64656	0.06512	16.92088	0.06115	16.55614	0.00291	16.55614	0.24953	92.96735
15VP11-041	51.50450	3.54701	55.83226	10.00869	445.68700	353.73900	0.0802	6.91624	0.05653	15.51482	0.05113	13.71422	0.00318	20.60949	0.20207	79.03661
15VP11-042	51.51986	3.41695	50.74851	14.50371	321.16465	616.6400	0.0802	6.63404	0.04634	14.15945	0.04634	12.53374	0.00274	20.53374	0.30053	-25.54581
15VP11-043	51.57320	4.06787	54.74510	9.80616	395.95762	352.26368	0.0803	7.97979	0.05540	18.64789	0.05004	16.95958	0.00376	13.05543	0.03809	73.67087
15VP11-044	51.57713	3.68668	71.40769	13.66682	607.39684	322.12802	0.0804	8.04123	0.06800	21.57131	0.06800	20.34811	0.00441	19.31559	0.13754	93.48344
15VP11-045	51.57731	2.60159	49.58068	5.41370	226.02175	607.997	0.0806	5.62741	0.05430	11.84714	0.05310	10.43203	0.00217	10.43203	0.14173	84.81349
15VP11-046	51.60217	3.07799	76.24905	15.80770	387.05171	387.05171	0.0807	7.91543	0.07012	22.68821	0.07012	21.08166	0.00473	21.08166	0.14317	94.43358
15VP11-047	51.82991	3.09823	69.58884	11.72396	730.39118	313.46610	0.0807	6.03223	0.07085	17.35189	0.06369	16.49335	0.00355	22.66672	0.24631	93.20203
15VP11-048	51.87511	3.27790	64.73931	11.31439	678.88463	313.29575	0.0809	6.45051	0.06483	18.42327	0.06012	16.96262	0.00237	15.83905	0.24893	92.96735
15VP11-049	51.88335	3.00010	57.31599	7.74336	290.46032	266.41369	0.0808	6.80705	0.05807	13.94794	0.05214	12.88151	0.00264	14.88470	0.12518	82.14983
15VP11-050	51.90597	3.69561	65.33214	13.86669	589.81348	392.83497	0.0808	7.15058	0.05965	12.77703	0.05965	10.50960	0.00347	18.57295	0.18746	91.19968

Table 4. LA-ICP-MS Zircon Isotope and Age Data Table: 156201: Mardun-Goyuk volcanic

Sample/Grain #	Dates (Ma)		Isotopic Ratios													
	207Pb/235U age	±2σ	207Pb/235U age	±2σ	207Pb/206Pb age	±2σ	207Pb/235U c	±2σ	207Pb/235U c	±2σ	207Pb/206Pb c	±2σ	208Pb/232Th c	±2σ	Th/U (a)	δ ⁷¹⁰ b
156201																
15G1-069	71.64040	5.5840	70.65731	6.07350	71.50734	100.45457	0.01138	7.80530	0.02707	8.92492	0.04679	4.32798	0.00321	21.25453	0.87340	-91.00370
15G1-056	73.23392	5.71751	77.85820	11.12078	222.20420	269.60925	0.01143	7.85511	0.07970	14.91954	0.05061	12.68424	0.00340	24.35878	0.48073	67.04206
15G1-049	74.01874	5.52419	82.10409	10.42430	323.15643	231.43697	0.01155	7.50735	0.08422	13.28475	0.05290	10.46012	0.00345	22.59370	0.53514	77.11721
15G1-062	76.131274	6.17232	94.25040	15.39891	633.70186	291.11154	0.01159	8.35648	0.09727	17.21644	0.06087	15.07518	0.00640	28.41613	0.41056	88.27234
15G1-035	74.78218	5.38256	75.97376	7.17021	113.62420	149.42975	0.01167	7.25956	0.07769	9.82990	0.04811	6.61159	0.00318	21.58237	0.72177	34.18464
15G1-058	75.12693	5.60480	76.99781	8.18363	135.40019	181.09795	0.01172	7.50726	0.07878	11.08106	0.04876	8.15052	0.00318	20.97780	0.69313	44.53947
15G1-063	73.13139	5.80940	88.45248	12.57385	464.66516	260.08704	0.01172	7.78098	0.09102	14.93821	0.05634	12.75372	0.00362	23.92104	0.46365	83.83037
15G1-027	75.31849	5.49027	78.85881	7.03847	187.46258	129.70870	0.01175	7.28029	0.08076	9.30871	0.04986	5.80062	0.00318	21.22155	0.76091	59.82159
15G1-089	75.33653	5.73397	82.10358	9.62458	281.61845	205.65900	0.01176	8.05911	0.08414	12.27116	0.05194	6.00311	0.00311	22.12278	0.59684	73.24872
15G1-034	75.41464	5.64023	112.10771	10.57073	984.47426	128.87273	0.01177	7.52608	0.11674	10.01121	0.07198	6.60170	0.00435	20.93165	0.72177	92.33960
15G1-026	75.46599	5.86489	80.58209	11.11526	355.02352	258.02762	0.01178	7.82070	0.08260	14.42711	0.05089	12.12346	0.00296	22.79308	0.49605	67.89033
15G1-082	75.53198	5.71282	73.50529	7.30086	81.07197	169.16145	0.01179	7.61122	0.07508	10.62750	0.04621	7.40274	0.00401	20.62442	0.70425	-855.23178
15G1-059	75.64037	6.07951	81.84022	9.47954	266.77219	194.64784	0.01180	8.08845	0.08394	12.11250	0.05160	9.01607	0.00312	22.06647	0.64452	71.64608
15G1-083	75.65434	5.65318	76.04306	8.74566	88.27841	207.59736	0.01181	7.51961	0.07772	11.98852	0.04780	9.33702	0.00326	22.36342	0.95932	14.30029
15G1-061	75.66797	5.80339	79.07445	11.04019	383.18852	265.48160	0.01181	7.72079	0.08099	14.59218	0.04977	12.38229	0.00320	24.82363	0.48274	58.68943
15G1-012	76.01287	5.47556	78.44885	7.85077	152.07319	167.14156	0.01186	7.24720	0.08032	10.49397	0.04912	7.51390	0.00313	21.35132	0.67200	50.18994
15G1-095	76.04787	5.70004	88.38770	12.26554	455.47839	256.07044	0.01187	7.54937	0.09095	14.57760	0.05034	12.47437	0.00314	22.65563	0.48272	52.55296
15G1-060	76.17139	5.92910	79.33342	11.01416	175.63478	262.52265	0.01189	7.83318	0.08126	14.51136	0.04961	12.21535	0.00319	24.47590	0.49142	66.63800
15G1-029	76.22735	5.84677	89.81491	14.92446	470.33827	311.93710	0.01189	7.71913	0.09159	17.47700	0.05648	15.07995	0.00323	21.96710	0.41518	83.79308
15G1-028	76.28129	6.00629	80.61656	10.88578	210.39523	290.63992	0.01190	7.92004	0.08163	14.12741	0.05037	11.05957	0.00318	22.73844	0.52123	63.83568
15G1-093	76.33890	5.92842	86.28239	13.31111	170.93704	291.34249	0.01191	7.81559	0.08869	16.19807	0.05402	14.18781	0.00297	24.73978	0.42445	79.41998
15G1-022	76.36497	5.71618	81.91633	10.33688	246.95833	221.13884	0.01192	7.53111	0.08402	13.20176	0.05116	10.84553	0.00344	23.22529	0.53808	69.07723
15G1-036	76.43395	5.29139	73.26121	7.98615	-25.73365	201.31644	0.01193	6.96662	0.07492	11.32836	0.04558	8.93121	0.00330	21.74262	0.58937	397.02721
15G1-025	76.44165	5.57052	75.51728	8.68426	146.56564	200.07032	0.01193	7.57675	0.07721	11.98381	0.04606	9.23464	0.00318	21.92171	0.58793	-64.90882
15G1-032	76.45761	5.73539	74.59656	11.35622	186.55512	101.19193	0.01193	7.54933	0.07623	11.16034	0.04632	8.21954	0.00338	22.44672	0.65224	-397.89356
15G1-008	76.64439	5.60925	82.04789	8.32400	242.33843	166.90009	0.01196	7.36313	0.08416	10.60412	0.05106	7.62884	0.00311	22.81472	0.66611	68.37300
15G1-048	76.67479	5.73732	84.07579	14.92446	299.20351	396.57962	0.01197	7.52588	0.08831	19.05252	0.05234	17.30313	0.00309	22.12382	0.36924	74.37370
15G1-071	76.69075	5.93921	108.74462	10.10940	683.86455	330.32664	0.01197	8.33815	0.11904	9.85229	0.06854	6.57412	0.00295	22.24504	0.71465	139.32325
15G1-090	76.74361	5.70149	84.64935	10.53758	313.80090	226.41840	0.01198	7.47688	0.08694	13.04216	0.05267	10.68617	0.00795	21.15045	0.54285	75.54885
15G1-033	77.13340	8.83110	82.14067	10.16107	230.29251	225.35017	0.01204	7.60851	0.08426	12.94208	0.05079	10.46938	0.00329	23.13342	0.54176	66.50033
15G1-011	77.13391	5.53733	83.20229	14.21167	579.09953	286.78482	0.01204	7.19870	0.09626	16.05133	0.05802	14.34679	0.00315	23.09039	0.40838	85.43780
15G1-003	77.18946	5.57556	75.17790	8.65235	131.59555	215.54115	0.01205	7.21976	0.07885	11.99150	0.04629	9.57451	0.00295	21.96537	0.56772	-668.30999
15G1-019	77.28597	6.00322	82.40017	11.14715	223.36165	251.88405	0.01206	7.81784	0.08454	14.16156	0.05086	11.80081	0.00311	23.89937	0.50434	66.88146
15G1-023	77.30195	5.61812	76.57389	7.64635	53.90818	167.69638	0.01206	7.31392	0.07833	10.40598	0.04711	7.40011	0.00302	22.57850	0.68027	-43.39558
15G1-066	77.32753	5.77385	86.45289	10.44734	346.30994	215.68453	0.01207	7.51238	0.08887	12.67126	0.05344	10.10416	0.00306	23.21814	0.61742	77.67487
15G1-065	77.40266	6.40978	89.42338	8.68426	-197.66456	304.55333	0.01208	8.36106	0.07076	15.79719	0.04620	13.34416	0.00354	22.96781	0.47521	139.18255
15G1-037	77.41364	5.78684	81.10213	8.68081	191.14514	181.91599	0.01208	7.52357	0.08315	11.18445	0.04994	8.27574	0.00330	21.42799	0.65308	59.50008
15G1-080	77.43355	5.59299	83.21707	252.13272	185.19726	0.01208	7.26957	0.08541	11.20768	0.05355	10.28026	0.00355	25.81376	0.62009	69.33722	
15G1-092	77.51235	5.55370	76.56667	8.70020	47.14602	210.46518	0.01210	7.21119	0.07852	11.84740	0.04698	9.33998	0.00307	22.72500	0.58258	-64.40913
15G1-086	77.52000	5.49876	79.26850	7.30661	132.22780	151.20838	0.01210	7.13894	0.08120	9.88800	0.04870	8.61244	0.00311	21.48008	0.76811	41.32739
15G1-002	77.53587	5.30865	73.30865	5.82795	582.60795	246.61529	0.01210	7.93069	0.09914	14.62703	0.05945	12.29041	0.00345	24.03128	0.49037	86.69159
15G1-015	77.54252	5.80927	100.60397	11.12866	688.61022	179.72224	0.01210	7.54027	0.10415	11.68280	0.06245	9.82369	0.00423	22.77853	0.62061	88.73927
15G1-067	77.55185	6.03235	78.73315	9.32632	114.73287	211.72952	0.01210	7.81720	0.08963	12.36737	0.04834	9.58499	0.00345	23.14326	0.61190	32.40660
15G1-094	77.72304	6.30991	79.44964	10.42262	131.68673	239.24659	0.01213	8.23027	0.08139	13.79869	0.04869	10.95664	0.00335	22.76566	0.37096	40.97884
15G1-040	77.72606	5.83353	79.98741	8.46905	148.06473	179.07779	0.01213	7.55399	0.08196	11.05654	0.04903	8.07367	0.00322	22.72736	0.66246	47.50535
15G1-085	77.81626	7.85997	74.08648	7.85997	-44.67459	184.47092	0.01214	7.58158	0.07569	11.04363	0.04522	8.02813	0.00312	22.55756	0.68251	274.18460
15G1-088	77.89417	5.63590	75.21484	6.98425	-5.46910	146.88009	0.01216	7.25046	0.07700	9.65532	0.04596	6.34664	0.00318	21.91939	0.73127	1524.25814
15G1-030	77.91040	5.69584	80.63466	8.20443	162.07927	173.07136	0.01216	7.31006	0.08365	10.62720	0.04932	7.13165	0.00319	21.44487	0.67001	51.92950
15G1-070	78.00649	5.77867	79.11838	11.82755	168.44091	0.01217	7.45619	0.08104	10.58889	0.04840	10.99400	0.00300	21.99404	0.67995	30.86220	
15G1-079	78.04812	6.05198	79.94255	8.93967	136.92335	192.33752	0.01218	7.80486	0.08191	11.67994	0.04879	6.68937	0.00348	21.92339	0.63844	43.00243
15G1-066	78.11234	5.87081	79.40384	9.35447	118.43998	214.07718	0.01219	7.56493	0.08134	12.30410	0.04861	9.70975	0.00299	22.77824	0.59541	34.04800
15G1-015	78.15329	6.12913	91.46781	13.01021	454.51825	295.96716	0.01220	7.88977	0.09426	14.98978	0.05007	12.71886	0.00311	23.33040	0.49613	82.79724
15G1-006	78.26195	5.52313	83.25220	228.86810	0.01222	7.10120	0.08545	7.05219	0.05076	8.42906	0.00274	21.44479	0.61755	65.80478		
15G1-021	78.32114	5.66204	84.93716	9.52090	274.38443	198.43975	0.01222	7.27646	0.08723	11.74231	0.05178	9.21603	0.00346	22.43175	0.58556	74.47648
15G1-072	78.32632	5.71310	99.03192	12.96192	631.47502	234.10101	0.0122									

Table 5: LA-ICP-MS Zircon Isotopic and Age Data Table (IGOR PRO): 15YP12 & 15YP13: SGTFW-SGTWH Basement/Volcanoclastic

Sample Grain #	Dates (Ma)				Isotopic Ratios								Rho (g)	% disc b
	206Pb/238U age	±2σ	207Pb/235U age	±2σ	207Pb/206Pb age	±2σ	206Pb/238U c	±2σ	207Pb/235U c	±2σ	207Pb/206Pb c	±2σ		
15YP12														
15YP12-004.FIN2	312.7	4	315.1	6.6	313	43	0.04970	1.30785	0.36430	2.44304	0.05280	3.00300	0.09531	0.09585
15YP12-036.FIN2	313	5.2	314.8	8.7	346	37	0.04976	1.68810	0.36500	3.28767	0.05280	3.59848	0.22171	9.53757
15YP12-017.FIN2	313.4	4.2	318.1	7.1	357	29	0.04982	1.38499	0.36860	2.60445	0.05320	2.63158	0.35239	12.21289
15YP12-070.FIN2	314.1	6.6	311.3	8.3	300	40	0.04990	2.20441	0.35900	3.06407	0.05240	2.86260	0.37943	-4.70000
15YP12-007.FIN2	314.9	4.8	313.4	9.2	296	42	0.05007	1.55782	0.36200	3.31492	0.05200	3.84615	-0.04820	-6.38514
15YP12-064.FIN2	315	11	364	11	719	60	0.05000	3.80000	0.43000	3.72093	0.06340	3.47003	0.64211	56.18915
15YP12-058.FIN2	316.8	6.4	321.3	8.3	388	28	0.05040	1.98413	0.37100	2.96496	0.05370	2.79330	0.51548	18.35052
15YP12-018.FIN2	317.1	7.2	312	15	380	66	0.05040	2.38095	0.35700	5.32213	0.05250	5.14286	0.25083	16.55263
15YP12-042.FIN2	317.2	4.6	316.4	9.3	337	41	0.05045	1.48662	0.36400	3.57143	0.05270	3.41556	0.33073	5.87537
15YP12-048.FIN2	317.2	4.2	315.5	5.4	326	31	0.05044	1.36796	0.36470	1.97423	0.05270	2.27704	0.21964	2.69939
15YP12-065.FIN2	317.3	8.9	312.2	7.9	343	37	0.05050	2.97000	0.36200	3.02867	0.05290	3.12361	0.50430	7.49371
15YP12-006.FIN2	317.4	3.1	325.1	5.1	359	30	0.05047	0.99069	0.37770	1.80037	0.05410	2.21811	0.24563	11.58774
15YP12-038.FIN2	317.5	4.6	320	5.3	344	27	0.05049	1.48544	0.37090	1.94122	0.05310	2.25989	0.39586	7.70349
15YP12-011.FIN2	319	5.2	323	11	396	53	0.05074	1.65550	0.37900	4.30712	0.05340	-0.01013	-0.01013	19.44444
15YP12-023.FIN2	319	3.5	319.4	6.2	351	29	0.05073	1.10388	0.37020	2.29606	0.05280	2.65152	0.22755	9.11681
15YP12-009.FIN2	319.3	4	324.7	7.9	348	44	0.05078	1.29972	0.37800	2.91005	0.05360	3.17164	0.08310	8.24713
15YP12-010.FIN2	319.6	4.2	321.9	8.4	364	42	0.05074	1.37958	0.37200	2.95699	0.05330	3.18949	0.11171	12.19780
15YP12-015.FIN2	319.8	3.8	324.6	5.9	362	33	0.05086	1.21903	0.37620	2.09995	0.05310	2.44821	0.13047	11.65746
15YP12-068.FIN2	320.3	7	320.6	7.3	405	34	0.05100	2.15686	0.36990	2.64936	0.05320	3.00752	0.36629	20.91358
15YP12-014.FIN2	320.8	3.8	322.2	6.4	294	39	0.05103	1.21497	0.37110	2.20965	0.05210	2.68714	-0.11565	-9.11565
15YP12-044.FIN2	320.9	4.3	323.9	5.7	327	27	0.05104	1.37147	0.37450	1.92256	0.05350	2.24299	0.30504	6.18959
15YP12-024.FIN2	321.1	4.3	315.7	7.1	332	41	0.05107	1.39025	0.36410	2.52678	0.05330	3.11891	-0.02880	3.28313
15YP12-069.FIN2	321.2	7.5	317.6	8.6	324	37	0.05110	2.34834	0.36800	3.26087	0.05370	3.67055	0.28455	0.86420
15YP12-003.FIN2	321.3	4.1	328.7	5.5	372	36	0.05111	1.31090	0.38110	2.02047	0.05410	2.21811	0.36882	13.62903
15YP12-053.FIN2	321.7	6.7	318	7	294	28	0.05120	2.14844	0.36850	2.55088	0.05240	2.67176	0.53909	-9.42177
15YP12-025.FIN2	324	4.8	329	7.6	450	37	0.05155	1.53249	0.39700	2.51889	0.05530	2.51645	0.57151	28.00000
15YP12-034.FIN2	324	4.1	326.6	6.3	362	42	0.05154	1.29996	0.38000	2.26316	0.05350	2.80374	0.23538	10.9724
15YP12-062.FIN2	325.3	6.4	339.9	7.6	429	43	0.05180	1.93050	0.39900	2.75689	0.05560	2.51799	0.46031	24.17249
15YP12-021.FIN2	325.8	3.9	327.8	6.2	321	36	0.05184	1.21528	0.38060	2.25959	0.05320	2.63158	0.12066	-1.49533
15YP12-041.FIN2	326.4	5.6	328.5	8	349	40	0.05195	1.75168	0.38000	2.89474	0.05330	2.81426	0.44650	6.47564
15YP12-052.FIN2	327.6	5.1	326.9	6.1	346	35	0.05214	1.61105	0.37930	2.24097	0.05320	2.63158	0.22603	5.31792
15YP12-002.FIN2	328	4.8	326.7	5.9	343	35	0.05220	1.51341	0.38000	2.10526	0.05300	2.83019	0.11175	4.37318
15YP12-055.FIN2	328	5.7	316.1	7.2	292	31	0.05221	1.78127	0.36590	2.65100	0.05140	2.72374	0.37430	-12.32877
15YP12-061.FIN2	328	5.5	329.5	7.4	364	35	0.05220	1.70498	0.38400	2.60417	0.05320	2.44361	0.52026	9.89011
15YP12-047.FIN2	328.8	5.5	329.6	6.9	336	29	0.05233	1.71985	0.38010	2.39411	0.05360	2.42537	0.39477	12.14886
15YP12-040.FIN2	329	5	325.1	6	314	22	0.05237	1.56578	0.37700	2.14854	0.05240	2.29008	0.52882	-4.77707
15YP12-043.FIN2	329.1	4.3	327.2	9.1	335	41	0.05238	1.35548	0.37800	3.17460	0.05320	3.37143	0.20377	17.16219
15YP12-051.FIN2	331	5.5	330.3	9.8	375	43	0.05260	1.71103	0.38600	3.36788	0.05360	3.54478	0.30648	11.72333
15YP12-049.FIN2	331.2	5.3	331	6.4	361	40	0.05272	1.63126	0.38580	2.25505	0.05380	2.78810	0.12537	5.84885
15YP12-022.FIN2	332.8	6.4	325	11	281	38	0.05300	1.88679	0.37800	3.96825	0.05220	4.99770	-0.05052	-18.43416
15YP12-026.FIN2	333.5	5.5	327	9.7	307	40	0.05310	1.67608	0.38100	3.41207	0.05140	3.96650	-0.21416	-8.63192
15YP12-037.FIN2	336.9	5.2	331.1	9	470	37	0.05366	1.58405	0.41300	2.80517	0.05650	3.00885	0.37350	28.31915
15YP12-066.FIN2	338	10	346.2	8.9	417	40	0.05380	3.15985	0.40700	2.94840	0.05460	3.29670	0.42688	18.94484
15YP12-016.FIN2	344.6	6.1	354	11	426	49	0.05490	1.82149	0.41600	3.84615	0.05450	3.85321	0.31116	19.10798
15YP12-001.FIN2	345.8	5.4	335.6	9.5	317	46	0.05511	1.61495	0.38900	3.34190	0.05110	3.71820	0.02322	-9.08517
15YP12-031.FIN2	349.2	5.6	345.2	6.7	340	32	0.05568	1.63434	0.40540	2.31870	0.05270	2.27704	0.53887	-2.70588
15YP12-039.FIN2	351	5.4	356.2	6.9	398	30	0.05596	1.59042	0.41980	2.33444	0.05480	2.18978	0.62135	11.80905
15YP12-060.FIN2	352.6	5.4	353.6	9.8	405	37	0.05622	1.58307	0.41800	3.34928	0.05410	3.14233	0.49966	12.93827
15YP12-045.FIN2	353.1	5.3	352.4	7.9	357	32	0.05631	1.56278	0.41100	2.67640	0.05410	2.58780	0.39160	1.09244
15YP12-029.FIN2	353.6	6	339.4	8.1	283	43	0.05639	1.73790	0.39600	2.77778	0.05090	3.14342	0.26390	-24.94700
15YP12-027.FIN2	357.7	5.7	360.4	8.4	376	29	0.05706	1.62986	0.42700	2.81030	0.05360	2.61194	0.47617	4.86702
15YP12-028.FIN2	360.7	7.2	364	11	374	50	0.05760	2.08333	0.43200	3.47222	0.05500	4.00000	0.21815	3.55615
15YP12-008.FIN2	471.4	5.3	471.5	9.8	449	38	0.07587	1.17306	0.59000	2.54237	0.05570	2.69300	0.23221	-4.98886
15YP12-067.FIN2	483	16	502	19	594	52	0.07790	3.59435	0.64100	4.99220	0.05900	4.06780	0.57285	18.88687
15YP12-046.FIN2	570.2	7.5	567.6	7.7	574	24	0.09250	1.40541	0.75000	1.73333	0.05950	2.01681	0.49761	0.66202
15YP12-059.FIN2	602.3	9.9	607	24	684	87	0.09800	1.73469	0.82400	5.21845	0.06130	5.56449	0.08328	11.94444
15YP12-063.FIN2	608	16	617	17	662	27	0.09900	2.72727	0.84000	3.80952	0.06090	3.28407	0.63321	8.15710
15YP12-035.FIN2	839	16	830	16	843	32	0.13880	2.01729	1.27000	2.83465	0.06690	2.84006	0.40613	0.47450
15YP12-013.FIN2	1691	27	1695	21	1673	30	0.29940	1.83701	4.53000	2.54042	0.10250	2.73171	0.38934	-1.07591
15YP12-012.FIN2	2512	28	2606	17	2669	19	0.47660	1.34285	12.04000	1.82724	0.18190	1.92413	0.54821	5.88235
15YP13:15YP13														
15YP13-014.FIN2	66	1	63.9	1.9	152	25	0.01029	1.55491	0.06500	3.07892	0.04670	3.64026	0.04677	56.57895
15YP13-094.FIN2	78.2	1.2	78.9	2.2	179	32	0.01220	1.55738	0.08060	2.97767	0.04810	3.11850	0.21600	56.31285
15YP13-006.FIN2	78.4	1.4	80.4	2.3	200	35	0.01224	1.79739	0.08250	3.03030	0.04870	3.28542	0.22673	60.80000
15YP13-061.FIN2	78.6	1.3	81.7	2.6	149	42	0.01227	1.62999	0.08380	3.34129	0.04820	3.11203	0.33370	47.24832
15YP13-018.FIN2	78.9	1.6	75.6	3.4	278	44	0.01231	2.03087	0.07740	4.65116	0.04610	5		

Table 5 cont: LA-ICP-MS Zircon Isotopic and Age Data Table (IGOR PRO): 15YP12 & 15YP13: SGTFW/SGTWH Basement/Volcanoclastic

Sample-Grain #	Dates (Ma)				Isotopic Ratios								Rho (ρ)	% disc b
	206Pb/238U age	±2σ	207Pb/235U age	±2σ	206Pb/238U c	±2σ	207Pb/235U c	±2σ	207Pb/206Pb c	±2σ				
15YP12-046.FIN2	570.2	7.5	567.6	7.7	574	24	0.00250	1.40541	0.75000	1.73333	0.05950	2.01681	0.49761	0.62002
15YP12-059.FIN2	602.3	9.9	607	24	684	87	0.09800	1.73469	0.82400	5.21845	0.06130	5.54649	0.08328	11.94444
15YP12-063.FIN2	608	16	617	17	662	27	0.09900	2.72727	0.84000	3.80952	0.06090	3.28407	0.63321	8.15710
15YP12-035.FIN2	839	16	830	16	843	32	0.13880	2.01729	1.27000	2.83465	0.06690	2.84006	0.40613	0.47450
15YP12-013.FIN2	1691	27	1695	21	1673	30	0.29940	1.83701	4.33000	2.54042	0.10250	2.73371	0.38934	-1.07591
15YP12-012.FIN2	2512	28	2606	17	2669	19	0.47660	1.34285	12.04000	1.82724	0.18190	1.92413	0.54821	5.88235
15YP13:15YP13														
15YP13-014.FIN2	66	1	63.9	1.9	152	25	0.01029	1.55491	0.06500	3.07692	0.04670	3.64026	0.04677	56.57895
15YP13-094.FIN2	78.2	1.2	78.9	2.2	179	32	0.01220	1.55738	0.08060	2.97767	0.04810	3.11850	0.21600	56.31285
15YP13-006.FIN2	78.4	1.4	80.4	2.3	200	35	0.01224	1.79739	0.08250	3.03030	0.04870	3.28542	0.22673	60.80000
15YP13-061.FIN2	78.6	1.3	81.7	2.6	149	42	0.01227	1.62999	0.08380	3.34129	0.04820	3.11203	0.33370	47.24832
15YP13-018.FIN2	78.9	1.6	75.6	3.4	278	44	0.01231	2.03087	0.07740	4.65116	0.04610	5.42299	-0.15802	71.61871
15YP13-068.FIN2	79.3	1.7	77.5	1.9	114	27	0.01238	2.10016	0.07940	2.51889	0.04680	2.77778	0.43293	30.43860
15YP13-012.FIN2	79.5	1.1	79.5	1.8	160	29	0.01242	1.36876	0.08150	2.33129	0.04750	2.79584	0.20385	50.31250
15YP13-015.FIN2	79.5	1	80.6	2.1	170	36	0.01241	1.28928	0.08260	2.66344	0.04770	3.14465	0.06538	53.23529
15YP13-025.FIN2	79.8	1.6	81.4	4.3	374	53	0.01246	2.00642	0.08370	5.49582	0.04680	5.37370	0.05223	78.66310
15YP13-027.FIN2	80	1	80.2	2.1	189	37	0.01249	1.28102	0.08220	2.67640	0.04760	3.15126	0.08377	57.67196
15YP13-119.FIN2	80.1	1.2	79.6	6.4	160	160	0.01250	1.60000	0.08160	8.70098	0.04690	8.95522	0.33474	49.93750
15YP13-055.FIN2	80.3	1.8	82.8	2.3	215	33	0.01253	1.91540	0.08470	2.83553	0.04840	2.89256	0.36362	62.65116
15YP13-072.FIN2	80.3	1.8	78.5	2.7	186	30	0.01254	2.23285	0.08400	3.60697	0.04670	3.64026	0.41692	56.82796
15YP13-104.FIN2	80.3	1.4	80.5	4.3	174	88	0.01254	1.75439	0.08260	5.69007	0.04780	5.02092	0.16679	58.85057
15YP13-070.FIN2	80.4	1.6	80.5	2.5	250	43	0.01255	1.99203	0.08250	3.27273	0.04840	3.71901	0.24712	67.84000
15YP13-076.FIN2	80.4	1.3	79.5	2.0	193	34	0.01256	1.59236	0.08150	2.57669	0.04710	2.97240	0.14851	58.34197
15YP13-121.FIN2	80.4	1.1	80.9	2.1	201	31	0.01255	1.35458	0.08300	2.65060	0.04840	3.09917	0.16721	60.00000
15YP13-004.FIN2	80.5	1.3	79.5	2.2	108	44	0.01257	1.59109	0.08120	2.83251	0.04750	3.38842	0.17071	59.34343
15YP13-002.FIN2	80.6	1.3	81.5	3	241	47	0.01258	1.58983	0.08360	3.82775	0.04830	3.72671	0.43747	66.55602
15YP13-009.FIN2	80.6	1.1	79.7	2.4	153	24	0.01258	1.35135	0.08170	3.05998	0.04700	3.40426	0.18681	47.32026
15YP13-071.FIN2	80.6	1.6	81.6	2.5	178	26	0.01258	2.06677	0.08350	3.11377	0.04860	3.29218	0.30935	54.73100
15YP13-073.FIN2	80.6	1.8	80	2.8	207	36	0.01259	2.30342	0.08210	3.53228	0.04670	3.85439	0.27375	61.06280
15YP13-088.FIN2	80.6	1.3	81.9	2.3	234	40	0.01259	1.58856	0.08400	2.85714	0.04780	3.34738	0.09385	65.55556
15YP13-034.FIN2	80.7	1.3	81.1	2.1	204	36	0.01260	1.66667	0.08350	2.69637	0.04680	2.66393	0.23211	60.44118
15YP13-042.FIN2	80.7	1.3	81.4	2.2	169	31	0.01260	1.56730	0.08360	2.75120	0.04770	3.14465	0.19600	52.24852
15YP13-101.FIN2	80.7	1.2	79.2	3.4	240	47	0.01260	1.50794	0.08080	4.43545	0.04690	4.90405	-0.06467	66.37500
15YP13-085.FIN2	80.8	1.1	80	2	133	26	0.01261	1.42744	0.08200	2.56098	0.04680	2.77778	0.18277	39.24812
15YP13-087.FIN2	80.8	1.5	78.8	2.6	211	34	0.01261	1.82395	0.08070	3.34572	0.04740	3.38650	0.38839	61.70616
15YP13-013.FIN2	80.9	1.1	80	2.1	170	37	0.01262	1.34707	0.08200	2.80488	0.04700	3.19149	0.26552	52.41176
15YP13-005.FIN2	81	1	80.1	2.2	199	34	0.01264	1.26582	0.08150	2.93040	0.04760	3.15126	0.24852	59.29648
15YP13-045.FIN2	81.1	1.3	79.9	2.6	205	48	0.01267	1.65746	0.08150	3.55828	0.04640	3.66379	0.15853	60.43902
15YP13-107.FIN2	81.1	1.2	79.1	2.6	217	41	0.01266	1.50079	0.08110	3.32922	0.04640	4.09483	-0.02103	62.62673
15YP13-020.FIN2	81.2	1.4	80	3.2	238	47	0.01267	1.73639	0.08210	4.14129	0.04740	4.43038	-0.01154	65.88235
15YP13-031.FIN2	81.2	1.2	81.6	2.3	176	35	0.01267	1.49961	0.08370	2.98686	0.04800	3.33333	0.24101	53.86364
15YP13-078.FIN2	81.3	1.4	80.3	2.6	288	37	0.01269	1.65485	0.08460	3.12500	0.04880	3.48631	0.26158	65.84034
15YP13-114.FIN2	81.4	1.2	81	1.7	141	31	0.01271	1.41621	0.08310	2.16606	0.04700	2.55319	0.23671	42.26950
15YP13-022.FIN2	81.5	1.5	78.7	3.2	277	56	0.01273	1.80676	0.08070	4.21114	0.04600	4.95622	-0.01114	70.57762
15YP13-003.FIN2	81.6	1.3	80.1	2.2	151	28	0.01273	1.64965	0.08220	2.79805	0.04710	3.18471	0.22905	45.96226
15YP13-036.FIN2	81.7	1.3	81.6	3.2	288	50	0.01276	1.64577	0.08380	4.05728	0.04710	4.67091	0.11342	71.63194
15YP13-058.FIN2	81.7	1.1	83.7	2.2	206	30	0.01276	1.33229	0.08600	2.79070	0.04880	2.66393	0.34948	60.33981
15YP13-041.FIN2	81.8	1.2	82.3	2.5	183	29	0.01277	1.48786	0.08450	3.19527	0.04770	3.35430	0.00106	55.30055
15YP13-115.FIN2	81.8	1.2	80.2	6.2	340	100	0.01278	2.66041	0.07770	8.48421	0.04450	8.31461	-0.06071	75.94118
15YP13-091.FIN2	81.9	1.2	79.8	2.1	199	37	0.01279	1.40735	0.08180	2.68949	0.04650	3.44086	0.06479	58.84422
15YP13-034.FIN2	82	1.5	82.9	4	311	47	0.01280	1.87500	0.08530	5.04103	0.04800	5.20833	0.13984	73.63344
15YP13-044.FIN2	82	1.1	83.3	5.8	170	110	0.01280	1.32813	0.08550	7.60234	0.04820	7.46888	0.30652	51.76471

Table 5 cont: LA-ICP-MS Zircon Isotopic and Age Data Table (IGOR PRO): 15YP12 & 15YP13: SGTFW/SGTWH Basement/Volcanoclastic

Sample-Grain #	Dates (Ma)				Isotopic Ratios								Rho (ρ)	% disc b
	206Pb/238U age	±2σ	207Pb/235U age	±2σ	206Pb/238U c	±2σ	207Pb/235U c	±2σ	207Pb/206Pb c	±2σ				
15YP13-056.FIN2	82	1.3	79.1	2.2	189	36	0.01280	1.64063	0.08110	2.95931	0.04610	3.47072	0.12375	56.61376
15YP13-067.FIN2	82	2	81.7	2.7	212	41	0.01280	2.50000	0.08380	3.46062	0.04740	3.58650	0.34661	61.32075
15YP13-079.FIN2	82	1.2	80.5	2	167	29	0.01280	1.48438	0.08260	2.66344	0.04730	2.95983	0.28642	50.89820
15YP13-116.FIN2	82	1.4	79.6	4.4	199	59	0.01280	1.71875	0.08120	5.66502	0.04870	5.94843	0.04007	79.44862
15YP13-060.FIN2	82.1	1.2	83.4	2.7	353	53	0.01282	1.40406	0.08530	3.51700	0.04770	3.35430	0.31063	46.33987
15YP13-075.FIN2	82.1	1.7	83.5	2.4	182	37	0.01282	2.02808	0.08580	3.03030	0.04760	2.94118	0.45718	54.89011
15YP13-097.FIN2	82.2	1.3	81.1	3.6	258	41	0.01283	1.63679	0.08330	4.56182	0.04710	4.88223	-0.02336	68.13953
15YP13-021.FIN2	82.3	1.5	86.7	2.6	242	36	0.01285	1.86770	0.08920	3.13901	0.04970	3.21932	0.12101	65.99174
15YP13-063.FIN2	82.3	1.5	82.3	2	145	28	0.01285	1.86770	0.08440	2.48815	0.04740	2.53165	0.54488	43.24138
15YP13-089.FIN2	82.3	1.1	80.4	2.3	169	28	0.01285	1.40078	0.08250	3.03030	0.04680	3.20513	0.19726	51.30178
15YP13-062.FIN2	82.4	1.1	82.3	2.4	181	32	0.01287	1.38860	0.08450	2.95858	0.04740	3.16456	0.20644	54.47514
15YP13-026.FIN2	82.5	1.5	87.1	4.4	259	80	0.01288	1.86335	0.08960	5.35714	0.05000	5.00000	0.05730	68.14272
15YP13-040.FIN2	82.5	1.2	85.5	2.8	233	35	0.01289	1.47401	0.08800	3.40909	0.04930	3.65112	-0.01402	64.95227
15YP13-049.FIN2	82.5	1.4	76	47	190	310	0.01288	5.35714	0.07800	87.17949	0.04400	59.00001	-0.15501	56.57895
15YP13-100.FIN2	82.5	1.3	82.8	2.4	193	37	0.01289	1.55159	0.08440	2.96209	0.04830	3.10559	0.31497	57.25389
15YP13-117.FIN2	82.5	1.2	80.8	2.1	183	34	0.01288	1.47516	0.08280	2.77778	0.04690	2.98007	0.31887	54.91803
15YP13-037.FIN2	82.6	1.4	80.2	2.9	228	39	0.01290	1.78295	0.08220	3.77129	0.04630	4.10367	0.22025	63.77193
15YP13-084.FIN2	82.8	1.4	86.9	2.7	304	39	0.01293	1.77881	0.08950	3.24022	0.05030	3.57853	0.18384	72.76316
15YP13-095.FIN2	82.8	2	81.5	6.8	421	81	0.01							

Table 5 cont: LA-ICP-MS Zircon isotopic and Age Data Table (IGOR PRO): 1591P12 & 1591P13: SGTWH/SGTWH Basement/Volcanoclastic

Sample-Grain #	Dates (Ma)		207Pb/235U age		207Pb/206Pb age		Isotopic Ratios		207Pb/235U c		207Pb/206Pb c		Rho (g)	% disc b
	206Pb/238U age	±2σ	±2σ	±2σ	±2σ	±2σ	206Pb/238U c	±2σ	±2σ	±2σ	±2σ			
1591P13-110.FIN2	88	1.7	87.8	2.3	180	26	0.01375	1.80991	0.09030	2.78855	0.04820	2.69710	0.45762	51.11111
1591P13-124.FIN2	89.1	1.6	110.5	3.7	592	62	0.01392	1.79598	0.11510	3.56212	0.06030	3.64842	0.11708	84.94932
1591P13-001.FIN2	89.2	1.7	101.2	7	326	98	0.01394	1.93687	0.10520	7.60456	0.05480	8.39416	0.38844	72.63804
1591P13-081.FIN2	89.3	1.7	90.4	2.2	164	36	0.01395	1.93548	0.09310	2.57787	0.04770	2.72537	0.40129	45.54878
1591P13-120.FIN2	90	1.4	87.9	2.4	130	32	0.01405	1.56584	0.09050	2.76243	0.04690	2.98507	0.27420	38.76923
1591P13-064.FIN2	92	1.7	222	1.8	1820	160	0.01437	1.87891	0.24900	8.83534	0.12200	8.19672	0.40200	94.94505
1591P13-058.FIN2	92.4	1.6	107.4	3.6	419	70	0.01441	1.80430	0.11170	3.49150	0.05540	4.15162	0.22777	77.94749
1591P13-065.FIN2	100.4	2.8	111.4	7.4	592	64	0.01570	2.80255	0.11680	7.20555	0.05220	7.27969	0.13230	83.04054
1591P13-082.FIN2	101.9	2.5	102.6	3	252	44	0.01593	2.44821	0.10640	3.00752	0.04720	3.17797	0.10400	59.56349
1591P13-046.FIN2	105.3	4.2	102	13	670	120	0.01647	4.00729	0.10800	12.96296	0.04700	12.76596	0.12761	84.28358
1591P13-047.FIN2	107.8	2.8	107.1	7.2	468	79	0.01687	2.73673	0.11010	7.17530	0.04690	6.82303	0.11778	76.56581
1591P13-074.FIN2	112.3	3	112.4	6.5	437	69	0.01760	2.67045	0.11590	6.38481	0.04700	6.38298	0.23917	74.25629
1591P13-028.FIN2	114.5	2.6	116.9	6	413	72	0.01790	2.92950	0.12160	5.92111	0.04960	6.25000	-0.00964	72.32446
1591P13-090.FIN2	166.6	3.9	175	9.7	444	77	0.02618	3.26822	0.18990	5.82011	0.05280	6.43999	-0.11064	62.47748
1591P13-125.FIN2	172.9	3.3	175.4	7.5	332	47	0.02718	1.94996	0.18930	4.64871	0.05060	4.74908	0.19235	47.92169
1591P13-048.FIN2	211.3	4.4	213.9	8.2	401	50	0.03933	2.13021	0.23500	4.25532	0.05070	4.33925	0.32941	47.30673
1591P13-048.FIN2	215.6	3.8	278.9	4.1	300	27	0.04360	1.42202	0.31630	1.70724	0.05250	1.90476	0.43483	8.13333
1591P13-032.FIN2	299	25	453	62	1270	180	0.04760	8.40336	0.64000	18.75000	0.08620	10.09281	0.95146	76.45669
1591P13-038.FIN2	325.3	4.5	321.9	6.5	390	35	0.05176	1.41036	0.37370	2.32807	0.05180	2.70270	-0.00560	-8.43333
1591P13-007.FIN2	327.9	3	325.4	4.3	319	26	0.05218	0.93906	0.37800	1.53439	0.05271	1.78334	0.56609	-2.78997
1591P13-033.FIN2	379.8	4.7	396	9	476	34	0.06069	1.26874	0.47800	2.71967	0.05610	2.82025	20.21008	48.33333
1591P13-011.FIN2	388.9	4.8	387.7	7.3	390	34	0.06210	1.23994	0.46500	2.15054	0.05390	2.59740	0.19275	0.28205
1591P13-039.FIN2	492.4	5.9	492.6	6.6	478	30	0.07939	1.24701	0.62500	1.76000	0.05680	2.11268	0.15514	-0.01255
1591P13-112.FIN2	573.6	7.3	563	10	538	38	0.09310	1.28894	0.74300	2.42261	0.05770	2.72756	0.13264	-6.61710
1591P13-080.FIN2	631.1	8.2	625.5	8.4	590	32	0.10290	1.36054	0.85000	1.76471	0.05900	2.20339	0.35051	-9.96510
1591P13-122.FIN2	634.2	7.8	639.3	8.7	643	27	0.10340	1.25725	0.87800	1.82233	0.06140	1.95440	0.57471	1.36858
1591P13-108.FIN2	680.2	6.9	671.3	9	643	26	0.11130	1.07817	0.93800	1.81237	0.06110	2.17766	0.25811	-5.78538
1591P13-008.FIN2	824.7	8.7	826.8	7.8	849	19	0.13650	1.09890	1.25900	1.35028	0.06740	1.78042	0.45459	2.86219
1591P13-029.FIN2	950	11	967	12	994	23	0.15870	1.26024	1.59300	1.82046	0.07260	2.06612	0.46551	4.42656
1591P13-109.FIN2	2464	22	2511	11	2579	15	0.46570	1.09513	11.08000	2.26354	0.17200	1.45349	0.45499	4.59909

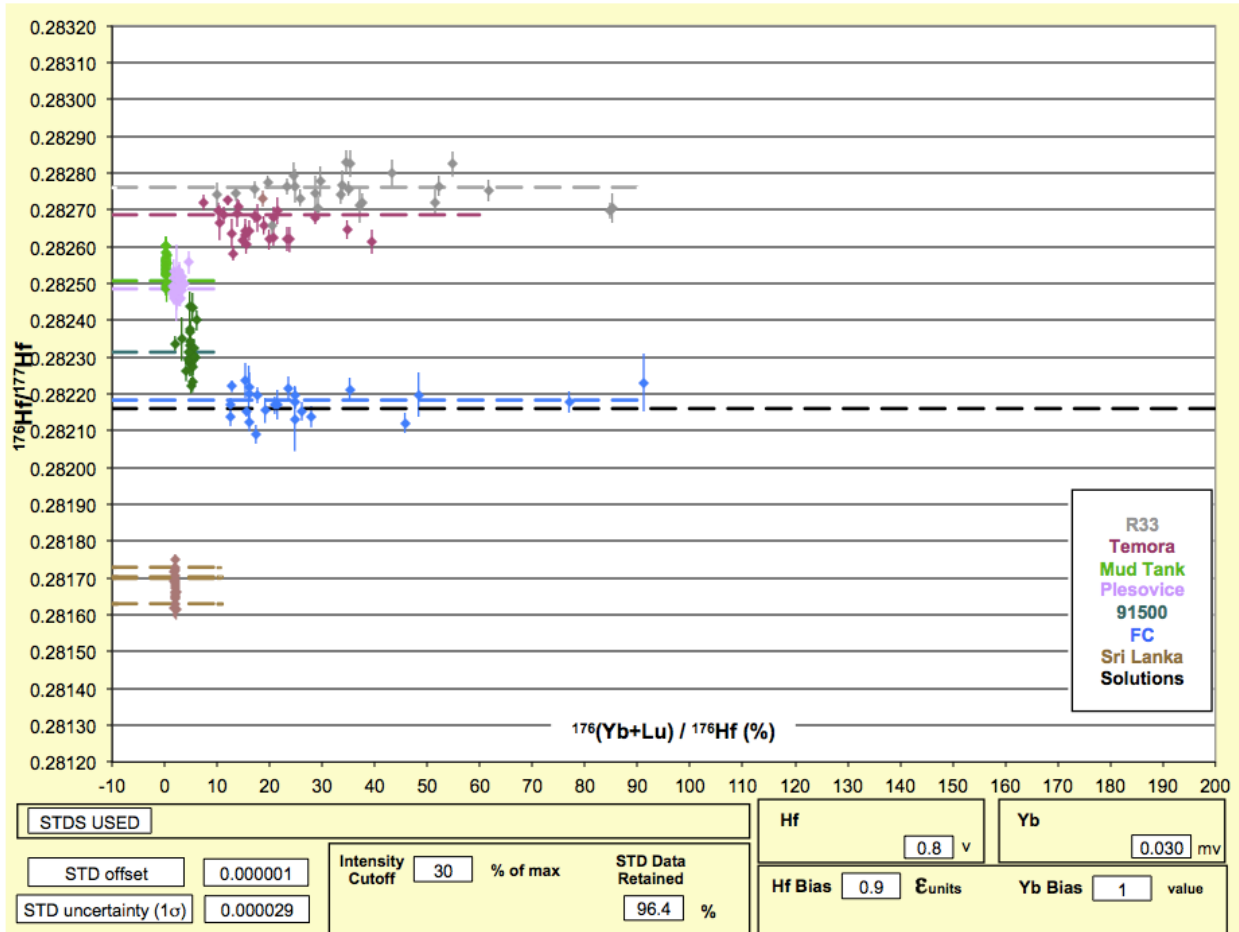
Table 6: LA-ICP-MS Zircon isotopic and Age Data Table 1591P14: SGTWH Xenocryst

Sample-Grain #	Dates (Ma)		207Pb/235U age		207Pb/206Pb age		Isotopic Ratios		207Pb/235U c		207Pb/206Pb c		Rho (g)	% disc b
	206Pb/238U age	±2σ	±2σ	±2σ	±2σ	±2σ	206Pb/238U c	±2σ	±2σ	±2σ	±2σ			
1591P14-093	75.51208	3.59249	74.86964	5.84970	52.33517	149.9087	0.01178	4.78676	0.07646	8.13472	0.04708	6.57729	0.03941	17.03398
1591P14-022	76.51551	3.63479	84.65259	9.02026	320.77530	214.39552	0.01194	4.77999	0.08095	11.67953	0.05284	10.00284	0.00337	18.30498
1591P14-067	77.34865	2.87292	76.84836	6.61214	64.40788	183.6099	0.01207	2.74555	0.07879	8.97909	0.04732	8.12002	0.00390	17.39946
1591P14-115	78.25347	3.36858	78.93119	5.14144	118.83444	0.01221	4.35359	0.08082	6.78811	0.04802	5.20944	0.62122	0.16539	21.30808
1591P14-091	78.73509	4.29646	104.93110	13.37479	750.44111	241.0538	0.01229	5.89318	0.10887	13.50496	0.06430	12.33729	0.00402	20.93700
1591P14-039	78.79211	4.05343	81.02014	8.63037	149.10423	215.97231	0.01229	5.18172	0.08306	11.13000	0.04905	9.80201	0.00370	47.18861
1591P14-011	78.78603	2.80800	81.02014	4.80722	168.75543	202.67590	0.01229	3.84919	0.08317	6.12866	0.04846	4.29186	0.00343	15.48065
1591P14-034	78.78255	3.11322	77.38435	5.30880	30.08866	116.64241	0.01230	3.98448	0.07905	7.15581	0.04665	5.84386	0.00346	16.02252
1591P14-096	79.12303	3.40486	80.73027	4.83974	127.95021	220.39042	0.01232	4.33086	0.08273	10.92326	0.04861	10.02802	0.00356	16.72466
1591P14-085	79.18461	3.32449	80.97533	6.42174	134.14648	193.19390	0.01236	4.23553	0.08301	8.27706	0.04874	7.11126	0.00377	16.47316
1591P14-090	79.30052	3.24660	78.88037	6.18869	65.90009	160.22806	0.01238	4.12124	0.08178	8.17316	0.04875	7.02034	0.00360	16.38113
1591P14-122	79.34341	3.83188	78.78249	3.34351	138.24448	186.92426	0.01239	5.28689	0.07972	16.48279	0.04671	15.62245	0.00360	138.39004
1591P14-094	79.49740	3.27168	80.38373	4.94832	106.04127	253.87398	0.01241	4.17158	0.08126	12.32000	0.04816	11.86252	0.00338	25.03633
1591P14-033	79.60117	3.03268	76.03921	5.09802	34.54130	138.00004	0.01242	3.81029	0.07776	6.97913	0.04541	5.84963	0.00338	16.74795
1591P14-099	79.99389	2.92881	80.79100	6.45528	104.39342	187.81802	0.01249	3.88490	0.08282	8.93976	0.04813	7.48000	0.00347	17.03588
1591P14-038	80.45604	3.71057	78.93237	5.90809	33.04855	258.54541	0.01256	4.64209	0.08084	12.57894	0.04670	11.69105	0.00371	21.25425
1591P14-002	80.62293	3.12727	86.51973	8.51987	143.56887	0.01259	3.90414	0.08284	7.43242	0.04776	6.33444	0.00358	16.65459	
1591P14-108	80.62275	3.45259	88.40883	6.28137	304.54495	131.84335	0.01259	4.29947	0.09106	7.45311	0.05246	6.06663	0.00401	16.56800
1591P14-017	81.54525	3.39025	84.28789	7.12640	162.78353	173.88810	0.01275	4.18778	0.08555	8.95411	0.04934	7.80153	0.00367	16.00077
1591P14-116	81.57439	3.89885	83.68838	5.85895	121.25559	214.89301	0.01273	4.54652	0.08507	10.76564	0.04847	9.74466	0.00379	23.62315
1591P14-097	81.58484	3.93885	79.93803	5.11320	131.62270	165.54888	0.01274	4.26263	0.08335	6.66599	0.04668	5.04092	0.00377	16.74475
1591P14-125	81.76240	3.95999	83.09055	7.40041	119.46537	185.29133	0.01277	4.11767	0.08523	8.31406	0.04844	8.83259	0.00382	17.74443
1591P14-052	81.90121	3.67292	80.80960	8.00806	90.42699	207.86748	0.01282	4.44646	0.08402	8.30875	0.04876	9.82521	0.00378	17.33320
1591P14-105	82.09920	3.85246	80.33146	9.48880	28.07048	252.82705	0.01282	4.72380	0.08233	12.34437	0.04661	11.40478	0.00356	17.74556
1591P14-072	82.11141	2.79823	83.83507	6.92244	133.25166	176.90500	0.01282	3.57999	0.08607	6.83217	0.04872	5.92525	0.00342	15.84918
1591P14-109	82.11489	4.75728	79.24244	11.28986	5.90355	301.13807	0.01282	5.83243	0.08119	14.88884	0.04995	13.68692	0.00328	25.34480
1591P14-098	82.13814	3.92221	81.02511	5.97551	140.24600	183.01334	0.01282	4.93280	0.08459	7.12900	0.04821	5.72488	0.00378	16.40197
1591P14-140	82.98800	3.55045	84.38729	7.26145	124.37139	176.20697	0.01296	4.30742	0.08666	8.99957	0.04853	7.90380	0.00373	33.27983
1591P14-000	83.51887	3.59075	79.28726	46.44441	221.02018	0.01304	4.32845	0.08122	6.73733	0.04519	5.14295	0.00362	17.46611	
1591P14-107	83.57271	4.09592	86.96981	11.72997	181.16258	279.17135	0.01305	5.45249	0.08944	14.15248	0.04973	13.07278	0.00386	27.11895
1591P14-115	84.16682	3.26236	84.82906	7.04941	108.42204	176.61774	0.01314	3.90229	0.08704	8.80952	0.04817	7.89149	0.00356	17.37378
1591P14-138	84.24271	3.72796	81.03847	5.29218	-13.94517	120.95992	0.01315	4.65552	0.08306	6.81388	0.04582	5.15351	0.00393	16.99709
1591P14-089	86.64735	6.55121	85.33242	8.29075	101.29338	0.01333	5.40667	0.08904	6.97023	0.04769	4.93909	0.00335	16.06452	
1591P14-088	99.60532													

Table 6 cont: LA-ICP-MS Zircon Isotope and Age Data Table 155001: Murdumu-Geymuk volcanic

Sample-Grain #	Dates (Ma)		Isotopic Ratios										δ ²⁷ S	δ ³⁴ S	δ ³³ S	
	207Pb/235U age	ε ₂₀₇	207Pb/235U age	ε ₂₀₇	207Pb/206Pb age	ε ₂₀₇	206Pb/238U	ε ₂₀₆	207Pb/235U c	ε ₂₀₇	207Pb/206Pb c	ε ₂₀₇				208Pb/232Th c
151914-075	377.48066	13.40921	376.37567	21.21014	369.08339	124.52912	0.06250	3.61136	0.44871	6.81111	0.05399	5.74026	0.01608	16.05232	0.47021	-3.20403
151914-052	379.50392	14.45422	377.85778	19.42194	367.78082	105.04791	0.06264	3.92632	0.45083	6.21483	0.05395	4.81747	0.01673	16.20668	0.59554	-3.18752
151914-041	388.64977	13.20696	390.45788	18.14337	401.18237	96.23257	0.06214	3.50522	0.46894	5.64754	0.05475	4.28111	0.01699	15.79037	0.59184	3.12404
151914-001	389.41580	12.61519	393.10068	16.08954	414.83467	80.33975	0.06227	3.34512	0.47277	4.97558	0.05509	3.68486	0.01774	16.48970	0.65118	6.12747
151914-095	397.14386	23.91421	388.36437	16.62071	332.66451	82.48517	0.06364	3.61121	0.46092	5.18254	0.05112	3.71117	0.01655	16.02045	0.60951	-19.49135
151914-045	397.78280	13.08487	401.23300	18.50275	421.15001	97.40482	0.06365	3.39317	0.48461	6.63362	0.05524	4.49862	0.01740	15.96449	0.57346	5.54843
151914-053	402.95793	14.99602	335.57846	21.02015	-108.62490	149.62359	0.06450	3.84448	0.39166	7.43252	0.04404	6.36161	0.01281	16.04014	0.49357	470.96277
151914-020	404.02491	15.01234	402.71007	18.28970	395.17420	87.52489	0.06468	3.83782	0.48677	5.55151	0.05461	4.01129	0.01736	15.33018	0.67930	-2.23970
151914-019	404.04049	23.88916	394.86252	15.65420	337.40218	83.01137	0.06479	3.49467	0.47333	5.12384	0.05123	3.76056	0.01754	16.78566	0.61610	-19.81789
151914-045	405.37874	18.04040	395.11637	18.04040	335.49936	87.77788	0.06490	3.88111	0.47570	5.66092	0.05318	3.90602	0.01715	15.55408	0.68678	-30.82647
151914-106	405.52203	13.66176	411.81035	18.69683	447.20560	93.95675	0.06493	3.47469	0.57409	5.57409	0.05590	4.34564	0.01820	16.78886	0.60134	9.32171
151914-007	406.10507	14.84524	444.56383	21.24614	648.42504	96.13918	0.06502	3.77621	0.54934	5.96359	0.06130	4.61569	0.01820	17.45270	0.59939	37.40916
151914-104	410.25980	15.23908	398.90640	18.42022	390.02127	91.22983	0.06513	3.82711	0.48129	5.63456	0.05365	4.13757	0.01775	15.20885	0.65897	-18.52205
151914-062	411.21542	14.52709	433.88551	18.40822	550.60683	80.79702	0.06503	3.64213	0.53113	5.26102	0.05658	3.79647	0.01884	16.50491	0.67528	25.13436
151914-078	415.39226	16.87935	395.86849	19.53414	383.38286	95.62849	0.06566	4.20139	0.47679	6.01644	0.05198	4.30659	0.01956	16.38153	0.68149	-46.58341
151914-057	418.11713	15.93866	400.12819	18.12796	298.89273	86.08912	0.06701	3.94029	0.48129	5.22865	0.05233	3.87633	0.02039	15.83221	0.70052	-19.88869
151914-110	440.21183	15.83880	438.72479	21.26602	399.11389	103.80934	0.07168	3.07127	0.54046	6.02811	0.06471	4.79560	0.02065	16.41616	0.57614	-11.75966
151914-027	455.84496	19.00443	489.75531	22.08739	551.66830	79.22336	0.07127	4.32657	0.61985	5.74890	0.06138	3.78483	0.04317	16.04319	0.73607	30.04054
151914-124	458.78345	18.73277	537.49922	22.65996	887.93094	70.51932	0.07376	4.23631	0.69809	5.48951	0.06867	3.49118	0.04009	16.58158	0.76237	48.31138
151914-100	469.12106	16.03880	460.43885	20.05044	469.19429	88.08106	0.07382	3.62622	0.57437	5.46641	0.05646	4.09051	0.02371	19.73859	0.64140	2.18791
151914-066	469.84906	40.92087	452.12018	27.58129	377.64412	137.25885	0.07455	4.27385	0.56091	7.68187	0.05394	6.02811	0.02851	15.52126	0.51967	-17.54086
151914-087	470.21930	15.83188	456.86022	16.16971	390.20739	135.48510	0.07567	3.49994	0.56822	7.20560	0.05449	6.29850	0.01852	18.48380	0.44166	-50.54097
151914-103	474.68096	15.21341	474.55392	22.89698	470.93981	109.46480	0.07641	3.23835	0.59578	6.10857	0.06257	5.12218	0.02132	16.90334	0.49957	-0.15638
151914-121	475.73784	16.58193	463.19300	21.77347	401.26444	101.57967	0.07660	3.62007	0.57003	5.91737	0.05476	4.68085	0.02417	18.93917	0.58245	-18.57034
151914-081	519.64033	18.80747	571.97521	24.61020	702.01515	90.44461	0.08721	3.05029	0.75447	6.06561	0.06265	4.37545	0.02949	12.59809	0.42776	22.20519
151914-032	542.37258	19.31881	558.49575	23.15688	542.37258	89.44381	0.08778	3.71807	0.61951	5.60460	0.05782	4.13757	0.02342	16.30142	0.58380	3.89842
151914-021	557.03816	20.73955	547.83036	20.04500	509.71825	109.83638	0.09025	3.89562	0.71520	6.47340	0.05750	5.17225	0.02156	15.43380	0.57388	8.28554
151914-061	559.45189	16.00055	570.88221	26.00055	616.67014	101.81188	0.09066	3.55690	0.60309	6.03101	0.06009	4.07408	0.02482	15.16964	0.56130	9.27858
151914-063	571.79032	24.64010	570.88119	24.38147	588.00834	72.29513	0.09274	4.48016	0.75476	5.65492	0.05905	3.44117	0.02325	15.17058	0.70156	-16.68656
151914-066	584.77657	24.65278	604.52461	41.96505	641.24055	109.85850	0.09666	4.34734	0.81369	9.40515	0.06108	3.84012	0.02525	16.97600	0.37121	7.24611
151914-003	589.95125	19.75471	597.00345	22.38442	585.82053	76.99490	0.09754	4.34561	0.80031	5.01419	0.05954	6.63520	0.02745	15.89545	0.66206	-2.41212
151914-136	602.32448	22.86128	594.84403	23.49998	543.75662	74.94124	0.09896	3.94516	0.79649	5.28103	0.05840	3.51070	0.02713	16.76020	0.73779	-11.87477
151914-068	613.73933	24.13346	615.77027	25.49417	632.93986	79.27928	0.09989	4.22995	0.83390	5.59558	0.06057	3.97652	0.02983	15.18640	0.71554	1.51485
151914-127	617.12978	26.36676	596.47602	25.39795	518.69931	93.19463	0.10046	4.32414	0.79938	6.14937	0.05773	4.37224	0.02912	16.30142	0.68555	-18.97640
151914-059	620.11850	23.74580	617.65734	25.08538	608.64732	78.71547	0.10097	4.02177	0.83711	5.48863	0.06017	3.71287	0.03441	20.16587	0.72092	-1.88470
151914-088	612.75045	19.84984	611.21149	29.13251	565.01775	115.49593	0.10160	3.34889	0.82568	6.43885	0.05987	5.49895	0.02609	19.49115	0.64623	-10.39484
151914-084	624.22837	24.63377	609.02035	35.07624	557.35766	138.79001	0.10168	4.04062	0.82337	7.78817	0.05976	6.56067	0.03863	15.51235	0.44431	-12.04622
151914-046	627.14695	45.84942	636.82100	52.27333	617.30250	169.52020	0.10218	7.65995	0.87231	11.39394	0.06195	8.36541	0.02905	19.60071	0.64714	6.57761
151914-008	644.71062	28.82027	634.55266	24.93975	598.53415	81.02208	0.10518	3.72616	0.86813	5.34962	0.05989	6.38551	0.02889	15.32501	0.67596	-7.71493
151914-028	652.39907	26.21148	653.99815	28.35815	659.13009	87.59960	0.10580	4.23034	0.90425	5.96632	0.06161	4.20173	0.02730	15.25265	0.68125	1.07958
151914-051	655.53491	23.42352	661.24007	29.78221	682.49381	102.19669	0.10700	3.78616	0.91788	6.21191	0.06234	4.94264	0.03731	15.38952	0.57586	3.85571
151914-111	656.70621	48.28698	672.26521	48.28698	179.41568	179.41568	0.10724	4.58563	0.93882	10.66788	0.06935	8.96170	0.02798	16.07998	0.38118	9.39842
151914-134	899.15977	38.36012	932.65671	34.05700	1022.67278	64.41032	0.14968	4.58429	1.50560	6.57653	0.07299	3.34772	0.04379	17.89404	0.80521	11.20025
151914-073	919.48426	35.43226	953.49922	33.72467	1009.37994	73.88330	0.15510	4.10479	1.57576	5.54538	0.07387	3.72852	0.04606	15.16964	0.72884	7.91636
151914-079	918.57336	32.86666	913.33028	30.88864	950.90551	49.11865	0.15673	3.82891	1.50776	5.18979	0.06978	3.47786	0.04048	15.26968	0.73048	-1.93211
151914-013	995.35888	28.95391	985.68378	27.15208	964.19970	60.52024	0.16696	3.14830	1.63991	4.86275	0.07127	3.02212	0.04605	14.89445	0.71091	-1.23271
151914-114	1006.29775	30.01683	999.62752	31.87025	985.02836	77.20110	0.18095	3.78684	1.67443	5.41330	0.07200	3.88881	0.04648	15.74716	0.68851	-2.15947
151914-083	1040.61130	32.11508	1029.38796	32.23145	1005.90523	75.14139	0.17919	3.95027	1.75403	5.06189	0.07273	3.79422	0.04551	15.38040	0.63889	-1.48340
151914-064	1128.15065	39.03382	1124.99611	39.62402	1118.99751	60.15528	0.19525	3.78296	2.02815	4.87520	0.07095	3.07520	0.05003	15.70123	0.76265	0.82486
151914-123	1865.62448	62.26558	1850.17168	44.66828	1822.81128	45.97717	0.33664	3.86230	5.18509	5.36472	0.12206	0.79966	0.07966	16.52006	0.68889	8.89895
151914-060	1899.99535	67.92572	2201.30897	43.17510	1898.79338	43.33142	0.34277	4.14956	7.75766	4.90373	0.14442	2.61299	0.10001	15.12556	0.84274	23.96349
151914-126	1938.22810	57.85639	1952.31689	40.36367	1925.99378	57.37734	0.35076	3.47479	5.70626	4.70396	0.11804	3.26513	0.09324	18.41367	0.71555	-0.63470
151914-005	1975.16796	53.10082	1959.05340	40.75788	1942.69397	63.40281	0.38652	3.12418	5.88713	4.79138	0.11915	3.61422	0.08778	15.27962	0.61460	-1.67133
151914-012	2017.13740	53.89990	2018.44024	34.31912	2011.79508	43.11323	0.36740	3.12								

Appendix 6: Zircon Hafnium Standard plot



Appendix 7: LA-MC-ICP-MS Zircon Hafnium Data Tables

Table 1: 15KZ01; LA-MC-ICP-MS Zircon Hafnium Data

Order	Sample	$(^{176}\text{Yb} + ^{176}\text{Lu}) / ^{176}\text{Hf}$ (%)	Volts Hf	$^{176}\text{Hf}/^{177}\text{Hf}$	\pm (1s)	$^{176}\text{Lu}/^{177}\text{Hf}$	$^{176}\text{Hf}/^{177}\text{Hf}$ (T)	E-Hf (0)	E-Hf (0) \pm (1s)	E-Hf (T)	Age (Ma)
1	CAMPBELL-15KZ01-002	22.7	3.2	0.282701	0.000024	0.001443	0.282694	-3.0	0.8	2.2	244
2	CAMPBELL-15KZ01-003	19.1	3.0	0.282161	0.000028	0.001107	0.282155	-22.1	1.0	-15.3	314
3	CAMPBELL-15KZ01-004	15.4	2.9	0.282636	0.000033	0.000982	0.282632	-5.3	1.2	0.2	254
4	CAMPBELL-15KZ01-050	9.0	4.1	0.281783	0.000029	0.000591	0.281772	-35.4	1.0	-12.5	1042
5	CAMPBELL-15KZ01-049	4.3	4.5	0.281974	0.000025	0.000255	0.281971	-28.7	0.9	-14.5	640
6	CAMPBELL-15KZ01-006	27.3	3.8	0.282623	0.000031	0.001648	0.282616	-5.7	1.1	-0.6	241
7	CAMPBELL-15KZ01-007	18.9	3.5	0.282669	0.000031	0.001557	0.282662	-4.1	1.1	1.1	245
8	CAMPBELL-15KZ01-009	19.2	3.7	0.282466	0.000019	0.001194	0.282459	-11.3	0.7	-4.1	335
9	CAMPBELL-15KZ01-010	18.3	3.5	0.282660	0.000030	0.001131	0.282655	-4.4	1.1	0.9	245
10	CAMPBELL-15KZ01-051	18.3	3.3	0.282482	0.000031	0.001120	0.282475	-10.7	1.1	-3.2	348
11	CAMPBELL-15KZ01-054	40.4	3.5	0.282659	0.000029	0.002387	0.282648	-4.5	1.0	0.7	250
12	CAMPBELL-15KZ01-055	20.4	3.4	0.282347	0.000027	0.001126	0.282339	-15.5	1.0	-7.7	363
13	CAMPBELL-15KZ01-056	6.1	4.6	0.281305	0.000023	0.000395	0.281292	-52.3	0.8	-13.7	1739
14	CAMPBELL-15KZ01-057	20.0	2.9	0.282593	0.000030	0.001266	0.282588	-6.8	1.1	-1.4	252
15	CAMPBELL-15KZ01-058	20.0	3.2	0.281703	0.000026	0.001668	0.281670	-38.3	0.9	-16.2	1038
16	CAMPBELL-15KZ01-039	7.1	3.2	0.281273	0.000032	0.000410	0.281257	-53.5	1.1	-7.8	2048
17	CAMPBELL-15KZ01-060	13.9	2.7	0.281982	0.000031	0.000767	0.281973	-28.4	1.1	-13.8	669
18	CAMPBELL-15KZ01-013	8.5	3.7	0.281343	0.000023	0.000545	0.281324	-51.0	0.8	-10.1	1844
19	CAMPBELL-15KZ01-015	17.8	3.8	0.282699	0.000040	0.001377	0.282693	-3.0	1.4	2.3	252
20	CAMPBELL-15KZ01-017	13.9	3.7	0.282644	0.000032	0.000882	0.282639	-5.0	1.1	0.9	270
21	CAMPBELL-15KZ01-018	13.3	3.5	0.282450	0.000031	0.001193	0.282443	-11.8	1.1	-5.0	320
22	CAMPBELL-15KZ01-019	36.1	4.3	0.282370	0.000041	0.001990	0.282357	-14.7	1.5	-7.6	340
23	CAMPBELL-15KZ01-021	22.1	3.4	0.282563	0.000032	0.001356	0.282557	-7.8	1.1	-2.8	235
24	CAMPBELL-15KZ01-028	21.9	3.8	0.282478	0.000028	0.001402	0.282469	-10.9	1.0	-3.4	350
25	CAMPBELL-15KZ01-025	17.6	3.9	0.282334	0.000029	0.001105	0.282320	-15.9	1.0	-1.1	688

Table 1: 15KZ01; LA-MC-ICP-MS Zircon Hafnium Data

Order	Sample	$(^{176}\text{Yb} + ^{176}\text{Lu}) / ^{176}\text{Hf}$ (%)	Volts Hf	$^{176}\text{Hf}/^{177}\text{Hf}$	\pm (1s)	$^{176}\text{Lu}/^{177}\text{Hf}$	$^{176}\text{Hf}/^{177}\text{Hf}$ (T)	E-Hf (0)	E-Hf (0) \pm (1s)	E-Hf (T)	Age (Ma)
26	CAMPBELL-15KZ01-071	17.8	3.1	0.282437	0.000028	0.001223	0.282430	-12.3	1.0	-5.3	325
27	CAMPBELL-15KZ01-073	8.5	2.0	0.281024	0.000030	0.000567	0.280995	-62.3	1.1	-1.4	2722
28	CAMPBELL-15KZ01-069	17.2	1.9	0.282656	0.000035	0.001207	0.282650	-4.6	1.2	0.8	248
29	CAMPBELL-15KZ01-067	24.9	3.5	0.282686	0.000039	0.001848	0.282678	-3.5	1.4	1.5	238
30	CAMPBELL-15KZ01-075	15.4	2.2	0.282653	0.000032	0.001006	0.282640	-4.7	1.1	9.7	664
31	CAMPBELL-15KZ01-077	7.6	4.2	0.282584	0.000035	0.000546	0.282576	-7.1	1.2	9.8	771
32	CAMPBELL-15KZ01-078	11.9	4.1	0.282618	0.000026	0.000814	0.282606	-5.9	0.9	10.9	773
33	CAMPBELL-15KZ01-065	9.1	3.5	0.282518	0.000027	0.001102	0.282511	-9.4	1.0	-2.6	317
34	CAMPBELL-15KZ01-079	18.6	3.3	0.282566	0.000036	0.001352	0.282558	-7.7	1.3	-0.9	322
35	CAMPBELL-15KZ01-080	10.0	4.3	0.282358	0.000026	0.000598	0.282354	-15.1	0.9	-7.7	341
36	CAMPBELL-15KZ01-082	17.8	3.5	0.282547	0.000026	0.001185	0.282540	-8.4	0.9	-1.5	322
37	CAMPBELL-15KZ01-083	6.9	3.6	0.282487	0.000030	0.000724	0.282483	-10.5	1.1	-3.8	311
38	CAMPBELL-15KZ01-084	12.0	3.7	0.282616	0.000026	0.000769	0.282612	-6.0	0.9	-0.4	259
39	CAMPBELL-15KZ01-087	14.4	3.8	0.282632	0.000027	0.000988	0.282628	-5.4	1.0	0.0	250
40	CAMPBELL-15KZ01-090	11.5	3.5	0.282425	0.000024	0.000709	0.282421	-12.7	0.9	-5.7	321
41	CAMPBELL-15KZ01-091	12.1	2.7	0.282630	0.000038	0.000782	0.282627	-5.5	1.3	0.0	251
42	CAMPBELL-15KZ01-093	19.3	1.9	0.282601	0.000034	0.001347	0.282595	-6.5	1.2	-1.6	228
43	CAMPBELL-15KZ01-094	9.1	3.3	0.282087	0.000039	0.000654	0.282079	-24.7	1.4	-10.8	636
44	CAMPBELL-15KZ01-095	31.1	3.5	0.282637	0.000030	0.001770	0.282628	-5.2	1.1	0.2	258
45	CAMPBELL-15KZ01-096	46.2	3.1	0.282648	0.000026	0.002880	0.282635	-4.9	0.9	-0.2	229
46	CAMPBELL-15KZ01-097	23.3	2.6	0.282553	0.000045	0.001769	0.282542	-8.2	1.6	-1.5	318
47	CAMPBELL-15KZ01-098	14.8	3.6	0.282517	0.000041	0.000962	0.282511	-9.5	1.4	-2.6	317
48	CAMPBELL-15KZ01-099	13.3	3.4	0.282508	0.000025	0.000794	0.282504	-9.8	0.9	-2.6	330
49	CAMPBELL-15KZ01-100	23.1	3.4	0.282440	0.000036	0.001486	0.282431	-12.2	1.3	-5.2	329

Table 2: 15YP11; LA-MC-ICP-MS Zircon Hafnium Data

Order	Sample	$(^{176}\text{Yb} + ^{176}\text{Lu}) / ^{176}\text{Hf}$ (%)	Volts Hf	$^{176}\text{Hf}/^{177}\text{Hf}$	\pm (1s)	$^{176}\text{Lu}/^{177}\text{Hf}$	$^{176}\text{Hf}/^{177}\text{Hf}$ (T)	E-Hf (0)	E-Hf (0) \pm (1s)	E-Hf (T)	Age (Ma)
50	CAMPBELL-15YP11-003	17.8	3.4	0.282851	0.000021	0.001435	0.282849	2.3	0.7	3.5	55
51	CAMPBELL-15YP11-008	33.0	3.5	0.282845	0.000019	0.002264	0.282843	2.1	0.7	3.2	51
52	CAMPBELL-15YP11-009	8.9	3.6	0.282926	0.000015	0.000889	0.282925	5.0	0.5	6.1	51
53	CAMPBELL-15YP11-010	17.0	3.4	0.282942	0.000022	0.001287	0.282941	5.6	0.8	6.7	51
54	CAMPBELL-15YP11-017	16.3	3.5	0.282858	0.000017	0.001331	0.282857	2.6	0.6	3.7	53
55	CAMPBELL-15YP11-146	21.0	3.2	0.282909	0.000018	0.001780	0.282907	4.4	0.6	5.5	51
56	CAMPBELL-15YP11-028	18.3	4.0	0.282917	0.000018	0.001417	0.282916	4.7	0.6	5.7	50
57	CAMPBELL-15YP11-029	19.9	3.6	0.282992	0.000020	0.001567	0.282991	7.3	0.7	8.4	51
58	CAMPBELL-15YP11-129	25.0	3.3	0.282953	0.000018	0.001855	0.282952	6.0	0.6	7.1	53
59	CAMPBELL-15YP11-125	31.0	3.3	0.282933	0.000026	0.002234	0.282931	5.2	0.9	6.3	50
60	CAMPBELL-15YP11-042	20.1	3.6	0.282926	0.000021	0.001478	0.282925	5.0	0.7	6.1	51
61	CAMPBELL-15YP11-121	22.4	3.4	0.282892	0.000020	0.001849	0.282890	3.8	0.7	4.9	52
62	CAMPBELL-15YP11-120	23.0	3.5	0.282937	0.000020	0.001783	0.282935	5.4	0.7	6.5	54
63	CAMPBELL-15YP11-119	12.2	3.6	0.282869	0.000015	0.000998	0.282868	3.0	0.5	4.1	54
64	CAMPBELL-15YP11-118	16.1	3.6	0.282914	0.000022	0.001197	0.282913	4.6	0.8	5.7	51
65	CAMPBELL-15YP11-058	17.7	3.6	0.282895	0.000016	0.001314	0.282894	3.9	0.6	4.9	50
66	CAMPBELL-15YP11-059	21.3	3.4	0.282926	0.000018	0.001593	0.282924	5.0	0.6	6.1	55
67	CAMPBELL-15YP11-062	19.9	3.4	0.282875	0.000019	0.001535	0.282873	3.2	0.7	4.3	52
68	CAMPBELL-15YP11-065	15.7	3.6	0.282980	0.000023	0.001128	0.282979	6.9	0.8	8.0	50
69	CAMPBELL-15YP11-095	21.0	3.3	0.282854	0.000022	0.001765	0.282852	2.4	0.8	3.5	52
70	CAMPBELL-15YP11-071	15.8	3.2	0.282914	0.000023	0.001433	0.282913	4.6	0.8	5.6	47
71	CAMPBELL-15YP11-074	15.1	3.5	0.282898	0.000016	0.001189	0.282897	4.0	0.6	5.1	52

Table 3:15YP04; LA-MC-ICP-MS Zircon Hafnium Data

Order	Sample	$(^{176}\text{Yb} + ^{176}\text{Lu}) / ^{176}\text{Hf}$ (%)	Volts Hf	$^{176}\text{Hf}/^{177}\text{Hf}$	\pm (1s)	$^{176}\text{Lu}/^{177}\text{Hf}$	$^{176}\text{Hf}/^{177}\text{Hf}$ (T)	E-Hf (0)	E-Hf (0) \pm (1s)	E-Hf (T)	Age (Ma)
72	CAMPBELL-15YP04-004	16.9	2.0	0.282627	0.000037	0.000978	0.282622	-5.6	1.3	1.3	318
73	CAMPBELL-15YP04-008	16.9	1.1	0.282085	0.000037	0.001123	0.282078	-24.7	1.3	-17.7	329
74	CAMPBELL-15YP04-010	8.7	4.7	0.281911	0.000027	0.000542	0.281901	-30.9	0.9	-7.8	1049
75	CAMPBELL-15YP04-011	16.3	3.2	0.282438	0.000026	0.001088	0.282431	-12.3	0.9	-5.4	320
76	CAMPBELL-15YP04-012	21.7	3.1	0.282433	0.000030	0.001351	0.282425	-12.4	1.1	-5.6	322
77	CAMPBELL-15YP04-013	70.6	2.0	0.282389	0.000071	0.004285	0.282360	-14.0	2.5	-7.2	352
78	CAMPBELL-15YP04-015	19.2	2.5	0.282497	0.000036	0.001412	0.282488	-10.2	1.3	-3.3	322
79	CAMPBELL-15YP04-016	12.5	2.8	0.282378	0.000026	0.000740	0.282374	-14.4	0.9	-7.4	321
80	CAMPBELL-15YP04-018	14.6	2.5	0.282403	0.000033	0.000897	0.282397	-13.5	1.2	-6.5	325
81	CAMPBELL-15YP04-021	21.1	3.4	0.282381	0.000039	0.001311	0.282373	-14.3	1.4	-7.2	330
82	CAMPBELL-15YP04-032	12.8	3.7	0.282439	0.000023	0.000843	0.282434	-12.2	0.8	-5.1	328
83	CAMPBELL-15YP04-034	15.8	3.8	0.282331	0.000025	0.001034	0.282324	-16.1	0.9	-9.0	326
84	CAMPBELL-15YP04-047	17.5	3.6	0.282359	0.000017	0.001084	0.282352	-15.1	0.6	-8.1	323
85	CAMPBELL-15YP04-048	25.8	2.2	0.282359	0.000020	0.001439	0.282349	-15.1	0.7	-7.1	376
86	CAMPBELL-15YP04-050	20.1	3.0	0.282401	0.000016	0.001274	0.282393	-13.6	0.6	-6.4	337
87	CAMPBELL-15YP04-049	7.6	2.8	0.281789	0.000019	0.000450	0.281784	-35.2	0.7	-22.2	592
88	CAMPBELL-15YP04-052	27.8	2.1	0.282407	0.000031	0.001559	0.282397	-13.4	1.1	-6.1	342
89	CAMPBELL-15YP04-056	16.8	4.2	0.282521	0.000019	0.001152	0.282513	-9.4	0.7	-2.2	335
90	CAMPBELL-15YP04-061	31.9	2.6	0.282404	0.000023	0.002126	0.282391	-13.5	0.8	-6.7	325
91	CAMPBELL-15YP04-062	28.4	1.5	0.281970	0.000039	0.001525	0.281954	-28.8	1.4	-17.3	544
92	CAMPBELL-15YP04-066	14.8	1.6	0.281718	0.000026	0.001011	0.281696	-37.7	0.9	-12.6	1156
93	CAMPBELL-15YP04-071	24.4	1.8	0.282417	0.000026	0.001530	0.282407	-13.0	0.9	-6.2	322
94	CAMPBELL-15YP04-079	13.4	3.4	0.282379	0.000021	0.000867	0.282374	-14.4	0.8	-7.3	324
95	CAMPBELL-15YP04-080	18.4	3.0	0.282440	0.000021	0.001175	0.282433	-12.2	0.8	-5.1	331
96	CAMPBELL-15YP04-081	14.2	3.3	0.282473	0.000017	0.000843	0.282468	-11.0	0.6	-4.0	322
97	CAMPBELL-15YP04-082	14.1	3.5	0.281994	0.000022	0.000787	0.281985	-28.0	0.8	-14.8	607
98	CAMPBELL-15YP04-087	44.0	2.7	0.282369	0.000024	0.002628	0.282352	-14.7	0.9	-8.0	328
99	CAMPBELL-15YP04-089	32.4	1.6	0.282464	0.000024	0.001904	0.282452	-11.4	0.9	-4.3	338
100	CAMPBELL-15YP04-090	13.4	1.8	0.282750	0.000028	0.000934	0.282739	-1.2	1.0	12.5	632
101	CAMPBELL-15YP04-096	29.4	3.0	0.282375	0.000025	0.001575	0.282366	-14.5	0.9	-7.6	326
102	CAMPBELL-15YP04-100	20.1	2.0	0.282507	0.000027	0.001456	0.282498	-9.8	1.0	-2.8	329
103	CAMPBELL-15YP04-108	17.0	1.4	0.282415	0.000036	0.001104	0.282403	-13.1	1.3	-0.6	580
104	CAMPBELL-15YP04-111	16.7	2.8	0.282420	0.000023	0.001056	0.282414	-12.9	0.8	-5.9	326
105	CAMPBELL-15YP04-133	4.1	3.1	0.282303	0.000020	0.000241	0.282302	-17.0	0.7	-9.7	331
106	CAMPBELL-15YP04-132	10.1	2.6	0.282093	0.000021	0.000826	0.282082	-24.5	0.8	-9.6	684
107	CAMPBELL-15YP04-135	21.6	4.2	0.282485	0.000019	0.001383	0.282476	-10.6	0.7	-3.5	336
108	CAMPBELL-15YP04-131	8.3	3.7	0.282311	0.000022	0.000572	0.282303	-16.8	0.8	-1.9	678

Table 4:15YP14; LA-MC-ICP-MS Zircon Hafnium Data

Order	Sample	$(^{176}\text{Yb} + ^{176}\text{Lu}) / ^{176}\text{Hf}$ (%)	Volts Hf	$^{176}\text{Hf}/^{177}\text{Hf}$	\pm (1s)	$^{176}\text{Lu}/^{177}\text{Hf}$	$^{176}\text{Hf}/^{177}\text{Hf}$ (T)	E-Hf (0)	E-Hf (0) \pm (1s)	E-Hf (T)	Age (Ma)
111	CAMPBELL-15YP14-012	5.0	2.2	0.281647	0.00028	0.000279	0.281637	-40.2	1.0	5.0	2017
112	CAMPBELL-15YP14-009	13.9	1.8	0.282512	0.00024	0.000979	0.282506	-9.7	0.9	-2.7	321
113	CAMPBELL-15YP14-022	20.6	1.4	0.282901	0.00027	0.001486	0.282899	4.1	1.0	5.7	77
114	CAMPBELL-15YP14-025	9.1	1.3	0.280990	0.00037	0.000570	0.280960	-63.5	1.3	-3.1	2702
115	CAMPBELL-15YP14-031	23.3	1.3	0.283059	0.00039	0.001596	0.283056	9.7	1.4	11.8	100
116	CAMPBELL-15YP14-032	7.3	1.9	0.282752	0.00030	0.000514	0.282747	-1.2	1.1	10.7	542
117	CAMPBELL-15YP14-036	8.8	2.4	0.281362	0.00024	0.000675	0.281330	-50.3	0.8	4.8	2475
118	CAMPBELL-15YP14-039	20.2	2.3	0.282750	0.00024	0.001465	0.282748	-1.2	0.8	0.4	79
119	CAMPBELL-15YP14-048	18.5	3.3	0.282955	0.00025	0.001342	0.282952	6.0	0.9	8.1	100
120	CAMPBELL-15YP14-049	24.1	2.6	0.282617	0.00023	0.002053	0.282604	-5.9	0.8	1.1	339
121	CAMPBELL-15YP14-051	10.5	1.6	0.282549	0.00029	0.000591	0.282542	-8.3	1.0	6.0	655
122	CAMPBELL-15YP14-052	26.4	2.5	0.282603	0.00022	0.001755	0.282590	-6.4	0.8	1.6	380
123	CAMPBELL-15YP14-054	19.6	3.3	0.282344	0.00019	0.001253	0.282335	-15.6	0.7	-6.9	405
124	CAMPBELL-15YP14-056	11.5	2.9	0.282347	0.00020	0.000758	0.282340	-15.5	0.7	-5.3	469
125	CAMPBELL-15YP14-057	22.2	2.7	0.282385	0.00027	0.001526	0.282373	-14.2	0.9	-5.3	418
126	CAMPBELL-15YP14-058	17.6	1.3	0.282484	0.00032	0.001051	0.282479	-10.6	1.1	-4.8	271
127	CAMPBELL-15YP14-055	29.5	1.5	0.282856	0.00031	0.002111	0.282852	2.5	1.1	4.6	102
128	CAMPBELL-15YP14-060	15.9	3.2	0.281181	0.00026	0.000862	0.281150	-56.7	0.9	-15.0	1900
129	CAMPBELL-15YP14-061	20.2	3.6	0.282424	0.00020	0.001324	0.282410	-12.8	0.7	-0.8	559
130	CAMPBELL-15YP14-064	24.3	2.0	0.282232	0.00037	0.001542	0.282199	-19.5	1.3	4.6	1128
131	CAMPBELL-15YP14-068	24.5	2.8	0.282224	0.00022	0.001382	0.282208	-19.9	0.8	-6.7	614
132	CAMPBELL-15YP14-071	26.7	2.8	0.282574	0.00027	0.001873	0.282563	-7.5	0.9	-0.7	320
133	CAMPBELL-15YP14-088	32.7	2.6	0.282503	0.00018	0.001934	0.282481	-10.0	0.6	3.2	624
134	CAMPBELL-15YP14-075	12.1	3.1	0.282725	0.00017	0.000788	0.282720	-2.1	0.6	6.1	377
135	CAMPBELL-15YP14-083	7.7	1.9	0.282152	0.00029	0.000466	0.282143	-22.4	1.0	0.6	1041
136	CAMPBELL-15YP14-080	8.0	1.9	0.282603	0.00031	0.000521	0.282600	-6.4	1.1	0.4	312
138	CAMPBELL-15YP14-099	24.2	3.6	0.282720	0.00022	0.001545	0.282717	-2.3	0.8	-0.6	82
139	CAMPBELL-15YP14-096	21.9	3.4	0.282739	0.00017	0.001419	0.282737	-1.6	0.6	0.1	79
140	CAMPBELL-15YP14-098	15.4	4.0	0.282587	0.00016	0.001109	0.282579	-7.0	0.6	0.9	365
141	CAMPBELL-15YP14-095	13.5	3.5	0.282318	0.00020	0.000857	0.282311	-16.5	0.7	-7.9	398
142	CAMPBELL-15YP14-091	16.2	3.4	0.282806	0.00020	0.000972	0.282805	0.8	0.7	2.4	79
143	CAMPBELL-15YP14-089	41.2	2.5	0.282665	0.00032	0.002498	0.282661	-4.3	1.1	-2.5	87
144	CAMPBELL-15YP14-107	9.0	1.6	0.282678	0.00035	0.000854	0.282677	-3.8	1.3	-2.0	84
145	CAMPBELL-15YP14-104	22.9	2.6	0.282313	0.00023	0.001499	0.282301	-16.7	0.8	-8.0	411
146	CAMPBELL-15YP14-100	16.6	2.0	0.282236	0.00025	0.000941	0.282228	-19.4	0.9	-9.5	459
147	CAMPBELL-15YP14-114	24.1	1.5	0.282200	0.00031	0.001306	0.282175	-20.7	1.1	1.0	1006
148	CAMPBELL-15YP14-119	24.4	2.2	0.282768	0.00028	0.001439	0.282761	-0.6	1.0	5.2	271
149	CAMPBELL-15YP14-122	20.4	2.0	0.282774	0.00028	0.001474	0.282772	-0.4	1.0	1.3	79
150	CAMPBELL-15YP14-123	7.3	3.5	0.281493	0.00019	0.000428	0.281478	-45.7	0.7	-4.1	1866
151	CAMPBELL-15YP14-135	20.1	2.8	0.282725	0.00024	0.001431	0.282723	-2.1	0.9	-0.3	84
152	CAMPBELL-15YP14-137	12.3	2.8	0.280753	0.00020	0.000647	0.280712	-71.9	0.7	2.3	3305
153	CAMPBELL-15YP14-134	26.9	3.0	0.282213	0.00031	0.001323	0.282190	-20.2	1.1	-0.9	899
154	CAMPBELL-15YP14-130	17.2	2.6	0.282555	0.00022	0.001170	0.282549	-8.1	0.8	-3.0	240
155	CAMPBELL-15YP14-131	17.4	3.3	0.282501	0.00018	0.001166	0.282494	-10.0	0.6	-2.6	347
156	CAMPBELL-15YP14-138	5.6	3.1	0.282446	0.00017	0.000492	0.282445	-12.0	0.6	-10.2	84
157	CAMPBELL-15YP14-116	9.9	2.7	0.282615	0.00017	0.000708	0.282614	-6.0	0.6	-4.2	82
158	CAMPBELL-15YP14-125	32.2	1.3	0.282500	0.00041	0.002075	0.282497	-10.1	1.4	-8.4	82
159	CAMPBELL-15YP14-127	22.1	2.5	0.282389	0.00029	0.001545	0.282371	-14.0	1.0	-0.9	617

Table 5:15YP09; LA-MC-ICP-MS Zircon Hafnium Data

Order	Sample	$(^{176}\text{Yb} + ^{176}\text{Lu}) / ^{176}\text{Hf}$ (%)	Volts Hf	$^{176}\text{Hf}/^{177}\text{Hf}$	\pm (1s)	$^{176}\text{Lu}/^{177}\text{Hf}$	$^{176}\text{Hf}/^{177}\text{Hf}$ (T)	E-Hf (0)	E-Hf (0) \pm (1s)	E-Hf (T)	Age (Ma)
160	CAMPBELL-15YP09-007	18.5	3.7	0.282274	0.000026	0.001228	0.282262	-18.1	0.9	-7.1	512
161	CAMPBELL-15YP09-010	4.3	3.2	0.280801	0.000025	0.000259	0.280787	-70.2	0.9	-6.5	2818
162	CAMPBELL-15YP09-015	19.7	2.7	0.282971	0.000024	0.001480	0.282968	6.6	0.9	9.0	115
163	CAMPBELL-15YP09-018	5.7	3.3	0.281101	0.000021	0.000357	0.281087	-59.6	0.7	-14.9	1999
164	CAMPBELL-15YP09-020	9.1	2.9	0.281182	0.000023	0.000540	0.281163	-56.7	0.8	-15.8	1844
165	CAMPBELL-15YP09-021	9.6	3.6	0.282173	0.000025	0.000646	0.282166	-21.6	0.9	-8.2	613
166	CAMPBELL-15YP09-036	8.6	3.4	0.282092	0.000027	0.000541	0.282083	-24.5	1.0	-3.7	943
167	CAMPBELL-15YP09-042	9.2	2.8	0.282133	0.000026	0.000699	0.282124	-23.1	0.9	-8.8	654
168	CAMPBELL-15YP09-045	15.5	3.8	0.281873	0.000019	0.000968	0.281855	-32.2	0.7	-10.2	1016
169	CAMPBELL-15YP09-047	15.3	3.0	0.282418	0.000032	0.000987	0.282411	-13.0	1.1	-4.4	396
170	CAMPBELL-15YP09-049	16.6	2.5	0.282712	0.000032	0.001373	0.282692	-2.6	1.1	14.0	774
171	CAMPBELL-15YP09-053	9.9	3.6	0.282527	0.000028	0.000593	0.282525	-9.1	1.0	-4.5	210
172	CAMPBELL-15YP09-054	8.5	1.9	0.281474	0.000027	0.000778	0.281455	-46.4	1.0	-17.9	1300
173	CAMPBELL-15YP09-055	18.0	1.8	0.282617	0.000033	0.001148	0.282602	-5.9	1.2	9.4	711
174	CAMPBELL-15YP09-061	11.9	2.2	0.281322	0.000026	0.000716	0.281298	-51.7	0.9	-11.8	1812
175	CAMPBELL-15YP09-071	9.6	3.1	0.282164	0.000027	0.000536	0.282154	-22.0	1.0	0.2	1006
176	CAMPBELL-15YP09-075	6.0	4.2	0.281960	0.000024	0.000371	0.281955	-29.2	0.8	-13.7	702
177	CAMPBELL-15YP09-078	24.9	2.1	0.282361	0.000027	0.001449	0.282346	-15.0	1.0	-2.8	573
178	CAMPBELL-15YP09-080	14.1	3.6	0.282587	0.000019	0.000939	0.282586	-7.0	0.7	-5.2	84
179	CAMPBELL-15YP09-085	28.6	2.8	0.280876	0.000027	0.001723	0.280768	-67.5	0.9	3.1	3252
180	CAMPBELL-15YP09-092	9.3	4.0	0.282061	0.000022	0.000572	0.282049	-25.6	0.8	-2.1	1067
181	CAMPBELL-15YP09-093	25.2	3.4	0.281667	0.000028	0.001507	0.281641	-39.5	1.0	-20.0	918
182	CAMPBELL-15YP09-094	7.7	2.6	0.282417	0.000024	0.000525	0.282413	-13.0	0.9	-4.4	391
183	CAMPBELL-15YP09-095	15.2	2.8	0.282269	0.000022	0.001021	0.282251	-18.2	0.8	2.5	954
184	CAMPBELL-15YP09-098	16.7	3.1	0.282295	0.000023	0.001034	0.282287	-17.3	0.8	-9.0	389
185	CAMPBELL-15YP09-100	19.0	2.8	0.282533	0.000020	0.001198	0.282524	-8.9	0.7	-1.1	365
186	CAMPBELL-15YP09-104	19.9	3.5	0.282601	0.000021	0.001203	0.282595	-6.5	0.7	-1.0	259
187	CAMPBELL-15YP09-107	9.8	3.3	0.281131	0.000022	0.000613	0.281102	-58.5	0.8	-4.7	2417
188	CAMPBELL-15YP09-108	15.8	3.5	0.282253	0.000025	0.000878	0.282242	-18.8	0.9	-4.0	681
189	CAMPBELL-15YP09-109	3.7	3.9	0.280990	0.000019	0.000308	0.280975	-63.5	0.7	-5.8	2565
190	CAMPBELL-15YP09-110	10.9	3.8	0.282452	0.000017	0.000739	0.282448	-11.8	0.6	-5.0	313
191	CAMPBELL-15YP09-119	8.1	2.7	0.282628	0.000023	0.000503	0.282621	-5.6	0.8	9.1	667
192	CAMPBELL-15YP09-120	26.7	3.0	0.281576	0.000021	0.001829	0.281502	-42.8	0.8	2.4	2110
193	CAMPBELL-15YP09-122	8.2	2.4	0.282537	0.000027	0.000639	0.282526	-8.8	1.0	9.6	836
194	CAMPBELL-15YP09-123	9.4	4.2	0.281794	0.000026	0.000750	0.281772	-35.1	0.9	-2.0	1502
195	CAMPBELL-15YP09-127	21.5	2.2	0.282688	0.000032	0.001425	0.282670	-3.4	1.1	10.9	669
196	CAMPBELL-15YP09-135	30.2	3.4	0.282520	0.000024	0.001856	0.282517	-9.4	0.9	-7.6	86
197	CAMPBELL-15YP09-136	16.6	3.9	0.281999	0.000021	0.000945	0.281985	-27.8	0.8	-10.1	813
198	CAMPBELL-15YP09-138	18.2	2.2	0.282416	0.000036	0.001094	0.282415	-13.0	1.3	-11.3	81
199	CAMPBELL-15YP09-142	13.0	3.6	0.282787	0.000024	0.000998	0.282777	0.1	0.9	11.8	539
200	CAMPBELL-15YP09-144	8.3	2.5	0.282429	0.000031	0.000520	0.282423	-12.6	1.1	0.7	606
201	CAMPBELL-15YP09-148	26.6	1.8	0.282273	0.000042	0.001542	0.282240	-18.1	1.5	6.1	1132
202	CAMPBELL-15YP09-149	35.3	3.7	0.282602	0.000024	0.002119	0.282599	-6.5	0.8	-4.7	83
203	CAMPBELL-15YP09-150	15.3	3.2	0.282586	0.000023	0.000982	0.282584	-7.0	0.8	-5.3	80

Table 5: 15G002; LA-MC-ICP-MS Zircon Hafnium Data

Order	Sample	$(^{176}\text{Yb} + ^{176}\text{Lu}) / ^{176}\text{Hf}$ (%)	Volts Hf	$^{176}\text{Hf}/^{177}\text{Hf}$	\pm (1s)	$^{176}\text{Lu}/^{177}\text{Hf}$	$^{176}\text{Hf}/^{177}\text{Hf}$ (T)	E-Hf (0)	E-Hf (0) \pm (1s)	E-Hf (T)	Age (Ma)
204	CAMPBELL-15G002-006	16.8	2.5	0.282369	0.000023	0.000993	0.282362	-14.7	0.8	-6.2	394
206	CAMPBELL-15G002-012	19.5	2.6	0.282398	0.000024	0.001136	0.282391	-13.7	0.9	-6.9	317
207	CAMPBELL-15G002-013	18.4	2.8	0.282834	0.000026	0.001182	0.282832	1.7	0.9	3.5	81
208	CAMPBELL-15G002-015	25.1	2.6	0.281876	0.000024	0.001576	0.281847	-32.1	0.9	-11.2	981
209	CAMPBELL-15G002-017	11.7	2.6	0.281230	0.000023	0.000681	0.281206	-55.0	0.8	-13.6	1872
210	CAMPBELL-15G002-018	25.5	2.5	0.282639	0.000026	0.001458	0.282632	-5.2	0.9	0.3	257
211	CAMPBELL-15G002-020	18.1	2.7	0.282765	0.000028	0.001248	0.282764	-0.7	1.0	1.0	79
212	CAMPBELL-15G002-021	11.2	3.2	0.282396	0.000019	0.000729	0.282392	-13.8	0.7	-7.3	298
213	CAMPBELL-15G002-024	22.2	2.9	0.282649	0.000021	0.001495	0.282647	-4.8	0.7	-3.0	83
214	CAMPBELL-15G002-025	15.4	2.7	0.282465	0.000020	0.000872	0.282459	-11.3	0.7	-4.6	312
215	CAMPBELL-15G002-026	9.4	3.1	0.282404	0.000020	0.000645	0.282400	-13.5	0.7	-6.4	325
217	CAMPBELL-15G002-035	15.5	1.9	0.281544	0.000037	0.001121	0.281493	-43.9	1.3	8.3	2377
218	CAMPBELL-15G002-042	8.8	3.1	0.282095	0.000018	0.000578	0.282088	-24.4	0.6	-11.3	598
219	CAMPBELL-15G002-043	16.1	2.3	0.282401	0.000035	0.001096	0.282394	-13.6	1.2	-6.3	336
220	CAMPBELL-15G002-047	18.4	2.0	0.282525	0.000022	0.001185	0.282508	-9.2	0.8	7.9	794
221	CAMPBELL-15G002-048	40.5	3.1	0.282349	0.000026	0.002107	0.282258	-15.4	0.9	32.9	2268
222	CAMPBELL-15G002-055	11.7	2.9	0.282732	0.000025	0.000747	0.282731	-1.9	0.9	-0.3	74
223	CAMPBELL-15G002-057	9.3	3.0	0.282357	0.000027	0.000588	0.282353	-15.1	1.0	-8.4	307
224	CAMPBELL-15G002-058	24.2	2.8	0.282449	0.000026	0.001499	0.282439	-11.9	0.9	-3.7	384
225	CAMPBELL-15G002-060	21.2	3.0	0.281873	0.000029	0.001365	0.281859	-32.2	1.0	-20.2	565
226	CAMPBELL-15G002-061	18.2	3.7	0.281427	0.000021	0.001110	0.281418	-48.0	0.8	-38.7	436
228	CAMPBELL-15G002-071	16.6	2.9	0.282072	0.000021	0.000991	0.282059	-25.2	0.7	-10.8	666
229	CAMPBELL-15G002-075	20.5	2.8	0.282718	0.000030	0.001384	0.282716	-2.4	1.1	-0.7	77
230	CAMPBELL-15G002-079	11.5	2.9	0.282542	0.000022	0.000761	0.282537	-8.6	0.8	-1.6	321
231	CAMPBELL-15G002-081	26.6	2.6	0.282693	0.000021	0.001573	0.282686	-3.3	0.8	1.6	230
232	CAMPBELL-15G002-084	30.2	3.1	0.282843	0.000019	0.002403	0.282832	2.1	0.7	7.5	264
233	CAMPBELL-15G002-089	22.4	3.1	0.282776	0.000025	0.001504	0.282774	-0.3	0.9	1.3	75
235	CAMPBELL-15G002-094	57.7	2.1	0.282755	0.000025	0.003989	0.282749	-1.1	0.9	0.5	79
236	CAMPBELL-15G002-096	21.3	2.7	0.282545	0.000021	0.001304	0.282536	-8.5	0.7	0.0	397
237	CAMPBELL-15G002-098	19.1	2.7	0.282527	0.000028	0.001294	0.282520	-9.1	1.0	-2.5	309
239	CAMPBELL-15G002-103	23.9	2.7	0.282757	0.000021	0.001579	0.282754	-1.0	0.8	0.7	82
240	CAMPBELL-15G002-106	13.7	2.9	0.282644	0.000026	0.000871	0.282641	-5.0	0.9	-0.4	213
241	CAMPBELL-15G002-109	31.9	2.6	0.282674	0.000030	0.002120	0.282645	-3.9	1.1	11.3	725
242	CAMPBELL-15G002-112	17.1	2.7	0.282423	0.000022	0.001000	0.282416	-12.8	0.8	-3.9	410
243	CAMPBELL-15G002-113	16.3	2.8	0.282717	0.000032	0.001052	0.282715	-2.4	1.1	-0.6	83
244	CAMPBELL-15G002-118	17.9	2.2	0.282512	0.000030	0.001072	0.282507	-9.6	1.0	-3.5	284
245	CAMPBELL-15G002-120	39.4	3.2	0.282577	0.000021	0.002796	0.282573	-7.4	0.7	-5.7	82
247	CAMPBELL-15G002-123	28.4	2.2	0.282460	0.000025	0.002006	0.282448	-11.5	0.9	-4.9	318
248	CAMPBELL-15G002-124	14.4	2.4	0.282572	0.000030	0.000953	0.282567	-7.5	1.0	-0.3	334
249	CAMPBELL-15G002-127	44.0	2.1	0.282706	0.000030	0.002975	0.282702	-2.8	1.1	-1.3	75
250	CAMPBELL-15G002-130	19.0	2.7	0.282790	0.000017	0.001508	0.282788	0.2	0.6	1.8	77
251	CAMPBELL-15G002-132	9.9	2.7	0.282117	0.000024	0.000622	0.282106	-23.6	0.8	-1.7	998
252	CAMPBELL-15G002-129	27.2	3.2	0.282406	0.000020	0.001647	0.282397	-13.4	0.7	-6.9	308
253	CAMPBELL-15G002-135	20.8	1.7	0.281582	0.000029	0.001383	0.281556	-42.6	1.0	-21.2	997
254	CAMPBELL-15G002-136	23.7	2.0	0.282624	0.000027	0.001770	0.282621	-5.7	1.0	-4.0	79
255	CAMPBELL-15G002-142	1.5	2.0	0.282207	0.000022	0.000103	0.282206	-20.4	0.8	0.4	935
256	CAMPBELL-15G002-143	40.4	1.9	0.282593	0.000024	0.002499	0.282590	-6.8	0.9	-5.1	81

Table 6: 15G001; LA-MC-ICP-MS Zircon Hafnium Data

Order	Sample	$(^{176}\text{Yb} + ^{176}\text{Lu}) / ^{176}\text{Hf}$ (%)	Volts Hf	$^{176}\text{Hf}/^{177}\text{Hf}$	\pm (1s)	$^{176}\text{Lu}/^{177}\text{Hf}$	$^{176}\text{Hf}/^{177}\text{Hf}$ (T)	E-Hf (0)	E-Hf (0) \pm (1s)	E-Hf (T)	Age (Ma)
257	CAMPBELL-15G001-003	14.4	2.2	0.282877	0.000023	0.000954	0.282876	3.3	0.8	4.9	77
258	CAMPBELL-15G001-012	15.1	2.5	0.282890	0.000036	0.001006	0.282888	3.7	1.3	5.3	76
259	CAMPBELL-15G001-015	19.7	2.5	0.282872	0.000025	0.001330	0.282870	3.1	0.9	4.7	78
260	CAMPBELL-15G001-016	13.3	2.4	0.282904	0.000031	0.000938	0.282903	4.2	1.1	5.9	80
261	CAMPBELL-15G001-021	14.9	2.5	0.282880	0.000029	0.001042	0.282878	3.4	1.0	5.0	78
262	CAMPBELL-15G001-028	13.0	2.5	0.282889	0.000021	0.000873	0.282887	3.7	0.7	5.3	76
263	CAMPBELL-15G001-034	35.0	2.1	0.282878	0.000025	0.002118	0.282876	3.3	0.9	4.9	75
264	CAMPBELL-15G001-039	24.5	1.9	0.282912	0.000024	0.001577	0.282910	4.5	0.8	6.2	79
265	CAMPBELL-15G001-051	15.6	2.2	0.282937	0.000027	0.001007	0.282936	5.4	0.9	7.1	80
267	CAMPBELL-15G001-064	23.2	2.2	0.282874	0.000025	0.001599	0.282872	3.1	0.9	4.8	80
268	CAMPBELL-15G001-063	23.0	2.1	0.282813	0.000023	0.001597	0.282811	1.0	0.8	2.6	75
269	CAMPBELL-15G001-072	25.1	2.0	0.282838	0.000030	0.001728	0.282835	1.9	1.0	3.5	78
270	CAMPBELL-15G001-077	13.9	2.3	0.282826	0.000020	0.000977	0.282824	1.4	0.7	3.2	82
271	CAMPBELL-15G001-079	26.1	2.0	0.282811	0.000031	0.001825	0.282809	0.9	1.1	2.6	78
272	CAMPBELL-15G001-080	20.9	2.0	0.282857	0.000028	0.001391	0.282855	2.6	1.0	4.2	77
273	CAMPBELL-15G001-089	15.7	2.2	0.282852	0.000024	0.001048	0.282851	2.4	0.8	4.0	75
274	CAMPBELL-15G001-091	22.5	2.0	0.282752	0.000026	0.001492	0.282750	-1.2	0.9	0.5	79
275	CAMPBELL-15G001-095	21.1	2.5	0.282829	0.000030	0.001356	0.282827	1.6	1.1	3.2	76

Table 7:15YP08; LA-MC-ICP-MS Zircon Hafnium Data

Order	Sample	$(^{176}\text{Yb} + ^{176}\text{Lu}) / ^{176}\text{Hf}$ (%)	Volts Hf	$^{176}\text{Hf}/^{177}\text{Hf}$	\pm (ls)	$^{176}\text{Lu}/^{177}\text{Hf}$	$^{176}\text{Hf}^{177}\text{Hf}$ (T)	E-Hf (0)	E-Hf (0) \pm (ls)	E-Hf (T)	Age (Ma)
276	CAMPBELL-15YP08-002	4.0	3.0	0.282231	0.000026	0.000245	0.282228	-19.6	0.9	-5.9	619
277	CAMPBELL-15YP08-004	19.0	3.1	0.282000	0.000026	0.001396	0.281973	-27.8	0.9	-6.0	1017
278	CAMPBELL-15YP08-005	11.5	3.6	0.282214	0.000025	0.000698	0.282206	-20.2	0.9	-6.3	637
279	CAMPBELL-15YP08-011	12.3	3.5	0.281778	0.000027	0.000789	0.281764	-35.6	0.9	-14.4	972
281	CAMPBELL-15YP08-013	13.4	3.4	0.282122	0.000028	0.000817	0.282108	-23.5	1.0	-3.8	900
282	CAMPBELL-15YP08-016	18.6	3.4	0.281177	0.000024	0.001254	0.281115	-56.9	0.8	-0.7	2569
283	CAMPBELL-15YP08-018	9.7	2.9	0.281975	0.000024	0.000609	0.281963	-28.6	0.8	-5.7	1044
284	CAMPBELL-15YP08-020	13.6	1.8	0.282481	0.000026	0.000963	0.282463	-10.8	0.9	11.4	1016
285	CAMPBELL-15YP08-021	10.1	3.9	0.281902	0.000020	0.000635	0.281890	-31.2	0.7	-8.4	1039
286	CAMPBELL-15YP08-026	9.8	2.3	0.282600	0.000028	0.000704	0.282591	-6.6	1.0	8.7	698
287	CAMPBELL-15YP08-029	5.9	3.6	0.281375	0.000025	0.000380	0.281361	-49.8	0.9	-5.9	1970
288	CAMPBELL-15YP08-031	13.9	3.2	0.282227	0.000024	0.000832	0.282215	-19.7	0.8	-1.9	817
289	CAMPBELL-15YP08-036	16.1	3.6	0.282426	0.000026	0.001131	0.282419	-12.7	0.9	-5.5	333
290	CAMPBELL-15YP08-037	14.7	2.4	0.282303	0.000027	0.001010	0.282291	-17.1	1.0	-3.8	611
291	CAMPBELL-15YP08-038	11.8	3.9	0.282327	0.000026	0.000698	0.282317	-16.2	0.9	0.0	739
292	CAMPBELL-15YP08-039	15.2	2.2	0.281947	0.000032	0.000901	0.281931	-29.6	1.1	-8.7	959
293	CAMPBELL-15YP08-040	7.5	2.0	0.282084	0.000029	0.000468	0.282076	-24.8	1.0	-4.9	904
294	CAMPBELL-15YP08-042	16.0	3.3	0.282501	0.000034	0.000953	0.282495	-10.0	1.2	-2.8	336
295	CAMPBELL-15YP08-043	4.5	3.0	0.282618	0.000033	0.000268	0.282615	-5.9	1.2	7.2	593
296	CAMPBELL-15YP08-044	11.0	1.5	0.282416	0.000034	0.000917	0.282402	-13.1	1.2	4.5	807
297	CAMPBELL-15YP08-046	21.1	4.2	0.281435	0.000034	0.001262	0.281386	-47.7	1.2	-3.7	2024
298	CAMPBELL-15YP08-049	17.5	2.4	0.281018	0.000032	0.000775	0.281014	-62.5	1.1	-55.9	305
299	CAMPBELL-15YP08-053	10.6	3.7	0.281965	0.000031	0.000697	0.281951	-29.0	1.1	-6.4	1032
300	CAMPBELL-15YP08-054	9.5	3.4	0.281911	0.000031	0.000626	0.281899	-30.9	1.1	-8.6	1016
301	CAMPBELL-15YP08-058	6.7	3.4	0.282133	0.000022	0.000413	0.282128	-23.0	0.8	-8.6	657
302	CAMPBELL-15YP08-059	7.4	3.4	0.282151	0.000025	0.000449	0.282146	-22.4	0.9	-8.6	630
303	CAMPBELL-15YP08-060	17.5	3.6	0.282627	0.000024	0.001055	0.282615	-5.6	0.8	8.0	627
304	CAMPBELL-15YP08-061	3.5	3.2	0.282835	0.000028	0.000279	0.282833	1.8	1.0	9.8	361
305	CAMPBELL-15YP08-64	49.1	2.0	0.282585	0.000034	0.003299	0.282568	-7.1	1.2	-1.5	275
306	CAMPBELL-15YP08-065	30.7	3.1	0.282468	0.000031	0.001774	0.282453	-11.2	1.1	-2.0	439
307	CAMPBELL-15YP08-066	12.7	3.2	0.281452	0.000022	0.000853	0.281421	-47.1	0.8	-5.3	1902
308	CAMPBELL-15YP08-070	16.3	2.1	0.282435	0.000033	0.001017	0.282427	-12.4	1.2	-2.8	443
309	CAMPBELL-15YP08-072	7.7	1.8	0.282092	0.000028	0.000513	0.282082	-24.5	1.0	-1.8	1028
310	CAMPBELL-15YP08-077	14.6	2.6	0.282610	0.000025	0.001241	0.282603	-6.2	0.9	1.0	336
311	CAMPBELL-15YP08-082	30.8	3.7	0.282453	0.000033	0.001738	0.282439	-11.7	1.2	-2.1	456
312	CAMPBELL-15YP08-089	12.6	2.4	0.282124	0.000027	0.000697	0.282116	-23.4	1.0	-9.9	616
313	CAMPBELL-15YP08-091	22.3	3.1	0.282544	0.000025	0.001584	0.282537	-8.5	0.9	-3.4	242
314	CAMPBELL-15YP08-098	14.7	1.4	0.282473	0.000039	0.001051	0.282460	-11.0	1.4	2.8	639
315	CAMPBELL-15YP08-101	6.6	3.0	0.282153	0.000025	0.000371	0.282149	-22.3	0.9	-9.0	605
316	CAMPBELL-15YP08-103	16.3	1.7	0.282188	0.000031	0.001145	0.282166	-21.1	1.1	0.8	1011
317	CAMPBELL-15YP08-109	25.7	2.8	0.282566	0.000033	0.001818	0.282548	-7.8	1.2	3.3	525
318	CAMPBELL-15YP08-114	14.1	3.1	0.282244	0.000032	0.000821	0.282235	-19.1	1.1	-6.1	600
319	CAMPBELL-15YP08-115	18.7	2.9	0.281633	0.000024	0.001254	0.281608	-40.7	0.8	-18.1	1053
320	CAMPBELL-15YP08-150	20.8	2.0	0.281383	0.000028	0.001177	0.281339	-49.6	1.0	-6.1	1994
321	CAMPBELL-15YP08-146	21.6	3.0	0.282223	0.000021	0.001139	0.282211	-19.9	0.8	-7.2	588
322	CAMPBELL-15YP08-145	21.8	2.7	0.282448	0.000030	0.001256	0.282438	-11.9	1.0	-2.3	450
323	CAMPBELL-15YP08-144	4.8	3.5	0.282069	0.000028	0.000341	0.282064	-25.3	1.0	-9.1	736

Table 7: 15YP12; LA-MC-ICP-MS Zircon Hafnium Data

Order	Sample	$(^{176}\text{Yb} + ^{176}\text{Lu}) / ^{176}\text{Hf}$ (%)	Volts Hf	$^{176}\text{Hf}/^{177}\text{Hf}$	\pm (1s)	$^{176}\text{Lu}/^{177}\text{Hf}$	$^{176}\text{Hf}^{177}\text{Hf}$ (T)	E-Hf (0)	E-Hf (0) \pm (1s)	E-Hf (T)	Age (Ma)
324	CAMPBELL-15YP12-002	32.6	2.2	0.282383	0.000031	0.002613	0.282367	-14.2	1.1	-7.5	328
325	CAMPBELL-15YP12-004	22.1	2.6	0.282387	0.000028	0.001424	0.282379	-14.1	1.0	-7.4	313
326	CAMPBELL-15YP12-011	14.2	3.0	0.282398	0.000028	0.001699	0.282388	-13.7	1.0	-7.0	319
327	CAMPBELL-15YP12-012	27.6	3.5	0.281205	0.000030	0.001677	0.281124	-55.9	1.1	-1.7	2512
328	CAMPBELL-15YP12-013	13.2	2.2	0.281774	0.000041	0.000822	0.281748	-35.7	1.5	1.4	1691
329	CAMPBELL-15YP12-014	37.6	3.3	0.282500	0.000030	0.002338	0.282486	-10.1	1.1	-3.4	321
330	CAMPBELL-15YP12-015	43.4	1.7	0.282525	0.000040	0.003187	0.282506	-9.2	1.4	-2.7	320
331	CAMPBELL-15YP12-023	42.6	3.4	0.282410	0.000025	0.002377	0.282396	-13.2	0.9	-6.7	319
332	CAMPBELL-15YP12-028	20.5	1.3	0.282373	0.000034	0.001870	0.282360	-14.6	1.2	-7.0	361
333	CAMPBELL-15YP12-029	38.4	1.6	0.282411	0.000044	0.002979	0.282391	-13.2	1.5	-6.1	354
334	CAMPBELL-15YP12-034	12.6	4.3	0.282567	0.000026	0.000871	0.282562	-7.7	0.9	-0.7	324
335	CAMPBELL-15YP12-035	19.5	3.8	0.282362	0.000026	0.001638	0.282336	-15.0	0.9	2.9	839
336	CAMPBELL-15YP12-037	21.1	3.3	0.282281	0.000022	0.001149	0.282274	-17.8	0.8	-10.6	337
337	CAMPBELL-15YP12-043	19.2	2.2	0.282405	0.000045	0.001519	0.282395	-13.4	1.6	-6.5	329
338	CAMPBELL-15YP12-046	14.4	2.2	0.282283	0.000025	0.001062	0.282272	-17.7	0.9	-5.4	570
339	CAMPBELL-15YP12-047	22.6	3.5	0.282393	0.000028	0.001445	0.282384	-13.9	1.0	-6.9	329
340	CAMPBELL-15YP12-070	25.8	2.5	0.282450	0.000033	0.001322	0.282442	-11.9	1.2	-5.1	314
341	CAMPBELL-15YP12-068	22.9	2.0	0.282467	0.000042	0.001445	0.282459	-11.2	1.5	-4.4	320
342	CAMPBELL-15YP12-067	11.9	2.3	0.282444	0.000028	0.000735	0.282437	-12.1	1.0	-1.5	483
343	CAMPBELL-15YP12-066	20.2	2.3	0.282324	0.000037	0.001190	0.282316	-16.3	1.3	-9.1	338
344	CAMPBELL-15YP12-062	32.4	1.9	0.282490	0.000042	0.002351	0.282476	-10.4	1.5	-3.7	325
345	CAMPBELL-15YP12-059	12.5	1.9	0.282221	0.000034	0.000811	0.282212	-19.9	1.2	-6.8	602

Table 8: 15YP13; LA-MC-ICP-MS Zircon Hafnium Data

Order	Sample	$(^{176}\text{Yb} + ^{176}\text{Lu}) / ^{176}\text{Hf}$ (%)	Volts Hf	$^{176}\text{Hf}/^{177}\text{Hf}$	\pm (1s)	$^{176}\text{Lu}/^{177}\text{Hf}$	$^{176}\text{Hf}/^{177}\text{Hf}$ (T)	E-Hf(0)	E-Hf(0) \pm (1s)	E-Hf(T)	Age (Ma)
346	CAMPBELL-15YP13-003	19.8	3.4	0.282596	0.000025	0.001365	0.282594	-6.7	0.9	-5.0	82
347	CAMPBELL-15YP13-004	35.4	2.7	0.282770	0.000031	0.002323	0.282767	-0.5	1.1	1.1	81
348	CAMPBELL-15YP13-127	39.4	2.9	0.282629	0.000034	0.002389	0.282625	-5.5	1.2	-3.7	85
349	CAMPBELL-15YP13-005	22.7	2.2	0.282697	0.000035	0.001611	0.282695	-3.1	1.2	-1.4	81
350	CAMPBELL-15YP13-006	12.3	2.2	0.282795	0.000037	0.000716	0.282794	0.4	1.3	2.1	78
351	CAMPBELL-15YP13-008	10.8	4.6	0.282435	0.000023	0.000640	0.282425	-12.4	0.8	5.7	825
352	CAMPBELL-15YP13-009	29.6	2.0	0.282769	0.000034	0.001929	0.282766	-0.6	1.2	1.1	81
353	CAMPBELL-15YP13-011	14.7	2.1	0.282360	0.000035	0.000969	0.282353	-15.0	1.2	-6.6	389
354	CAMPBELL-15YP13-013	53.9	2.4	0.282629	0.000035	0.003811	0.282624	-5.5	1.2	-3.9	81
355	CAMPBELL-15YP13-014	26.4	3.2	0.282672	0.000028	0.001935	0.282669	-4.0	1.0	-2.6	66
356	CAMPBELL-15YP13-022	15.7	3.9	0.282658	0.000023	0.001068	0.282656	-4.5	0.8	-2.7	82
357	CAMPBELL-15YP13-026	43.4	2.6	0.282725	0.000030	0.002646	0.282721	-2.1	1.1	-0.4	83
358	CAMPBELL-15YP13-027	25.9	3.1	0.282650	0.000020	0.001712	0.282648	-4.8	0.7	-3.1	80
359	CAMPBELL-15YP13-029	9.3	3.0	0.281964	0.000032	0.000671	0.281952	-29.0	1.1	-8.2	950
360	CAMPBELL-15YP13-032	25.6	2.6	0.282425	0.000026	0.001667	0.282416	-12.7	0.9	-6.4	299
361	CAMPBELL-15YP13-033	9.7	3.4	0.282772	0.000023	0.000660	0.282767	-0.5	0.8	7.8	380
362	CAMPBELL-15YP13-034	11.2	3.4	0.282696	0.000033	0.001230	0.282694	-3.2	1.2	-1.4	82
363	CAMPBELL-15YP13-037	18.7	3.3	0.282673	0.000022	0.001381	0.282671	-4.0	0.8	-2.2	83
364	CAMPBELL-15YP13-039	17.1	4.5	0.282318	0.000021	0.000773	0.282311	-16.5	0.7	-5.8	492
365	CAMPBELL-15YP13-042	27.2	3.3	0.282680	0.000028	0.002843	0.282676	-3.7	1.0	-2.1	81
366	CAMPBELL-15YP13-046	14.8	3.0	0.282880	0.000025	0.000984	0.282878	3.3	0.9	5.6	105
367	CAMPBELL-15YP13-047	10.6	3.5	0.282936	0.000021	0.000749	0.282935	5.3	0.7	7.7	108
368	CAMPBELL-15YP13-048	13.0	3.7	0.282593	0.000022	0.000966	0.282588	-6.8	0.8	-0.8	276
369	CAMPBELL-15YP13-054	32.2	3.1	0.282735	0.000038	0.002624	0.282731	-1.8	1.4	-0.1	83
370	CAMPBELL-15YP13-055	23.0	3.5	0.282728	0.000034	0.001557	0.282726	-2.0	1.2	-0.3	80
371	CAMPBELL-15YP13-059	25.0	3.0	0.282656	0.000029	0.001762	0.282653	-4.6	1.0	-2.8	84
372	CAMPBELL-15YP13-061	20.6	3.4	0.282707	0.000029	0.002135	0.282704	-2.8	1.0	-1.1	79
373	CAMPBELL-15YP13-062	21.8	3.0	0.282711	0.000023	0.001709	0.282708	-2.6	0.8	-0.9	82
374	CAMPBELL-15YP13-072	16.7	4.1	0.282628	0.000027	0.001089	0.282627	-5.5	0.9	-3.8	80
375	CAMPBELL-15YP13-074	21.7	2.9	0.282951	0.000022	0.001709	0.282948	5.9	0.8	8.3	113
376	CAMPBELL-15YP13-078	23.6	3.1	0.282674	0.000038	0.001689	0.282671	-3.9	1.3	-2.2	81
377	CAMPBELL-15YP13-080	7.9	2.4	0.282342	0.000034	0.000584	0.282335	-15.7	1.2	-1.8	631
378	CAMPBELL-15YP13-088	20.0	2.1	0.282823	0.000029	0.001376	0.282821	1.3	1.0	3.1	81
379	CAMPBELL-15YP13-090	11.5	1.7	0.282563	0.000047	0.000964	0.282560	-7.9	1.7	-4.3	167
380	CAMPBELL-15YP13-094	48.8	3.3	0.282862	0.000035	0.002794	0.282858	2.7	1.2	4.3	78
382	CAMPBELL-15YP13-109	7.0	3.7	0.280952	0.000023	0.000418	0.280933	-64.8	0.8	-9.6	2464
383	CAMPBELL-15YP13-120	42.4	1.6	0.282836	0.000060	0.003595	0.282830	1.8	2.1	3.6	90
384	CAMPBELL-15YP13-124	30.9	1.8	0.282782	0.000037	0.002209	0.282778	-0.1	1.3	1.7	89
385	CAMPBELL-15YP13-125	17.4	3.7	0.282774	0.000022	0.001132	0.282771	-0.4	0.8	3.3	173
386	CAMPBELL-15YP13-126	68.5	2.6	0.282918	0.000040	0.004808	0.282899	4.7	1.4	8.7	211

Table 9: 15YP07; LA-MC-ICP-MS Zircon Hafnium Data

Order	Sample	$(^{176}\text{Yb} + ^{176}\text{Lu}) / ^{176}\text{Hf}$ (%)	Volts Hf	$^{176}\text{Hf}/^{177}\text{Hf}$	\pm (1s)	$^{176}\text{Lu}/^{177}\text{Hf}$	$^{176}\text{Hf}/^{177}\text{Hf}$ (T)	E-Hf (0)	E-Hf (0) \pm (1s)	E-Hf (T)	Age (Ma)
387	CAMPBELL-15YP07-001	27.7	3.9	0.282959	0.000033	0.001976	0.282957	6.2	1.2	7.2	50
388	CAMPBELL-15YP07-003	34.5	3.2	0.282902	0.000044	0.002450	0.282900	4.1	1.6	5.2	52
389	CAMPBELL-15YP07-007	27.3	3.9	0.282904	0.000031	0.002103	0.282902	4.2	1.1	5.2	49
394	CAMPBELL-15YP07-018	32.9	3.7	0.282928	0.000041	0.002377	0.282926	5.1	1.5	6.0	46
395	CAMPBELL-15YP07-027	21.3	3.4	0.282897	0.000032	0.001510	0.282896	4.0	1.1	5.0	47
396	CAMPBELL-15YP07-029	23.7	3.7	0.282954	0.000026	0.001684	0.282953	6.0	0.9	7.0	48
397	CAMPBELL-15YP07-034	31.7	3.7	0.282954	0.000029	0.002308	0.282952	6.0	1.0	6.9	47
398	CAMPBELL-15YP07-035	27.4	3.8	0.282901	0.000033	0.002304	0.282899	4.1	1.2	5.1	50
399	CAMPBELL-15YP07-036	29.5	3.7	0.282918	0.000033	0.002151	0.282916	4.7	1.2	5.7	49
400	CAMPBELL-15YP07-044	32.9	3.8	0.282889	0.000029	0.002398	0.282887	3.7	1.0	4.6	46